UC Santa Barbara

UC Santa Barbara Electronic Theses and Dissertations

Title

To the edge of apoptotic cell death and back

Permalink

https://escholarship.org/uc/item/45q341km

Author

Conner, Christopher

Publication Date

2021

Peer reviewed|Thesis/dissertation

eScholarship.org Powered by the California Digital Library
University of California

UNIVERSITY OF CALIFORNIA

SANTA BARBARA

To the edge of apoptotic cell death and back

A dissertation submitted in partial satisfaction of the requirements for the degree Doctor of Philosophy in Molecular, Cellular, and Developmental Biology

by

Christopher Michael Conner

Committee

Professor Denise Montell, Chair

Professor Kathleen Foltz

Professor Anthony De Tomaso

Professor William Smith

March 2021

The dissertation of Christopher Michael Conner is approved

_____

Kathleen Foltz

_____

Anthony De Tomaso

_____

William Smith

_____

Denise Montell, Committee Chair

March 2021

Acknowledgements

I want to thank everyone who helped me throughout my life and doctoral career with mentorship, scientific feedback, and friendship.

Thank you, Denise. I am grateful to have done my doctorate research in your lab. Your mentorship and support for even my craziest hypotheses was essential to my research experience.

I would like to thank my committee members, Kathy Foltz, Tony De Tomaso, and Bill Smith for their feedback and support. I want to further thank Kathy for being a second mentor to me and for your support at each critical step in my career.

I want to thank every member of Denise's lab. Special thanks to Varuzhan Balasanyan, Maddalena Nano, and Gongping Sun for mentorship, great collaboration and friendship. I also want to thank Jim Mondo, Austin Ding, Xiaoran Guo, Allison Gabbert, Morgan Mutch, Guangxia Miao, Joseph Campanale, Sreesankar Easwaran, Abhinava Mishra, Alba Torres, Lauren Penfield, Christina Herron, Yewubdar Argaw, Adishthi Guraz, Josephine Nguyen, Juhi Gor, Salina Manibog, Lisa Schwartz, and Jackie Chen for being great lab mates and creating the environment that made this work possible.

Thanks to the department of Molecular, Cellular, and Developmental Biology for providing an excellent work environment. I want to thank Cassidy Arnold for her efforts as the stem cell facility director and for flow cytometry training and experiment advice. I want to thank Anthony Galaviz for his efforts as the graduate student advisor. I want to thank Connie Frank and Otto J. Holmok for providing me fellowship funding at critical points in my career. I want to thank my mentors prior to graduate school who without I would not have made it: Karine Le Roch, Serena Cervantes, Jacques Prudhomme, and Ernest Martinez.

I want to thank my family for providing the foundation that made it possible for me to pursue my interests.

Curriculum Vitae

Christopher Michael Conner

Education

2015 – 2021	Ph.D. Molecular, Cellular, and Developmental Biology
	University of California, Santa Barbara
2011 – 2015	B.S. Biological Sciences
	University of California, Riverside

Awards and Fellowships

2020	Otto J. Holmok Research Fellowship
2019	Connie Frank Research Fellowship
2014	Neil Campbell Undergraduate Award for Outstanding Research

Teaching Experience

2020	Teaching Assistant, Cell Division and Oncogenesis
2019	Teaching Assistant, Cell Division and Oncogenesis
2018	Teaching Assistant, Cell Division and Oncogenesis
2017	Teaching Assistant, Cell Division and Oncogenesis
2015	Teaching Assistant, Introduction to Biology Laboratory

Publications

- Gudipaty S, **Conner CM**, Rosenblatt J, Montell DJ. (2018). Unconventional ways to live and die: cell death and survival in development, homeostasis, and disease. *Annu. Rev. Cell Dev. Biol*.

- Sun G, Guzman E, Balasanyan V, **Conner CM**, Wong K, et al. (2017). A molecular signature for anastasis, recovery from the brink of apoptotic cell death. *J. Cell Biol*. jcb.201706134

- Cervantes S, Bunnik EM, Saraf A, **Conner CM**, Escalante A, et al. (2013) The multifunctional autophagy pathway in the human malaria parasite, Plasmodium falciparum. *Autophagy* 10:80–92

ABSTRACT

To the edge of apoptotic cell death and back

by

Christopher Michael Conner

Cell death is fundamental in animal development, tissue homeostasis, and disease. Approximately 50 billion cells die by apoptosis every day in an adult human. During apoptosis, mitochondrial permeabilization results in the activation of caspase proteases. Caspases cleave hundreds of protein targets killing the cell and fragmentating it into apoptotic bodies for immune clearance. Cell death research has long suggested that once mitochondrial dysfunction and caspase activation are observed, death is inevitable. However, a growing body of research challenges this long-standing assumption. A variety of normal and cancer cell types can survive transient activation of apoptosis via a survival process termed anastasis.

I study anastasis using human cancer cell lines, representing some of the most prevalent cancer types, as a model. I first document major phenotypic changes following transient treatment of the apoptosis inducer staurosporine (STS). I observed cancer cells recovering from STS induced mitochondrial collapse and damage. From these observations, I discovered that anastatic cancer cells survive with low mitochondrial membrane potential ($\Delta\Psi m$) and that low-$\Delta\Psi m$ correlated with nuclear health. This dissertation provides a cell biological description of anastasis in cervical cancer HeLa cells and reveals a previously unknown connection between apoptosis survival and metabolic reprogramming.

Table of Contents

PREFACE

This dissertation includes two published manuscripts and a manuscript in preparation.

The first chapter presents:

1. Gudipaty SA, **Conner CM**, Rosenblatt J, Montell DJ. Unconventional Ways to Live and Die: Cell Death and Survival in Development, Homeostasis, and Disease. Annu Rev Cell Dev Biol. 2018 Oct 6; 34:311-332. doi: 10.1146/annurev-cellbio-100616-060748.

The second chapter presents:

2. Sun G, Guzman E, Balasanyan V, **Conner CM**, Wong K, Zhou HR, Kosik KS, Montell DJ. A molecular signature for anastasis, recovery from the brink of apoptotic cell death. J Cell Biol. 2017 Oct 2;216(10):3355-3368. doi: 10.1083/jcb.201706134.

The third chapter is composed of research that will be published in the future.

I. Unconventional Ways to Live and Die: Cell Death and Survival in Development, Homeostasis, and Disease

©2018 Gudipaty et al. Originally published in *Annual Review of Cell and Developmental Biology*. https://doi.org/10.1146/annurev-cellbio-100616-060748

Swapna Gudipaty, Christopher M. Conner, Jody Rosenblatt, and Denise J. Montell

Abstract

Balancing cell death and survival is essential for normal development and homeostasis and for preventing diseases, especially cancer. Conventional cell death pathways include apoptosis, a form of programmed cell death controlled by a well-defined biochemical pathway, and necrosis, the lysis of acutely injured cells. New types of regulated cell death include necroptosis, pyroptosis, ferroptosis, phagoptosis, and entosis. Autophagy can promote survival or can cause death. Newly described processes of anastasis and resuscitation show that, remarkably, cells can recover from the brink of apoptosis or necroptosis. Important new work shows that epithelia achieve homeostasis by extruding excess cells, which then die by anoikis due to loss of survival signals. This mechanically regulated process both maintains barrier function as cells die and matches rates of proliferation and death. In this review, we describe these unconventional ways in which cells have evolved to die or survive, as well as the contributions that these processes make to homeostasis and cancer.

Introduction

The regulation of cell death and survival is fundamental for eukaryotic development and tissue homeostasis. It is as important for autoreactive T cells, supernumerary cells, and damaged cells to die as it is for stem cells, cardiomyocytes, and neurons to last our whole lives. Eukaryotic cells can die by accident, suicide, or murder. Accidental cell death, usually as a result of severe stress, is not under the control of specific genes or gene products, whereas regulated cell death, whether suicide or murder, is mediated genetically and tightly controlled (Galluzzi et al., 2015). Necrosis is a common form of accidental cell death characterized by cellular swelling and loss of membrane integrity (Vanlangenakker et al., 2012). Apoptosis, the most extensively studied form of regulated cell suicide, is characterized as a series of stereotyped morphological changes in response to the activation of proteolytic enzymes termed caspases (Kerr et al., 1972; Vaux, 2002). Autophagic cell death (ACD) occurs when cytosolic autophagic vacuoles consume the cell (Liu and Levine, 2015).

Since identification of these canonical cell death mechanisms, new studies have revealed strikingly diverse ways by which death pathways can be triggered, regulated, and even reversed. Death by pyroptosis, necroptosis, and ferroptosis turns out to be regulated rather than accidental. Additionally, death by live cell engulfment occurs in the processes of phagoptosis and entosis. Surprisingly, cells can recover from the brink of several forms of death, including apoptosis, necroptosis, and entosis, in some cases after passing through biochemical steps previously considered points of no return, such as activation

of executioner caspases. This review covers our current understanding of conventional and unconventional cell death and survival programs.

Conventional Forms of Cell Death

Apoptosis

Apoptosis, the best-characterized form of programmed cell death, is essential for normal animal development, tissue homeostasis, and disease and has been reviewed extensively elsewhere (Elmore, 2007; Fuchs and Steller, 2011; Taylor et al., 2008). Morphological hallmarks of apoptosis include cell shrinkage, membrane blebbing, nuclear condensation, and DNA fragmentation. Classical biochemical markers of apoptosis include mitochondrial outer membrane permeabilization (MOMP); activation of a group of proteases termed caspases; and the externalization of phosphatidylserine, which attracts phagocytes that engulf apoptotic cells without inducing an inflammatory response (Martin and Green, 1995; Taylor et al., 2008). Apoptosis can result from active prodeath signals or from loss of survival signals. Anoikis is a specific type of apoptosis resulting solely from loss of survival signals derived from attachment to extracellular matrix (ECM) and/or neighboring cells (Frisch and Francis, 1994). Anoikis is a common form of cellular murder whereby neighboring cells squeeze a cell out by the process of extrusion (Eisenhoffer et al., 2012; Rosenblatt et al., 2001).

Apoptosis is triggered when prodeath signals outweigh prosurvival signals. Once the balance is tipped, cells activate upstream initiator caspase-8 or −9; these caspases cleave and activate executioner caspases-3 and −7 (Salvesen and Ashkenazi, 2011).

Executioner caspases cleave hundreds of cellular targets, resulting in biochemical and morphological hallmarks and ultimately death (Coleman et al., 2001; Lakhani, 2006; Lüthi and Martin, 2007; Martin et al., 1995). If caspase activity is blocked, cells can still sometimes die by caspase-independent cell death (Tait and Green, 2008). Although activation of executioner caspases has been considered a point of no return in the apoptotic pathway (Green and Kroemer, 1998), in some circumstances cells can recover following executioner caspase activation, in a process termed anastasis (Sun and Montell, 2017), described further below.

Elimination of specific cells by apoptosis is critical for regulating cell numbers, sculpting tissues, and eliminating unwanted cells throughout animal development and adulthood. Classic examples of developmental apoptosis include removal of interdigital webs during limb formation, metamorphosis of the endocardial cushion into cardiac valves and septa, and elimination of surplus neurons (Abdelwahid et al., 2002; Dekkers et al., 2013; Fisher et al., 2000; Lindsten et al., 2000). Apoptosis also protects tissues by removing potentially harmful cells. For example, in the immune system, self-reactive lymphocytes are removed in the thymus by apoptosis to avoid their release into the circulation, which could lead to autoimmune reactions (Feig and Peter, 2007). The apoptotic program also removes cells with unrepaired DNA damage (Roos et al., 2016), which is important for tumor suppression. Additionally, apoptosis suppresses lymphomas and carcinomas by promoting the homeostatic turnover of cells such as B cells and epithelial cells, respectively. Genetic rearrangements that cause overexpression of the apoptosis-inhibiting Bcl2 gene cooperate with oncogenes to cause B cell lymphomas by delaying or

preventing the normal turnover of these cells by apoptosis (Yip and Reed, 2008). Moreover, p53, a critical promoter of apoptosis in cells with DNA damage, is the most commonly mutated gene in human cancer (Muller and Vousden, 2013). Additionally, tumor cells can induce apoptosis in tumor-reactive T cells by expressing programmed death ligand 1 (PDL1), thus suppressing the antitumor immune response (Dong et al., 2002). Apoptosis is, therefore, a biochemically well-defined process essential for normal development and homeostasis and plays complex roles in both causing and preventing disease.

Death by Extrusion and Anoikis

Cells within epithelia turn over at some of the fastest rates in the body, which may be why these are the tissues where most cancers arise. How do tissues match the numbers of cells that are dividing with those that are dying? Epithelia match the number of cells that divide with the number that die through mechanical force: When epithelial cells become too crowded, they extrude live cells that then die by anoikis (Eisenhoffer et al., 2012). Additionally, when cells within a monolayer are triggered to undergo apoptosis, they are extruded as they die (Andrade and Rosenblatt, 2011; Rosenblatt et al., 2001). To extrude, both live and dying cells produce and emit the bioactive lipid sphingosine-1-phosphate (S1P), which binds the G protein–coupled receptor sphingosine-1-phosphate receptor 2 (S1P2) in their neighboring cells to activate Rho-mediated contraction of an actomyosin ring (Gu et al., 2011; Slattum et al., 2009). Actomyosin contraction squeezes live cells apically out of the epithelial monolayer, while neighboring cells move in to prevent a gap from forming, thus preserving epithelial barrier function). While apoptotic stimuli can

simultaneously activate apoptosis and extrusion, during homeostatic turnover mechanical crowding activates the stretch-activated channel Piezo1 to activate live cell extrusion (Eisenhoffer et al., 2012). Once live cells extrude, they then die by anoikis because they are stripped from the matrix and neighboring cells that provide them with survival signals. In this way, cells are killed by their neighbors through extrusion to maintain constant cell numbers. In contrast, during Drosophila development, cells extrude basally (such extrusions are also termed delaminations) and die as a result of proapoptotic signaling, rather than loss of survival signals (Levayer et al., 2016; Meghana et al., 2011). Oncogenic mutations can disrupt the apical extrusion pathway, leading to cell masses at sites where cells would normally have extruded, underscoring the importance of apical extrusion in maintaining constant epithelial cell densities and suppressing tumor formation (Gu et al., 2015; Marshall et al., 2011; Slattum et al., 2014).

Autophagic Cell Death

Autophagy is a conserved catabolic process that degrades cellular contents and recycles damaged organelles (Kroemer et al., 2010; Takeshige et al., 1992). During autophagy, cells form autophagosomes that capture cellular contents and target them for degradation (Nakatogawa et al., 2009; Takeshige et al., 1992). By blocking growth signaling and promoting autophagosome formation, autophagy typically regulates protein levels and promotes survival in cells experiencing nutrient insufficiency and other types of stress. The molecular mechanism of autophagy requires several conserved Atg (autophagy-related) proteins and comprises three main steps: initiation, nucleation, and elongation (Kaur and Debnath, 2015). Autophagosome formation is initiated by phagophore (or

isolation membrane) assembly by the ULK1 complex and nucleation by the class III phosphatidylinositol kinase (PI3K)-Beclin1 (yeast Atg8) complex. Elongation and formation of the autophagosome require two ubiquitin-like conjugation systems. The Atg12-Atg5-Atg16 complex promotes lipidation of the microtubule-associated protein 1 light chain 3 (LC3) with phosphatidylethanolamine (PE) to form the LC3-II complex, which elongates the membranes of the forming autophagosome. The LC3-II complex remains covalently bound to the mature autophagosome until it fuses with the lysosome to form an autolysosome. Lysosomal hydrolases degrade the contents of the autolysosome, including internalized LC3, so that molecules, particularly amino acids, can be released into the cytosol to serve as building blocks to conserve energy and rebuild organelles (White, 2012). However, components of the autophagic machinery can also kill cells (Bursch, 2001). Large cytosolic autophagic vacuoles from accumulated autophagosomes, marked by LC3 labeling, are the most observable characteristics of ACD (Galluzzi et al., 2015). The mechanisms regulating ACD are not well understood, although the emerging roles of proapoptotic factors AMPK, MAPK, BNIP3, and cathepsin L in ACD suggest that there is likely cross talk between autophagy and apoptosis (Liu and Levine, 2015). It is likely for this reason that the term autophagic cell death is under debate. Currently, the term ACD should be used only in cases in which cell death (a) occurs independently of apoptosis, (b) shows increased autophagic flux (not just increased autophagic markers), and (c) is suppressed by inhibition or knockdown of essential autophagic proteins (Denton et al., 2012; Galluzzi et al., 2015).

Physiologically, ACD plays roles in Dictyostelium and Drosophila development. Dictyostelium discoideum lacks caspases and Bcl-2 family proteins. Starvation of this organism triggers single cells to aggregate into a multicellular structure that undergoes differentiation into stalk cells and spores. Stalk cells undergo Atg1-induced autophagy, which, together with a second signal, the differentiation inducing factor-1 (DIF-1) (Kay, 1987; Morris et al., 1987), eventually leads to stalk cell death. Thus, the DIF-1 signal converts autophagy into ACD (Giusti et al., 2009). Developmental ACD has also been characterized in Drosophila during salivary gland and midgut development (Tracy and Baehrecke, 2013). Even though flies have an intact apoptotic machinery, cell death in the midgut occurs primarily through ACD (Denton et al., 2009). In contrast, destruction of the salivary gland requires both caspase activity and autophagy pathways (Berry and Baehrecke, 2008).

In mammals, thus far, ACD has been reported only in cells with mutations in normal cell death pathways. For instance, ACD may be an important alternative death pathway for tumor cells with oncogenic RasV12 mutations that amplify autophagy for survival. Dying Ras mutant cells do not activate caspases or other apoptotic markers but do express Beclin, a central regulator of autophagy (Elgendy et al., 2011). Additionally, mouse embryonic fibroblasts deficient in proapoptotic Bax and Bak1 or multiple myeloma cells deficient in caspase-10 activity undergo Beclin-1-and Atg5-dependent autophagic death (Lamy et al., 2013; Shimizu et al., 2004). Thus, ACD appears to serve as a backup death program when apoptosis is insufficient or inhibited. Thus, certain cancer cells may be more vulnerable than normal cells to ACD, opening an avenue to exploit for treatment.

Finally, autosis represents a distinct cell death mechanism that is similar to ACD. Autosis is morphologically characterized by the disappearance of the endoplasmic reticulum and by convolution and swelling of the perinuclear space (Liu et al., 2013). Disruption of a Na+, K+-ATPase protects a variety of cell types from experimental induction of autosis (Liu and Levine, 2015), suggesting that the ATPase function promotes autosis, but the mechanism still remains mysterious.

Cultured cells that are starved or exposed to a Beclin1-derived peptide, neurons in cerebral ischemia, and hepatocytes of patients with severe anorexia nervosa exhibit hallmarks of autosis (Kheloufi et al., 2015; Liu et al., 2013; Xie et al., 2016a).

Necrosis

Necrosis, defined by cellular swelling and rupture of the plasma membrane, is the most common form of accidental cell death, typically in response to severe cellular, chemical, or physical stress (Vanlangenakker et al., 2012). Necrosis can also result when apoptotic cells are not phagocytosed after undergoing apoptosis, in a process termed secondary necrosis (Silva et al., 2008). In contrast to apoptosis, which can eliminate numerous cells without causing inflammation, necrosis activates an inflammatory response. Interestingly, secondary necrosis is no accident but rather is controlled by a specific biochemical pathway. Caspase-3 regulates secondary necrosis by cleaving DFNA5 (deafness-associated tumor suppressor), which converts it into a necrosis-promoting DFNA5-N fragment (Rogers et al., 2017). The DFNA5-N fragment inserts into the plasma membrane, forming a large pore that releases inflammatory molecules (Rogers et al.,

2017). Additional forms of regulated necrosis include necroptosis, pyroptosis, and ferroptosis, each of which is briefly summarized below (Table 1).

Table 1 Major cell death modalities with biochemical hallmarks

Cell death pathway	Biochemical hallmarks	Reference(s)
Apoptosis	Caspase-3/7 activation, phosphatidylserine (PS) exposure, MOMP	**Martin & Green 1995**, **Martin et al. 1995**, **Taylor et al. 2008**
Autophagic cell death and autosis	Dependency on autophagy machinery	**Bursch 2001**, **Liu et al. 2013**
Necrosis	Plasma membrane lysis	**Vanlangenakker et al. 2012**
Secondary necrosis	Caspase-3-dependent cleavage of DFNA5	**Rogers et al. 2017**
Pyroptosis	Inflammatory caspase—mediated cleavage of gasdermin D	**Cookson & Brennan 2001**, **Man et al. 2017**
Necroptosis	RIPK activation, MLKL activation, PS exposure	**Ashkenazi & Salvesen 2014**, **Cho et al. 2009**, **Gong et al. 2017b**, **Sun et al. 2012**
Ferroptosis	Glutathione peroxidase inactivation, iron-dependent ROS accumulation	**Dixon et al. 2012**, **Yang et al. 2014**
Phagoptosis	Exposure of eat-me signals, loss of don't-eat-me signals	**Brown & Neher 2012**
Entosis	Rho and ROCK activity, actomyosin contractions	**Overholtzer et al. 2007**
Cornification	Caspase-14 activation	**Eckhart et al. 2013**
Parthanatos	PARP-1 overactivation	**Fuchslocher Chico et al. 2017**
Linker cell–type death	HSF-1 induction of LET-70/UBE2D2	**Malin et al. 2016**
NETosis	NADPH oxidase activity, formation of NETs	**Remijsen et al. 2011**

Unconventional Forms of Cell Death

Necroptosis

The best-characterized form of regulated necrotic cell death is necroptosis, a pathway important in inflammation and viral infection (Ashkenazi and Salvesen, 2014; Weinlich et al., 2017). Necroptosis requires activation of the receptor-interacting kinases 1 and 3 (RIPK1 and −3) (Cho et al., 2009; Zhang et al., 2016), which results in the phosphorylation of the pseudokinase mixed lineage kinas-like (MLKL), causing its oligomerization and activation (Grootjans et al., 2017; Sun et al., 2012). Active MLKL then localizes to intracellular and plasma membranes, where it disrupts membrane integrity to kill the cell (Cai et al., 2014; Wang et al., 2014). Plasma membrane breakdown causes necroptotic cells to release damage-associated molecular patterns (DAMPs) important for activating the inflammatory pathway (Kaczmarek et al., 2013). During viral infection, necroptosis can act as a backup death pathway when viral proteins inhibit caspases. Mice lacking RIPK3 are more susceptible to viral and Yersinia infection (Jorgensen et al., 2017; Kaiser et al., 2013). However, necroptosis is not always beneficial. Some viruses and bacteria can induce immune cell necroptosis, resulting in reduced pathogen control and inflammation (Weinlich et al., 2017). Necroptotic death may also have important roles in cancer. Necroptosis of endothelial cells, for example, can promote tumor extravasation facilitating metastasis, and low MLKL expression is correlated with poor prognosis of patients with gastric and cervical cancers (Ertao et al., 2016; Grootjans et al., 2017; Ruan et al., 2015; Strilic et al., 2016).

Pyroptosis

Pyroptosis is an essential antimicrobial response that triggers a cell-autonomous inflammatory form of regulated cell death in response to bacteria, viral, fungal, and protozoan infections (Cookson and Brennan, 2001; Man et al., 2017). A set of caspases distinct from those used in apoptosis—caspase-1, human caspase-4, human caspase-5, and mouse caspase-11—activate the pyroptotic pathway in response to formation of an inflammasome (Man et al., 2017). The inflammasome is a multiprotein complex formed by activation of pattern recognition receptors like the Nod-like receptors (NLRs) (Bergsbaken et al., 2009). The inflammasome-activated caspases then cleave the propyroptotic protein Gasdermin D (GSDMD), which forms a pore in the plasma membrane and causes cell lysis (He et al., 2015; Liu et al., 2016). Interestingly, some chemotherapy drugs can increase inflammasome activity, which could potentially help mobilize the body's own immune response to a tumor (Thi and Hong, 2017). Thus, promoting pyroptosis over apoptosis of tumors is an important new line of investigation for cancer therapy (Kolb et al., 2014).

Ferroptosis

Ferroptosis, an iron-dependent form of regulated cell death (Xie et al., 2016b), was first discovered in cancer cells treated with erastin, a VDAC2 and VDAC3 inhibitor that selectively targets the oncogenic form of RAS (Dixon et al., 2012). Here, metabolic dysfunction causes iron-dependent reactive oxygen species (ROS) accumulation to promote cell death (Dixon et al., 2012). Reduction of the antioxidant glutathione or direct inhibition of glutathione peroxidase 4 leads to the accumulation of ROS, which activates

ferroptosis (Yang et al., 2014). In an effort to overcome apoptotic resistance and improve drug efficacy, researchers are now identifying drugs that induce ferroptotic death in cancer cell (Ma et al., 2016; Zhu et al., 2017). Ferroptosis has thus far been identified only in drug therapy responses, so whether it plays a role in normal physiology is not clear. Its therapeutic value may be greatest if it does not play a role in normal physiology, by limiting possible side effects.

Phagoptosis and Entosis

Phagoptosis is a form of cell murder that occurs when a phagocyte consumes an otherwise viable cell (Brown and Neher, 2012). This process is distinct from phagocytosis of apoptotic or necrotic cells. Yet, similarly to phagocytosis, cell surface exposure of the eat-me signal, phosphatidylserine, and/or loss of the don't-eat-me signal CD47 is critical for phagoptosis (Brown and Neher, 2012). The mechanisms that regulate phagoptosis are yet to be fully understood.

Physiologically, phagoptosis is responsible for erythrocyte and neutrophil turnover and, thus, may represent the most common death program used in the body (Brown and Neher, 2012). However, phagoptosis also has pathological roles. For instance, neuroinflammation can cause microglia to kill viable neurons by phagoptosis, possibly leading to neuronal degeneration (Neher et al., 2012). In contrast, human cancer cells can avoid phagoptosis by upregulating CD47 on their surfaces (Willingham et al., 2012).

In contrast to phagoptosis, entosis occurs when a live cell drives itself inside another cell, rather than passively being eaten (Overholtzer et al., 2007). Entosis does not require phosphatidylserine exposure. Rather, the entosing cell requires adherens junction proteins, ROCK activity, and actomyosin contractions to physically force its way into an adjacent cell (Overholtzer et al., 2007). Following entosis, the internalized cell has three different fates: cell death, cell division, or exit). Internalized cells are surrounded by an entotic vacuole membrane that recruits LC3, a component of autophagosomes (Florey et al., 2011). The LC3-targeted entotic vacuole membrane then recruits lysosomes to degrade the internalized cell, resulting in death of the entosed cell (Florey et al., 2011).

Entosis has also been noted in mice to remove cells within the epithelial barrier during normal implantation (Li et al., 2015). Furthermore, soft agar assays suggest that entosis may inhibit tumor growth, as the inhibition of entosis increases colony formation (Overholtzer et al., 2007; Sun et al., 2014). Thus, entosis may function as an additional mechanism to eliminate matrix-detached cells.

Other Forms of Cell Death

Oher forms of unconventional cell death remain the subject of active research, and the list is likely to continue to grow. Here, we briefly mention a few types, indicating where to find more information. Cornification is a form of programmed cell death specific to outer epidermal keratinocytes, where dead cell layers remain attached to live layers to provide a thicker protective barrier until the former are eventually sloughed off from the skin (Eckhart et al., 2013). Parthanatos is a form of regulated necrosis caused by PARP-1

overactivation during traumatic brain injury, excitotoxicity, and ischemia and in many neurodegenerative disorders (Fuchslocher Chico et al., 2017). NETosis is a form of pathogen-induced neutrophil death, which causes release of NETs (neutrophil extracellular traps) made of DNA following cell lysis (Remijsen et al., 2011). Here, the DNA forms massive nets that bind and capture more pathogens to aid the immune response. In male Caenorhabditis elegans larvae, a single cell, termed the linker cell, migrates from the middle of the larva to the posterior cloaca, pulling the gonad along behind it, and then dies through a cell-autonomous, nonapoptotic process termed linker cell death (Abraham et al., 2007; Malin et al., 2016). During Drosophila oogenesis, support cells termed nurse cells die after contributing most of their cytoplasm to the developing oocyte. This physiological death incorporates morphological and biochemical elements of apoptosis, necrosis, and phagoptosis of the germline nurse cells by the somatic follicle cells (Peterson et al., 2015). When female flies are starved or otherwise stressed, they activate these mechanisms earlier during egg development to recoup nutrients and limit energy expenditure. The relatively large size of the polypoid nurse cells may engender the need to mobilize multiple death pathways to eliminate them.

The diversity of death mechanisms described above presents a challenge if the goal is to enhance or block all cellular demise. But this same diversity might offer opportunities if the goal is selective cell killing or rescue. If all cells died by the same mechanism, it would be difficult to kill tumor cells without harming beneficial cells. The diversity of death mechanisms may allow for identification of specific vulnerabilities of cancer cells while fostering the health and well-being of tissue stem cells, cardiomyocytes, and neurons.

Furthermore, appreciating the diversity of mechanisms by which harmful cells can die may reveal strategies to trigger alternate cell death pathways if canonical death components are disabled by mutation or by other means. Next, we discuss mechanisms that cells have evolved to escape death in both normal physiology and disease.

Recovery from the Brink of Death

Earlier work suggested that cells commit irreversibly to death once they cross a biochemically defined point of no return. However, recent studies show that multiple cell types can reverse and survive biochemical hallmarks of apoptosis, entosis, and necroptosis (Figure 1, Table 2). Here, we describe examples in which cells can survive near-death experiences.

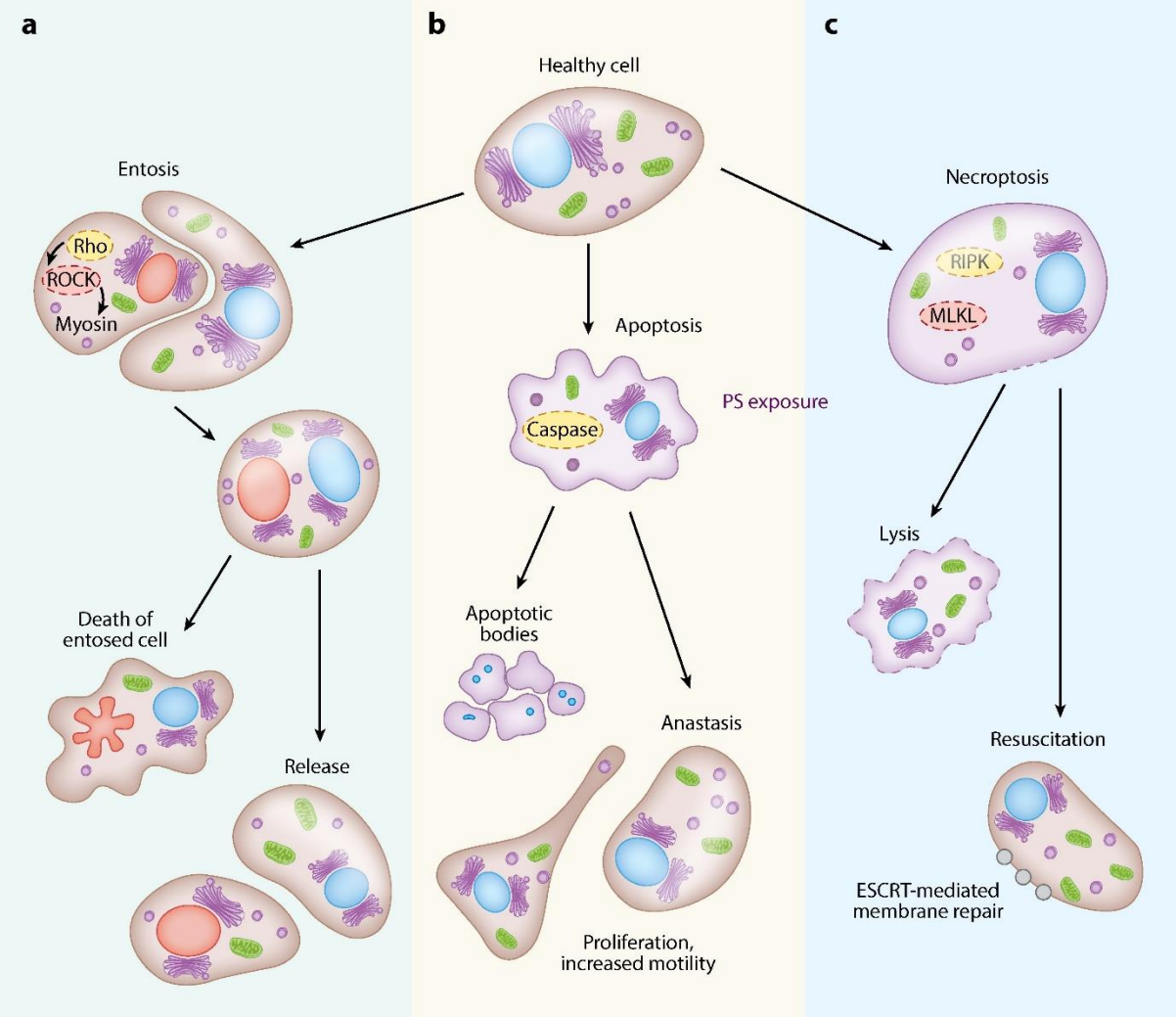

Figure 1. Recovery from the brink of death. Eukaryotic cells have been reported to survive the biochemical hallmarks of entosis, apoptosis, and necroptosis. (*a*) Entosis results when one cell pushes itself into another by Rho- and ROCK-driven myosin contraction. This results in a cell-in-cell structure. The entosed cell, whether a cancer cell or a normal cell, can either be degraded within the host cell or be released and survive. (*b*) Apoptosis results in cell shrinkage, membrane blebbing, and phosphatidylserine (PS) exposure (*purple*) due to executioner caspase activation. Cells with activated caspase can break into apoptotic bodies and die or can undergo anastasis and recover. Survival by anastasis can result in an elongated cell morphology and increased motility. (*c*) Necroptosis is a form of regulated necrosis carried out by the activation of RIPKs (receptor-interacting kinases) and MLKL (mixed lineage kinase–like). Active MLKL damages the plasma membrane of cells, results in PS exposure, and kills the cell by lysis. However, provided that MLKL activity is halted, cells can survive in a process termed resuscitation by ESCRT-mediated membrane repair.

Table 2 Major cell survival pathways

Survival pathway	Biochemical hallmarks	Reference(s)
Anastasis	Survival after caspase-3/7 activation	**Ding & Sun et al. 2016**, **Sun et al. 2017**, **Tang et al. 2012**
Necroptosis resuscitation	Survival after MLKL activation	**Gong et al. 2017a**,**b**; **Zargarian et al. 2017**
Overriding anoikis	EGFR upregulation, PI3K/AKT activation	**Frisch et al. 2013**, **Hanahan & Weinberg 2011**, **Kim et al. 2012**
Hijacking entosis	E-cadherin overexpression, glucose starvation	**Sun et al. 2014**
Basal extrusion	Mutations in K-Ras, APC, and $S1PR_2$; disruption in S1P trafficking	**Slattum et al. 2014**

Anastasis: Cell Survival Following Apoptotic Activation of Caspase-3

Caspase-3 activation was widely considered a point of no return in terms of activation of apoptosis, yet recent findings show that this is not the case. A variety of cultured mammalian cells, including primary cells, cell lines, and cancer cells, can survive caspase-3 activation by using a process termed anastasis, a Greek word meaning rising to life (Sun and Montell, 2017; Tang et al., 2012). Anastasis occurs when cells are treated with potentially lethal doses of chemicals such as ethanol, DMSO, or staurosporine but survive, if the treatment is transient. Cells at the brink of chemically induced apoptosis show classic morphological signs such as shrinkage and blebbing, as well as biochemical hallmarks such as phosphatidylserine exposure and caspase-3 activation. If left in the toxins, the treated cells die. However, if the inducer of cell death is removed, most of the treated cells recover normal morphology, survive, and divide (Figure 1).

RNAseq of mammalian cancer cells undergoing anastasis has revealed two discrete phases, with different sets of genes transcribed during the first 4 h compared to the next 8 to 12 h of recovery (Sun et al., 2017). Strikingly, some mRNAs that are highly induced 1 h following removal of the apoptotic stimulus are already enriched in cells on the brink of apoptotic death. For example, the mRNA encoding the zinc-finger transcription factor Snail is enriched but not translated in cells treated with a potentially lethal dose of EtOH for 3 h. Once the EtOH is washed out, Snail mRNA is translated, which is required for anastasis (Sun et al., 2017).

Discovery of factors critical for anastasis could have important implications in disease. Radiation and chemotherapy for cancer induce apoptosis but are delivered transiently,

due to their toxicity. Therefore, if even a fraction of tumor cells undergo anastasis in vivo during or after treatment, they could sow the seeds for relapse. Survival from caspase activation can also result in genetic instability and oncogenic transformation, suggesting that anastasis may contribute to tumor initiation (Cartwright et al., 2017; Liu et al., 2015; Pérez et al., 2017; Tang et al., 2012). In addition, HeLa cells that undergo anastasis first proliferate and then increase motility (Sun et al., 2017) (Figure 1), properties associated with tumor progression, raising the possibility that anastasis contributes to tumor initiation, progression, and/or relapse following therapy.

In contrast to the potentially harmful consequences of anastasis in cancer, in normal cells, especially those that are difficult to replace such as neurons or cardiomyocytes, anastasis could help preserve cells following transient injury. In support of this idea, cardiomyocytes appear to undergo anastasis in vivo following transient ischemia (Kenis et al., 2010). In another example, in a mouse model of tau-mediated neurodegeneration, overexpression of a mutant form of human tau protein triggers caspase-3 activation in neurons. Simultaneous live imaging of caspase-3 activity and tau tangles in the brains of these mice shows that cells with transient caspase activity can survive long term (de Calignon et al., 2010). While caspase-3 activation precedes tangle formation, the precise relationship between caspase-3 and tangles is not clear. The observation that the neurons survive caspase-3 activation, however, suggests that they may represent another example of in vivo anastasis, in the context of neurodegenerative disease.

Another example of in vivo anastasis is the surprising discovery of developmental anastasis (Ding et al., 2016), which occurs in rapidly growing Drosophila epithelia. A particularly clear example is found in the developing pupal notum, where live imaging reveals that mechanical crowding leads to caspase-3 activation in a subset of cells, only some of which go on to die by apoptosis (Levayer et al., 2016). This finding is consistent with the idea that, rather than a single, all-or-none event, different rates and levels of caspase-3 activation likely influence whether a cell ultimately dies or retains the capacity to recover.

In a possibly related process, when a limited population of mitochondria permeabilize in a process termed minority MOMP, sublethal caspase activation occurs, promoting transformation and tumorigenesis (Ichim et al., 2015). However, minority MOMP does not cause sufficient caspase activation to result in the morphological hallmarks of apoptosis. Therefore, while both anastasis and minority MOMP can lead to survival of cells with DNA damage and oncogenic transformation, additional work is required to establish the mechanistic similarities and differences.

Resuscitation: Reversing Necroptosis

Human colon cancer cells (HT-29 cells), NIH3T3 cells, and Jurkat cells can reverse and survive necroptosis in a process termed resuscitation (Gong et al., 2017a; Zargarian et al., 2017). By controlling the activity of RIPK3 and MLKL, survival following necroptosis has been observed upon chemical inactivation of RIPK3 or MLKL (Gong et al., 2017a). These cells use ESCRT-III-mediated membrane repair to survive MLKL activation and

plasma membrane disruption (Gong et al., 2017a) (Figure 1). Recent work has reported that MLKL itself can regulate endosomal trafficking and extracellular vesicle generation (Yoon et al., 2017). Interestingly, this function of MLKL is RIPK3 independent and can result in the release of phosphorylated MLKL withholding necroptotic death (Yoon et al., 2017).

Both anastasis and resuscitation are processes that reverse cell death programs. To compare these processes at the molecular level, transcriptomes of cells undergoing anastasis versus resuscitation were evaluated. From this analysis, the processes appear to be mostly distinct, with the caveat that the transcriptomes are derived from different cell types (Gong et al., 2017b). Although there were more differences than similarities, both resuscitation and anastasis signatures show upregulated FGFR1, highlighting mitogenic signaling during both types of recovery (Gong et al., 2017b). Further research into the unique data sets will undoubtedly reveal new information about the mechanisms that control each of these processes and how they might be exploited therapeutically.

Autophagy as a Survival Mechanism in Normal Physiology

Although cells can die by ACD, the main function of autophagy is to promote cell survival during normal tissue homeostasis. The prosurvival function of autophagy is conserved from yeast to humans and plays an important role in adaptive metabolic responses to a variety of stresses, including nutrient deprivation, growth factor withdrawal, hypoxia, and infection (Kroemer et al., 2010). When cells lack essential nutrients, autolysosomal degradation of membrane lipids and proteins provides free macromolecules that can be

reused to generate energy and sustain protein synthesis (Rabinowitz and White, 2010). This recycling function of autophagy can preserve life during starvation. For example, in the mammalian liver, autophagy is activated during nutrient deficiency to produce glucose from amino acids to provide nutrients to the brain and erythrocytes (Ezaki et al., 2011).

In addition to autophagy playing a role in adaptive responses, basal levels of autophagy are seen in many cell types independently of nutrient status or stress. For example, in liver cells, selective turnover of specific cargos contributes to the basic hepatic functions of glyconeogenesis, gluconeogenesis, and β-oxidation (Singh et al., 2009). Basal autophagy helps maintain muscle mass and myofiber integrity, which protects against stress-induced muscle degeneration (Finn and Dice, 2006). Autophagy also serves an essential quality control function in cells by supporting nonselective turnover of cytoplasmic content and selective removal of damaged organelles such as mitochondria, large protein aggregates, and intracellular pathogens. In this way, autophagy promotes cell survival during aging or disease states (Kraft et al., 2010). However, autophagy also plays key roles in several pathological conditions, and its role in cancer progression can be especially complex, as described below.

Dysregulation of Cell Death and Survival in Cancer

Autophagy

Relative to normal cells, tumor cells can have high metabolic needs and experience oxygen and nutrient deficiencies as they enter new microenvironments, so enhancing autophagy can enable their survival (Rabinowitz and White, 2010). For example, tumors

experiencing hypoxia can stimulate adaptive autophagy through hypoxia-inducible factor 1 alpha (HIF1-α)-dependent activation of proapoptotic proteins that induce autophagy without triggering cell death (Mazure and Pouysségur, 2009). Similarly, under nutrient deprivation conditions, AMP kinase activates catabolic autophagy, which provides nutrients required for tumor survival (Kim et al., 2011).

Oncogenic mutations in K-Ras are common in a large percentage of poor-prognosis tumors, including lung, colon, and pancreatic cancers. Ras-driven cancers are notably addicted to autophagy, a process that likely promotes growth of the primary tumor, as well as survival after invasion, essential for metastasis (Guo et al., 2011, 2013; Lock et al., 2014; Yang et al., 2011). Expressing K-RasG12V or H-RasG12V activating mutations is sufficient to upregulate autophagy in cultured cells. Indeed, autophagy deficiency reduces growth of K-RasG12V-driven non–small cell lung carcinomas in genetically engineered mouse models (Guo et al., 2013). Autophagy deficiency actually diverts the tumors from adenomas and carcinomas to benign oncocytomas (Guo et al., 2013). These studies have suggested that blocking autophagy using chloroquine, an established antimalarial drug, could hold promise in treating these cancers. Clinical trials are under way to test this possibility (Manic et al., 2014).

Entosis

Entosis appears frequently in cancer, with a third of the cells in breast cancers showing internalized live cells (Kroemer and Perfettini, 2014; Overholtzer et al., 2007). Because the fate of an entosed cell can vary (Figure 1), entosis may either suppress or promote

tumor formation. Entosis may act as a tumor suppressor by internalizing and killing abnormally dividing cells and may account for another mechanism by which E-cadherin expression yields a better prognosis for tumors, since it is needed for entosis (Durgan et al., 2017; Sun et al., 2014) (Figure 1). However, entosis can also promote tumor formation, as entosed cells can interfere with cytokinesis of the host cell, leading to aneuploidy (Krajcovic et al., 2011). Entosed cancer cells may be able to survive and proliferate inside another cell during metabolic stress and starvation—conditions commonly seen in tumors. Entotic cell cannibalism also requires autophagic LC3 and lysosomal LAMP1, which could similarly release the contents of the digested entosed cell into the host cell, amplifying the latter cell's survival (Florey et al., 2011). Under such circumstances, autophagy may act as a potential mechanism to allow wild-type cells to acquire the tumorigenic properties of the entosed cancer cell, essentially non–cell autonomously spreading the tumor. Alternatively, entosis could allow tumor cells to internalize and replace wild-type cells and thus support tumor progression. Tumor cells are known to escape immune surveillance by a variety of mechanisms (Vinay et al., 2015). A large-scale survey of different cell types showed that heterotypic cell-in-cell structures are formed between a variety of tumor cell lines and immune cells, perhaps as a mechanism to escape immune attack (Chen et al., 2013). Entosed tumor cells can also emerge to live autonomously again (Figure 1). At this point, while entosis is a frequent hallmark in tumor pathology, what is not yet clear is whether it represents a way for the body to remove neoplastic cells or a way for tumors to spread and hide from the immune system. It is likely, as with many aspects of cancer, that both processes occur, thus limiting some cancers while promoting others.

Resisting Anoikis

Anoikis is an indispensable mechanism for maintaining tissue homeostasis by preventing cells from surviving at sites where they do not belong. Thus, resistance to anoikis is a critical step for tumor cell invasion (Frisch et al., 2013; Hanahan and Weinberg, 2011) and metastasis(Kim et al., 2012; Simpson et al., 2008) (Table 2). Cancer cells deploy several mechanisms to achieve anoikis resistance. Aside from using autophagy in response to metabolic stress to promote survival and resistance to anoikis (Fung et al., 2008), many aggressive cancers have adopted differential signaling to bypass anoikis and survive in places that normal cells cannot.

Many cancer cells aberrantly activate protein tyrosine kinases (PTKs) to escape anoikis (Gschwind et al., 2004), making them attractive targets for therapy. In particular, upregulation of epidermal growth factor receptor (EGFR) families plays an important role in overriding anoikis. Mammary epithelial cells that fail to grow on surfaces lacking ECM have reduced EGFR levels and increased levels of the proapoptotic protein Bim (Debnath et al., 2002; Reginato et al., 2005). Cancer cells that override anoikis, however, compensate for EGFR loss by either overexpressing ERBB2 (a member of the EGFR family) or activating the proto-oncogene Src, both of which suppress apoptosis by activating the ERK/MAPK pathway (Reginato et al., 2005). Additionally, ERBB2 can enable cell survival by stabilizing EGFR and β1 integrin, which usually degrade upon ECM detachment (Grassian et al., 2011). ERBB2 can also promote cell survival by upregulating α5 integrin, which activates Src (Haenssen et al., 2010) through regulation of HIFs (Whelan et al., 2013). Misregulated expression of another PTK, the insulin-like growth

factor 1 receptor, can also promote anoikis resistance by activating the PI3K/AKT pathway (Chen and Sharon, 2013; Dunn et al., 1998; Resnicoff et al., 1994). Other mechanisms of anoikis suppression include transforming growth factor β (TGF-β)-activated kinase 1–mediated WNT2 signaling in pancreatic circulating tumor cells (Yu et al., 2012) and stimulation of integrin-linked kinase activity in breast cancer cells (Attwell et al., 2000; Weigel et al., 2014).

Oncogenic mutations in K-Ras, HRas, or NRas not only increase autophagy, as described above, but also can upregulate survival signaling by constitutively activating PI3K/AKT signaling (Castellano and Downward, 2011), upregulating antiapoptotic Bcl-XL (Rosen et al., 2000), or downregulating caspase-2 (Yoo et al., 2011). Mutations in Raf kinases, downstream effectors of Ras, also promote survival upon matrix detachment through activation of PI3K or ERK pathways (Boisvert-Adamo and Aplin, 2006). Moreover, in cases in which extrusion signaling is inhibited, the lack of cell detachment from the matrix results in upregulation of focal adhesion kinase (FAK)—a kinase that is now being targeted in clinical trials of many cancers—and in chemotherapy resistance (Gu et al., 2015).

In contrast, Rho protein overexpression, seen in many human tumors, can have both positive and negative effects on anoikis (Sahai and Marshall, 2002). RhoG suppresses anoikis in HeLa cell lines in a PI3K-dependent manner (Yamaki et al., 2007). Yet RhoA and AKT prevent anoikis by activating FAK in B16F10 melanoma cells (Goundiam et al., 2012), and RhoA suppression in KRas-driven lung tumors also blocks anoikis (Ma et al.,

2007). Therefore, there may be discrepancies regarding RhoA roles in tumor cell survival, depending on the type of tumor or whether the studies are done in vivo or in culture. Another possibility is that Rho overrides anoikis by changing the identity of the tumor cell, rather than merely its survival. An example is the epithelial-tomesenchymal transition (EMT), in which polarized epithelial cells adopt a mesenchymal phenotype with increased migration, invasiveness, and resistance to apoptosis. During EMT, loss of E-cadherin, activation of TGF-β signaling via the transcription factors Twist and Snail, and N-cadherin expression can lead to anoikis resistance and increased tumor invasiveness (Araki et al., 2011; Derksen et al., 2006; Diamond et al., 2008; Lamouille et al., 2014; Yang et al., 2004).

Basal Extrusion

For epithelia to maintain a constant barrier in the face of high rates of cell death and division, cells fated to die are first extruded by concerted contraction of their neighboring cells. When cells extrude, the direction in which the cell extrudes determines its fate. Typically, in vertebrates, cells extrude apically into a lumen (Figure 2). Because the apically extruded cells detach from the matrix, which provides survival signaling, they die by anoikis. Extrusion is the chief mechanism by which epithelial cells apoptose, and thus extrusion may be thought of as tumor suppressive. However, in some instances, cells can extrude basally beneath the epithelial sheet (Figure 2), allowing them to take on different fates.

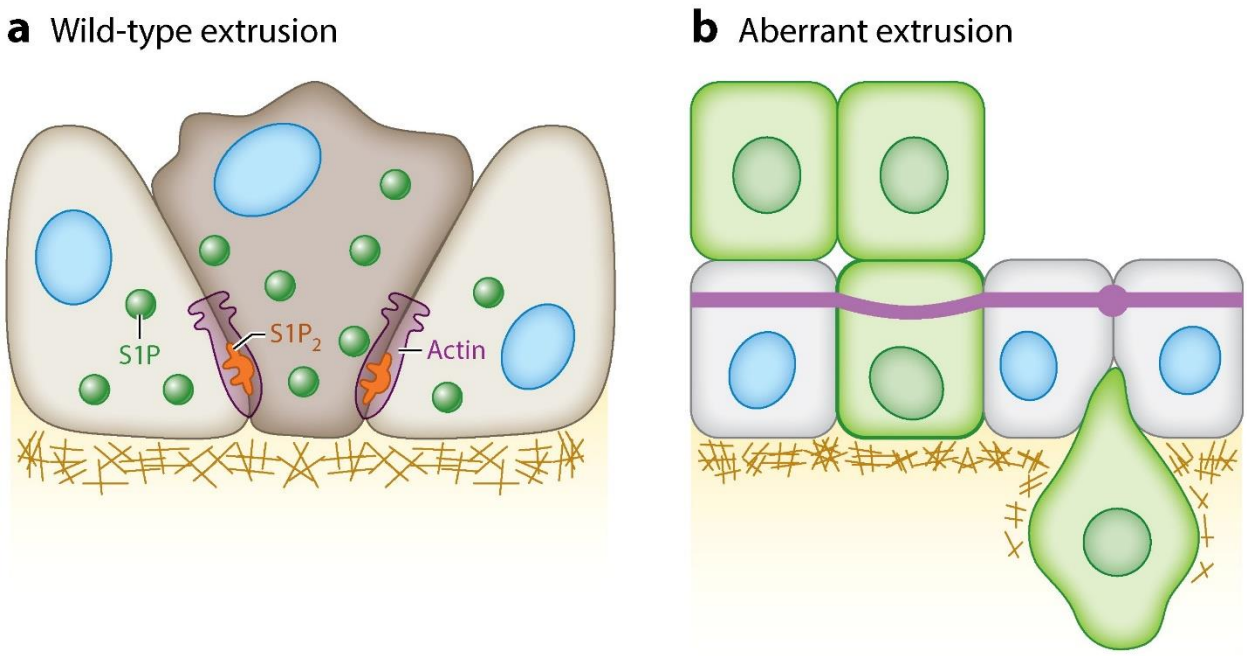

Figure 2. Extrusion removes epithelial cells in response to crowding forces during homeostasis or apoptotic stimuli. (*a*) During apoptotic apical extrusion, the cell destined to die produces the bioactive lipid sphingosine-1-phosphate (S1P), which binds to the sphingosine-1-phosphate 2 ($S1P_2$) receptor in the neighboring cells to activate actomyosin contraction and squeeze the extruding cell out. These cells then die by anoikis or death due to loss of matrix-dependent survival signaling. (*b*) Disruption of apical extrusion signaling in epithelial cells (*green; normal cells are shown in gray*) can lead to formation of masses at sites where cells should have extruded and died and to basal extrusion, which enables invasion and initiation of metastasis. Oncogenic mutations in K-Ras and APC, and downregulation of $S1P_2$, disrupt apical extrusion and may account for the chemoresistance and highly invasive nature of pancreatic, lung, and colon tumors driven by these mutations.

A class of oncogenic mutations (in K-Ras, APC, and S1P2) that drive aggressive, invasive cancers can hijack the apical extrusion pathway, causing cells normally fated for apoptosis to either accumulate in masses or extrude basally (Table 2, Figure 2). Basal extrusion of transformed cells may enable invasion and metastasis to other sites in the body. Each of these mutations appears to target different key signals in the apical extrusion pathway: APC truncation mutations disrupt S1P trafficking to neighboring cells (Marshall et al., 2011); unknown mechanisms in pancreatic, lung, and colon cancer epigenetically downregulate the S1P2 receptor essential for extrusion (Gu et al., 2015); and K-RasG12V causes lysosomal degradation of S1P through increased autophagy (Slattum and Rosenblatt, 2014; Slattum et al., 2014). Additionally, in K-RasG12V-driven pancreatic intraepithelial neoplasia mouse models, biallelic loss of the adherens junction protein P120 catenin causes extensive extrusion, both apically and basally (Hendley et al., 2016). The growing list of driver mutations of aggressive, invasive cancers that disrupt canonical apical extrusion suggests that extrusion is important not only for promoting apoptosis but also for preventing tumor invasion. Additionally, it suggests that epithelial cells expelled basally into the stroma may encounter enough survival signaling to avert anoikis or to change fate so as to become independent of the ECM for survival, as suggested above for EMT.

Summary and Open Questions

The discovery of programmed cell death pathways in normal development and disease, followed by the elucidation of biochemical and genetic mechanisms, raised hopes that antitumor therapies based on promoting tumor cell apoptosis would soon follow. The

complexities described here—multiple cell death pathways and the capacity of cells to resist death or recover from the brink of death—are one reason that therapies activating the core apoptosis machinery have limitations. Globally targeting canonical apoptotic mechanisms may not only fail to kill all tumor cells but may also eliminate beneficial cells, such as tumor-reactive T cells. The most recent successes in cancer therapy establish that selective cell killing is key. The power of anti-PDL1 therapy is that it enhances the immune response to tumors by rescuing tumor-reactive T cells from tumor-induced programmed cell death. This success underscores the importance of seeking therapies with better specificity, i.e., selectively targeting harmful cells while protecting beneficial cells.

We may be just beginning to understand the multifaceted tug of war between cell death and survival. Many questions remain unanswered. For example, under physiological conditions, how are only some types of cells targeted to die, and what protects surrounding cells? What sets the rate of turnover in different tissues? How does the microenvironment influence homeostatic cell death, and how do tumor cells manage to survive under these conditions? What are the true points of no return, if any, in the various cell death programs? What are the mechanisms by which cells reverse death processes to survive? Understanding how cell death and survival processes are controlled and intersect normally may yield insights into their roles in cancer and into the development of effective and cell type–specific combination therapies.

Summary Points

1. In addition to apoptosis, ACD, anoikis, and necrosis, unconventional, biochemically distinct forms of cell death have been discovered. These include regulated forms of necrosis, including pyroptosis, necroptosis, ferroptosis, and parthanatos, as well as cornification, NETosis, linker cell death, phagoptosis, and entosis.

2. Apical extrusion is an important mechanism that protects epithelial barrier function by removing apoptotic cells and preventing gaps in the epithelium. Importantly, extrusion also drives cell death during normal epithelial turnover. When epithelial monolayers become too crowded, they extrude live cells that go on to die by anoikis, which is a specific form of apoptosis.

3. Cells can recover from the brink of apoptotic cell death, even after executioner caspase activation, in a process termed anastasis, which is a Greek term meaning rising to life.

4. Necroptosis is an important immune-promoting cell death response, but its activation by RIPK3 and MLKL is not always sufficient to kill a cell. ESCRT-III complexes can act with MLKL to repair and maintain plasma membrane integrity, allowing for cell survival in a process termed necroptosis resuscitation.

5. The prosurvival function of autophagy is essential for homeostatic turnover of selective cargo and for metabolic response to a variety of stresses. However, tumor cells that have high metabolic needs upregulate adaptive autophagy to survive transient oxygen and nutrient deficiencies as they move to new microenvironments.6. Anoikis is an important mechanism to prevent cells from surviving at sites where they do not belong. Thus, resistance to anoikis is a critical step for tumor cell invasion, and many aggressive cancers adopt differential signaling mechanisms to override anoikis and to survive in places where normal cells cannot.

6. Because extrusion is the chief mechanism by which epithelial cells die, extrusion can be considered a tumor-suppressive mechanism. However, basal extrusion can permit survival. Oncogenic mutations that drive aggressive cancers can hijack the homeostatic apical extrusion pathway, override anoikis, and allow cells to accumulate in masses or escape by extruding basally and to survive.

Acknowledgements

We apologize to any authors whose work could not be cited due to space limitations. We would like to thank Sophie Nebeker for the figure illustrations.

Literature Cited

Abdelwahid E, Pelliniemi LJ, Jokinen E. 2002. Cell death and differentiation in the development of the endocardial cushion of the embryonic heart. *Microsc. Res. Tech.* 58(5):395–403

Abraham MC, Lu Y, Shaham S. 2007. A morphologically conserved nonapoptotic program promotes linker cell death in *Caenorhabditis elegans. Dev. Cell* 12(1):73–86

Andrade D, Rosenblatt J. 2011. Apoptotic regulation of epithelial cellular extrusion. *Apoptosis Int. J. Program. Cell Death* 16(5):491–501

Araki K, Shimura T, Suzuki H, Tsutsumi S, Wada W, et al. 2011. E/N-cadherin switch mediates cancer progression via TGF-β-induced epithelial-to-mesenchymal transition in extrahepatic cholangiocarcinoma.*Br. J. Cancer* 105(12):1885–93

Ashkenazi A, Salvesen G. 2014. Regulated cell death: signaling and mechanisms. *Annu. Rev. Cell Dev. Biol.* 30:337–56

Attwell S, Roskelley C, Dedhar S. 2000. The integrin-linked kinase (ILK) suppresses anoikis. *Oncogene* 19(33):3811–15

Bergsbaken T, Fink SL, Cookson BT. 2009. Pyroptosis: host cell death and inflammation.*Nat. Rev. Microbiol.*7(2):99–109

Berry DL, Baehrecke EH. 2008. Autophagy functions in programmed cell death. *Autophagy* 4(3):359–60

Boisvert-Adamo K, Aplin AE. 2006. B-RAF and PI-3 kinase signaling protect melanoma cells from anoikis. *Oncogene* 25(35):4848–56

Brown GC, Neher JJ. 2012. Eaten alive! Cell death by primary phagocytosis: “phagoptosis.” *Trends Biochem. Sci.* 37(8):325–32

Bursch W. 2001. The autophagosomal-lysosomal compartment in programmed cell death. *Cell Death Differ*. 8(6):569–81

Cai Z, Jitkaew S, Zhao J, Chiang H-C, Choksi S, et al. 2013. Plasma membrane translocation of trimerized MLKL protein is required for TNF-induced necroptosis. *Nat. Cell Biol.* 16(1):55–65

Cartwright IM, Liu X, Zhou M, Li F, Li C-Y. 2017. Essential roles of Caspase-3 in facilitating Myc-induced genetic instability and carcinogenesis. *eLife* 6:e26371

Castellano E, Downward J. 2011. RAS interaction with PI3K: more than just another effector pathway. *Genes Cancer* 2(3):261–74

Chen HX, Sharon E. 2013. IGF-1R as an anti-cancer target—trials and tribulations. *Chin. J. Cancer* 32(5):242–52

Chen Y, Wang S, He M, Wang Y, Zhao H, et al. 2013. Prevalence of heterotypic tumor/immune cell-in-cell structure in vitro and in vivo leading to formation of aneuploidy. *PLOS ONE* 8(3):e59418

Cho Y, Challa S, Moquin D, Genga R, Ray TD, et al. 2009. Phosphorylation-driven assembly of the RIP1-RIP3 complex regulates programmed necrosis and virus-induced inflammation. *Cell* 137(6):1112–23

Coleman ML, Sahai EA, Yeo M, Bosch M, Dewar A, Olson MF. 2001. Membrane blebbing during apoptosis results from caspase-mediated activation of ROCK I. *Nat. Cell Biol.* 3(4):339–45

Cookson BT, Brennan MA. 2001. Pro-inflammatory programmed cell death. *Trends Microbiol*. 9(3):113–14

de Calignon A, Fox LM, Pitstick R, Carlson GA, Bacskai BJ, et al. 2010. Caspase activation precedes and leads to tangles. *Nature* 464(7292):1201–4

Debnath J, Mills KR, Collins NL, Reginato MJ, Muthuswamy SK, Brugge JS. 2002. The role of apoptosis in creating and maintaining luminal space within normal and oncogene-expressing mammary acini. *Cell* 111(1):29–40

Dekkers MPJ, Nikoletopoulou V, Barde Y-A. 2013. Death of developing neurons: new insights and implications for connectivity. *J. Cell Biol*. 203(3):385–93

Denton D, Nicolson S, Kumar S. 2012. Cell death by autophagy: facts and apparent artefacts. *Cell Death Differ*. 19(1):87–95

Denton D, Shravage B, Simin R, Mills K, Berry DL, et al. 2009. Autophagy, not apoptosis, is essential for midgut cell death in *Drosophila. Curr. Biol*. 19(20):1741–46

Derksen PWB, Liu X, Saridin F, van der Gulden H, Zevenhoven J, et al. 2006. Somatic inactivation of Ecadherin and p53 in mice leads to metastatic lobular mammary carcinoma through induction of anoikis resistance and angiogenesis. *Cancer Cell* 10(5):437–49

Diamond ME, Sun L, Ottaviano AJ, Joseph MJ, Munshi HG. 2008. Differential growth factor regulation of N-cadherin expression and motility in normal and malignant oral epithelium. *J. Cell Sci.* 121(Pt 13):2197–207

Ding AX, Sun G, Argaw YG, Wong JO, Easwaran S, Montell DJ. 2016. CasExpress reveals widespread and diverse patterns of cell survival of caspase-3 activation during development in vivo. *eLife* 5:e10936

Dixon SJ, Lemberg KM, Lamprecht MR, Skouta R, Zaitsev EM, et al. 2012. Ferroptosis: an iron-dependent form of nonapoptotic cell death. *Cell* 149(5):1060–72

Dong H, Strome SE, Salomao DR, Tamura H, Hirano F, et al. 2002. Tumor-associated B7-H1 promotes T-cell apoptosis: a potential mechanism of immune evasion. *Nat. Med.* 8(8):793–800

Dunn SE, Ehrlich M, Sharp NJ, Reiss K, Solomon G, et al. 1998. A dominant negative mutant of the insulinlike growth factor-I receptor inhibits the adhesion, invasion, and metastasis of breast cancer. *Cancer Res*. 58(15):3353–61

Durgan J, Tseng Y-Y, Hamann JC, Domart M-C, Collinson L, et al. 2017. Mitosis can drive cell cannibalism through entosis. *eLife* 6:e27134

Eckhart L, Lippens S, Tschachler E, Declercq W. 2013. Cell death by cornification. *Biochim. Biophys. Acta Mol. Cell Res.* 1833(12):3471–80

Eisenhoffer GT, Loftus PD, Yoshigi M, Otsuna H, Chien C-B, et al. 2012. Crowding induces live cell extrusion to maintain homeostatic cell numbers in epithelia. *Nature* 484(7395):546–49

Elgendy M, Sheridan C, Brumatti G, Martin SJ. 2011. Oncogenic Ras-induced expression of Noxa and Beclin-1 promotes autophagic cell death and limits clonogenic survival. *Mol. Cell* 42(1):23–35

Elmore S. 2007. Apoptosis: a review of programmed cell death. *Toxicol. Pathol.* 35(4):495–516

Ertao Z, Jianhui C, Kang W, Zhijun Y, Hui W, et al. 2016. Prognostic value of mixed lineage kinase domain–like protein expression in the survival of patients with gastric cancer. *Tumour Biol. J. Int. Soc. Oncodev. Biol. Med.* 37(10):13679–85

Ezaki J, Matsumoto N, Takeda-Ezaki M, Komatsu M, Takahashi K, et al. 2011. Liver autophagy contributes to the maintenance of blood glucose and amino acid levels. *Autophagy* 7(7):727–36

Feig C, Peter ME. 2007. How apoptosis got the immune system in shape. *Eur. J. Immunol.* 37(Suppl. 1):61–70

Finn PF, Dice JF. 2006. Proteolytic and lipolytic responses to starvation. *Nutrition* 22(7–8):830–44

Fisher SA, Langille BL, Srivastava D. 2000. Apoptosis during cardiovascular development. *Circ. Res.* 87(10):856–64

Florey O, Kim SE, Sandoval CP, Haynes CM, Overholtzer M. 2011. Autophagy machinery mediates macroendocytic processing and entotic cell death by targeting single membranes. *Nat. Cell Biol.* 13(11):1335–43

Frisch SM, Francis H. 1994. Disruption of epithelial cell-matrix interactions induces apoptosis. *J. Cell Biol.* 124(4):619–26

Frisch SM, Schaller M, Cieply B. 2013. Mechanisms that link the oncogenic epithelial-mesenchymal transition to suppression of anoikis. *J. Cell Sci.* 126(Pt 1):21–29

Fuchs Y, Steller H. 2011. Programmed cell death in animal development and disease. *Cell* 147(4):742–58

Fuchslocher Chico J, Saggau C, Adam D. 2017. Proteolytic control of regulated necrosis. *Biochim. Biophys.Acta Mol. Cell Res.* 1864(11, Part B):2147–61

Fung C, Lock R, Gao S, Salas E, Debnath J. 2008. Induction of autophagy during extracellular matrix detachment promotes cell survival. *Mol. Biol. Cell* 19(3):797–806

Galluzzi L, Bravo-San Pedro JM, Vitale I, Aaronson SA, Abrams JM, et al. 2015. Essential versus accessory aspects of cell death: recommendations of the NCCD 2015. *Cell Death Differ*. 22(1):58–73

Giusti C, Tresse E, Luciani M-F, Golstein P. 2009. Autophagic cell death: Analysis in *Dictyostelium. Biochim.Biophys. Acta* 1793(9):1422–31

Gong Y-N, Guy C, Crawford JC, Green DR. 2017a. Biological events and molecular signaling following MLKL activation during necroptosis. *Cell Cycle* 16(19):1748–60

Gong Y-N, Guy C, Olauson H, Becker JU, Yang M, et al. 2017b. ESCRT-III acts downstream of MLKL to regulate necroptotic cell death and its consequences. *Cell* 169(2):286–300.e16

Goundiam O, Nagel M-D, Vayssade M. 2012. Akt and RhoA inhibition promotes anoikis of aggregated B16F10 melanoma cells. *Cell Biol. Int.* 36(3):311–19

Grassian AR, Schafer ZT, Brugge JS. 2011. ErbB2 stabilizes epidermal growth factor receptor (EGFR) expression via Erk and Sprouty2 in extracellular matrix–detached cells. *J. Biol. Chem.* 286(1):79–90

Green D, Kroemer G. 1998. The central executioners of apoptosis: caspases or mitochondria? *Trends Cell Biol*. 8(7):267–71

Grootjans S, Vanden Berghe T, Vandenabeele P. 2017. Initiation and execution mechanisms of necroptosis: an overview. *Cell Death Differ*. 24(7):1184–95

Gschwind A, Fischer OM, Ullrich A. 2004. The discovery of receptor tyrosine kinases: targets for cancer therapy. *Nat. Rev. Cancer* 4(5):361–70

Gu Y, Forostyan T, Sabbadini R, Rosenblatt J. 2011. Epithelial cell extrusion requires the sphingosine-1-phosphate receptor 2 pathway. *J. Cell Biol.* 193(4):667–76

Gu Y, Shea J, Slattum G, Firpo MA, Alexander M, et al. 2015. Defective apical extrusion signaling contributes to aggressive tumor hallmarks. *eLife* 4:e04069

Guo JY, Chen H-Y, Mathew R, Fan J, Strohecker AM, et al. 2011. Activated Ras requires autophagy to maintain oxidative metabolism and tumorigenesis. *Genes Dev*. 25(5):460–70

Guo JY, Karsli-Uzunbas G, Mathew R, Aisner SC, Kamphorst JJ, et al. 2013. Autophagy suppresses progression of K-ras-induced lung tumors to oncocytomas and maintains lipid homeostasis. *Genes Dev*. 27(13):1447–61

Haenssen KK, Caldwell SA, Shahriari KS, Jackson SR, Whelan KA, et al. 2010. ErbB2 requires integrin α5 for anoikis resistance via Src regulation of receptor activity in human mammary epithelial cells. *J. Cell Sci.* 123(8):1373–82

Hanahan D, Weinberg RA. 2011. Hallmarks of cancer: the next generation. *Cell* 144(5):646–74

He W, Wan H, Hu L, Chen P, Wang X, et al. 2015. Gasdermin D is an executor of pyroptosis and required for interleukin-1βsecretion. *Cell Res*. 25(12):1285–98

Hendley AM, Wang YJ, Polireddy K, Alsina J, Ahmed I, et al. 2016. p120 catenin suppresses basal epithelial cell extrusion in invasive pancreatic neoplasia. *Cancer Res*. 76(11):3351–63

Ichim G, Lopez J, Ahmed SU, Muthalagu N, Giampazolias E, et al. 2015. Limited mitochondrial permeabilization causes DNA damage and genomic instability in the absence of cell death. *Mol. Cell* 57(5):860–72

Jorgensen I, Rayamajhi M, Miao EA. 2017. Programmed cell death as a defense against infection. *Nat. Rev. Immunol.* 17(3):151–64

Kaczmarek A, Vandenabeele P, Krysko DV. 2013. Necroptosis: the release of damage-associated molecular patterns and its physiological relevance. *Immunity* 38(2):209–23

Kaiser WJ, Upton JW, Mocarski ES. 2013. Viral modulation of programmed necrosis. *Curr. Opin. Virol.* 3(3):296–306

Kaur J, Debnath J. 2015. Autophagy at the crossroads of catabolism and anabolism. *Nat. Rev. Mol. Cell Biol.* 16(8):461–72

Kay RR. 1987. Cell differentiation in monolayers and the investigation of slime mold morphogens. *Methods Cell Biol*. 28:433–48

Kenis H, Zandbergen HR, Hofstra L, Petrov AD, Dumont EA, et al. 2010. Annexin A5 uptake in ischemic myocardium: demonstration of reversible phosphatidylserine externalization and feasibility of radionuclide imaging. *J. Nucl. Med.* 51(2):259–67

Kerr JF, Wyllie AH, Currie AR. 1972. Apoptosis: a basic biological phenomenon with wide-ranging implications in tissue kinetics. *Br. J. Cancer* 26(4):239–57

Kheloufi M, Boulanger CM, Codogno P, Rautou P-E. 2015. Autosis occurs in the liver of patients with severe anorexia nervosa. *Hepatology* 62(2):657–58

Kim YK, Mbonye U, Hokello J, Karn J. 2011. T-cell receptor signaling enhances transcriptional elongation from latent HIV proviruses by activating P-TEFb through an ERK-dependent pathway. *J. Mol. Biol.* 410(5):896–916

Kim Y-N, Koo KH, Sung JY, Yun U-J, Kim H. 2012. Anoikis resistance: an essential prerequisite for tumor metastasis. *Int. J. Cell Biol.* 2012:306879

Kolb R, Liu G-H, Janowski AM, Sutterwala FS, Zhang W. 2014. Inflammasomes in cancer: a double-edged sword. *Protein Cell* 5(1):12–20

Kraft C, Peter M, Hofmann K. 2010. Selective autophagy: ubiquitin-mediated recognition and beyond. *Nat. Cell Biol.* 12(9):836–41

Krajcovic M, Johnson NB, Sun Q, Normand G, Hoover N, et al. 2011. A non-genetic route to aneuploidy in human cancers. *Nat. Cell Biol.* 13(3):324–30

Kroemer G, Marino G, Levine B. 2010. Autophagy and the integrated stress response. *Mol. Cell* 40(2):280–93

Kroemer G, Perfettini J-L. 2014. Entosis, a key player in cancer cell competition. *Cell Res*. 24(11):1280–81

Lakhani SA. 2006. Caspases 3 and 7: key mediators of mitochondrial events of apoptosis. *Science* 311(5762):847–51

Lamouille S, Xu J, Derynck R. 2014. Molecular mechanisms of epithelial-mesenchymal transition. *Nat. Rev. Mol. Cell Biol.* 15(3):178–96

Lamy L, Ngo VN, Emre NCT, Shaffer AL, Yang Y, et al. 2013. Control of autophagic cell death by caspase-10 in multiple myeloma. *Cancer Cell* 23(4):435–49

Levayer R, Dupont C, Moreno E. 2016. Tissue crowding induces caspase-dependent competition for space. *Curr. Biol.* 26(5):670–77

Li Y, Sun X, Dey SK. 2015. Entosis allows timely elimination of the luminal epithelial barrier for embryo implantation. *Cell Rep*. 11(3):358–65

Lindsten T, Ross AJ, King A, Zong WX, Rathmell JC, et al. 2000. The combined functions of proapoptotic Bcl-2 family members Bak and Bax are essential for normal development of multiple tissues. *Mol. Cell* 6(6):1389–99

Liu X, He Y, Li F, Huang Q, Kato TA, et al. 2015. Caspase-3 promotes genetic instability and carcinogenesis. *Mol. Cell* 58(2):284–96

Liu X, Zhang Z, Ruan J, Pan Y, Magupalli VG, et al. 2016. Inflammasome-activated gasdermin D causes pyroptosis by forming membrane pores. *Nature* 535(7610):153–58

Liu Y, Levine B. 2015. Autosis and autophagic cell death: the dark side of autophagy. *Cell Death Differ*. 22(3):367–76

Liu Y, Shoji-Kawata S, Sumpter RM, Wei Y, Ginet V, et al. 2013. Autosis is a Na+, K+-ATPase-regulated form of cell death triggered by autophagy-inducing peptides, starvation, and hypoxia-ischemia. *PNAS* 110(51):20364–71

Lock R, Kenific CM, Leidal AM, Salas E, Debnath J. 2014. Autophagy-dependent production of secreted factors facilitates oncogenic RAS-driven invasion. *Cancer Discov*. 4(4):466–79

Luthi AU, Martin SJ. 2007. The CASBAH: a searchable database of caspase substrates. *Cell Death Differ*. 14(4):641–50

Ma S, Henson ES, Chen Y, Gibson SB. 2016. Ferroptosis is induced following siramesine and lapatinib treatment of breast cancer cells. *Cell Death Dis*. 7(7):e2307

Ma Z, Myers DP, Wu RF, Nwariaku FE, Terada LS. 2007. p66Shc mediates anoikis through Rho A. *J. Cell Biol.* 179(1):23–31

Malin JA, Kinet MJ, Abraham MC, Blum ES, Shaham S. 2016. Transcriptional control of non-apoptotic developmental cell death in *C. elegans. Cell Death Differ*. 23(12):1985–94

Man SM, Karki R, Kanneganti T-D. 2017. Molecular mechanisms and functions of pyroptosis, inflammatory caspases and inflammasomes in infectious diseases. *Immunol. Rev*. 277(1):61–75

Manic G, Obrist F, Kroemer G, Vitale I, Galluzzi L. 2014. Chloroquine and hydroxychloroquine for cancer therapy. *Mol. Cell. Oncol.* 1(1):e29911

Marshall TW, Lloyd IE, Delalande JM, Nathke I, Rosenblatt J. 2011. The tumor suppressor adenomatous polyposis coli controls the direction in which a cell extrudes from an epithelium. *Mol. Biol. Cell* 22(21):3962–70

Martin SJ, Green DR. 1995. Protease activation during apoptosis: death by a thousand cuts? *Cell* 82(3):349–52

Martin SJ, Reutelingsperger CP, McGahon AJ, Rader JA, van Schie RC, et al. 1995. Early redistribution of plasma membrane phosphatidylserine is a general feature of apoptosis regardless of the initiating stimulus: inhibition by overexpression of Bcl-2 and Abl. *J. Exp. Med.* 182(5):1545–56

Mazure NM, Pouyssegur J. 2009. Atypical BH3-domains of BNIP3 and BNIP3L lead to autophagy in hypoxia. *Autophagy* 5(6):868–69

Meghana C, Ramdas N, Hameed FM, Rao M, Shivashankar GV, Narasimha M. 2011. Integrin adhesion drives the emergent polarization of active cytoskeletal stresses to pattern cell delamination. *PNAS* 108(22):9107–12

Morris HR, Taylor GW, Masento MS, Jermyn KA, Kay RR. 1987. Chemical structure of the morphogen differentiation inducing factor from *Dictyostelium discoideum. Nature* 328(6133):811–14

Muller PAJ, Vousden KH. 2013. p53 mutations in cancer. *Nat. Cell Biol.* 15(1):2–8
Nakatogawa H, Suzuki K, Kamada Y, Ohsumi Y. 2009. Dynamics and diversity in autophagy mechanisms: lessons from yeast. *Nat. Rev. Mol. Cell Biol.* 10(7):458–67

Neher JJ, Neniskyte U, Brown GC. 2012. Primary phagocytosis of neurons by inflamed microglia: potential roles in neurodegeneration. *Front. Pharmacol.* 3:27

Overholtzer M, Mailleux AA, Mouneimne G, Normand G, Schnitt SJ, et al. 2007. A nonapoptotic cell death process, entosis, that occurs by cell-in-cell invasion. *Cell* 131(5):966–79

Perez E, Lindblad JL, Bergmann A. 2017. Tumor-promoting function of apoptotic caspases by an amplification loop involving ROS, macrophages and JNK in *Drosophila. eLife* 6:e26747

Peterson JS, Timmons AK, Mondragon AA, McCall K. 2015. The end of the beginning. *Curr. Top. Dev. Biol*. 114:93–119

Rabinowitz JD, White E. 2010. Autophagy and metabolism. *Science* 330(6009):1344–48
Reginato MJ, Mills KR, Becker EBE, Lynch DK, Bonni A, et al. 2005. Bim regulation of lumen formation in cultured mammary epithelial acini is targeted by oncogenes. *Mol. Cell. Biol.* 25(11):4591–601

Remijsen Q, Kuijpers TW, Wirawan E, Lippens S, Vandenabeele P, Vanden Berghe T. 2011. Dying for a cause: NETosis, mechanisms behind an antimicrobial cell death modality. *Cell Death Differ*. 18(4):581–88

Resnicoff M, Coppola D, Sell C, Rubin R, Ferrone S, Baserga R. 1994. Growth inhibition of human melanoma cells in nude mice by antisense strategies to the type 1 insulin-like growth factor receptor. *Cancer Res*. 54(18):4848–50

Rogers C, Fernandes-Alnemri T, Mayes L, Alnemri D, Cingolani G, Alnemri ES. 2017. Cleavage of DFNA5 by caspase-3 during apoptosis mediates progression to secondary necrotic/pyroptotic cell death. *Nat. Commun.* 8:14128

Roos WP, Thomas AD, Kaina B. 2015. DNA damage and the balance between survival and death in cancer biology. *Nat. Rev. Cancer* 16(1):20–33

Rosen K, Rak J, Leung T, Dean NM, Kerbel RS, Filmus J. 2000. Activated *ras* prevents downregulation of Bcl-XL triggered by detachment from the extracellular matrix: a mechanism of *ras*-induced resistance to anoikis in intestinal epithelial cells. *J. Cell Biol.* 149(2):447–56

Rosenblatt J, Raff MC, Cramer LP. 2001. An epithelial cell destined for apoptosis signals its neighbors to extrude it by an actin- and myosin-dependent mechanism. *Curr. Biol.* 11(23):1847–57

Ruan J, Mei L, Zhu Q, Shi G, Wang H. 2015. Mixed lineage kinase domain–like protein is a prognostic biomarker for cervical squamous cell cancer. *Int. J. Clin. Exp. Pathol.* 8(11):15035–38

Sahai E, Marshall CJ. 2002. RHO-GTPases and cancer. *Nat. Rev. Cancer* 2(2):133–42
Salvesen GS, Ashkenazi A. 2011. Snapshot: caspases. *Cell* 147(2):476.e1

Shimizu S, Kanaseki T, Mizushima N, Mizuta T, Arakawa-Kobayashi S, et al. 2004. Role of Bcl-2 family proteins in a non-apoptotic programmed cell death dependent on autophagy genes. *Nat. Cell Biol.* 6(12):1221–28

Silva MT, do Vale A, dos Santos NMN. 2008. Secondary necrosis in multicellular animals: an outcome of apoptosis with pathogenic implications. *Apoptosis Int. J. Program. Cell Death* 13(4):463–82

Simpson CD, Anyiwe K, Schimmer AD. 2008. Anoikis resistance and tumor metastasis. *Cancer Lett*. 272(2):177–85

Singh R, Kaushik S, Wang Y, Xiang Y, Novak I, et al. 2009. Autophagy regulates lipid metabolism. *Nature* 458(7242):1131–35

Slattum G, Gu Y, Sabbadini R, Rosenblatt J. 2014. Autophagy in oncogenic K-Ras promotes basal extrusion of epithelial cells by degrading S1P. *Curr. Biol.* 24(1):19–28

Slattum G, McGee KM, Rosenblatt J. 2009. P115 Rho GEF and microtubules decide the direction apoptotic cells extrude from an epithelium. *J. Cell Biol.* 186(5):693–702

Slattum GM, Rosenblatt J. 2014. Tumour cell invasion: an emerging role for basal epithelial cell extrusion. *Nat. Rev. Cancer* 14(7):495–501

Strilic B, Yang L, Albarran-Juarez J, Wachsmuth L, Han K, et al. 2016. Tumour-cell-induced endothelial cell necroptosis via death receptor 6 promotes metastasis. *Nature* 536(7615):215–18

Sun G, Guzman E, Balasanyan V, Conner CM, Wong K, et al. 2017. A molecular signature for anastasis, recovery from the brink of apoptotic cell death. *J. Cell Biol.* 216(10):3355–68

Sun G, Montell DJ. 2017. Q&A: Cellular near death experiences—what is anastasis? *BMC Biol*. 15(1):92

Sun L, Wang H, Wang Z, He S, Chen S, et al. 2012. Mixed lineage kinase domain–like protein mediates necrosis signaling downstream of RIP3 kinase. *Cell* 148(1–2):213–27

Sun Q, Cibas ES, Huang H, Hodgson L, Overholtzer M. 2014. Induction of entosis by epithelial cadherin expression. *Cell Res*. 24(11):1288–98

Tait SWG, Green DR. 2008. Caspase-independent cell death: leaving the set without the final cut. *Oncogene* 27(50):6452–61

Takeshige K, Baba M, Tsuboi S, Noda T, Ohsumi Y. 1992. Autophagy in yeast demonstrated with proteinase deficient mutants and conditions for its induction. *J. Cell Biol.* 119(2):301–11

Tang HL, Tang HM, Mak KH, Hu S, Wang SS, et al. 2012. Cell survival, DNA damage, and oncogenic transformation after a transient and reversible apoptotic response. *Mol. Biol. Cell* 23(12):2240–52

Taylor RC, Cullen SP, Martin SJ. 2008. Apoptosis: controlled demolition at the cellular level. *Nat. Rev. Mol. Cell Biol.* 9(3):231–41

Thi HTH, Hong S. 2017. Inflammasome as a therapeutic target for cancer prevention and treatment. *J. Cancer Prev.* 22(2):62–73

Tracy K, Baehrecke EH. 2013. The role of autophagy in *Drosophila* metamorphosis. *Curr. Top. Dev. Biol.* 103:101–25

Vanlangenakker N, Vanden Berghe T, Vandenabeele P. 2012. Many stimuli pull the necrotic trigger, an overview. *Cell Death Differ*. 19(1):75–86

Vaux DL. 2002. Apoptosis timeline. *Cell Death Differ*. 9(4):349–54

Vinay DS, Ryan EP, Pawelec G, Talib WH, Stagg J, et al. 2015. Immune evasion in cancer: mechanistic basis and therapeutic strategies. *Semin. Cancer Biol.* 35:S185–98

Wang H, Sun L, Su L, Rizo J, Liu L, et al. 2014. Mixed lineage kinase domain–like protein MLKL causes necrotic membrane disruption upon phosphorylation by RIP3. *Mol. Cell* 54(1):133–46

Weigel KJ, Jakimenko A, Conti BA, Chapman SE, Kaliney WJ, et al. 2014. CAF-secreted IGFBPs regulate breast cancer cell anoikis. *Mol. Cancer Res.* 12(6):855–66

Weinlich R, Oberst A, Beere HM, Green DR. 2017. Necroptosis in development, inflammation and disease. *Nat. Rev. Mol. Cell Biol.* 18(2):127–36

Whelan KA, Schwab LP, Karakashev SV, Franchetti L, Johannes GJ, et al. 2013. The oncogene HER2/neu (ERBB2) requires the hypoxia-inducible factor HIF-1 for mammary tumor growth and anoikis resistance. *J. Biol. Chem.* 288(22):15865–77

White E. 2012. Deconvoluting the context-dependent role for autophagy in cancer. *Nat. Rev. Cancer* 12(6):401–10

Willingham SB, Volkmer J-P, Gentles AJ, Sahoo D, Dalerba P, et al. 2012. The CD47-signal regulatory protein alpha (SIRPa) interaction is a therapeutic target for human solid tumors. *PNAS* 109(17):6662–67

Xie C, Ginet V, Sun Y, Koike M, Zhou K, et al. 2016. Neuroprotection by selective neuronal deletion of Atg7 in neonatal brain injury. *Autophagy* 12(2):410–23

Xie Y, Hou W, Song X, Yu Y, Huang J, et al. 2016. Ferroptosis: process and function. *Cell Death Differ*. 23(3):369–79

Yamaki N, Negishi M, Katoh H. 2007. RhoG regulates anoikis through a phosphatidylinositol 3-kinasedependent mechanism. *Exp. Cell Res.* 313(13):2821–32

Yang J, Mani SA, Donaher JL, Ramaswamy S, Itzykson RA, et al. 2004. Twist, a master regulator of morphogenesis, plays an essential role in tumor metastasis. *Cell* 117(7):927–39

Yang S, Wang X, Contino G, Liesa M, Sahin E, et al. 2011. Pancreatic cancers require autophagy for tumor growth. *Genes Dev*. 25(7):717–29

Yang WS, Sri Ramaratnam R, Welsch ME, Shimada K, Skouta R, et al. 2014. Regulation of ferroptotic cancer cell death by GPX4. *Cell* 156(1–2):317–31

Yip KW, Reed JC. 2008. Bcl-2 family proteins and cancer. *Oncogene* 27(50):6398–406

Yoo BH, Wang Y, Erdogan M, Sasazuki T, Shirasawa S, et al. 2011. Oncogenic *ras*-induced down-regulation of pro-apoptotic protease caspase-2 is required for malignant transformation of intestinal epithelial cells. *J. Biol. Chem.* 286(45):38894–903

Yoon S, Kovalenko A, Bogdanov K, Wallach D. 2017. MLKL, the protein that mediates necroptosis, also regulates endosomal trafficking and extracellular vesicle generation. *Immunity* 47(1):51–65.e7

Yu M, Ting DT, Stott SL, Wittner BS, Ozsolak F, et al. 2012. RNA sequencing of pancreatic circulating tumour cells implicates WNT signaling in metastasis. *Nature* 487(7408):510–13

Zargarian S, Shlomovitz I, Erlich Z, Hourizadeh A, Ofir-Birin Y, et al. 2017. Phosphatidylserine externalization, “necroptotic bodies” release, and phagocytosis during necroptosis. *PLOS Biol*. 15(6):e2002711

Zhang J, Yang Y,HeW, Sun L. 2016. Necrosome core machinery: MLKL. *Cell. Mol. Life Sci.* 73(11–12):2153–63

Zhu S, Zhang Q, Sun X, Zeh HJ, Lotze MT, et al. 2017. HSPA5 regulates ferroptotic cell death in cancer cells. *Cancer Res*. 77(8):2064–77

II. A Molecular Signature for Anastasis, Recovery from the Brink of Apoptotic Cell Death

©2017 Sun et al. Originally published in *Journal of Cell Biology*.

https://doi.org/10.1083/jcb.201706134

Gongping Sun, Elmer Guzman, Varuzhan Balasanyan, Christopher M. Conner, Kirsten Wong, Hongjun Robin Zhou, Kenneth S. Kosik, and Denise J. Montell

Preface

To characterize gene expression during anastasis, our lab published an RNA-seq data set on HeLa cells throughout ethanol (EtOH) exposure and recovery. In collaboration with the lab, I developed an anastasis protocol using the apoptosis inducer staurosporine (STS). This data is highlighted in figure 4 and supplemental video 3 (found online).

Abstract

During apoptosis, executioner caspase activity has been considered a point of no return. However, recent studies show that cells can survive caspase activation following transient apoptotic stimuli, a process called anastasis. To identify a molecular signature, we performed whole-transcriptome RNA sequencing of untreated, apoptotic, and recovering HeLa cells. We found that anastasis is an active, two-stage program. During the early stage, cells transition from growth-arrested to growing. In the late stage, HeLa cells change from proliferating to migratory. Recovering cells also exhibited prolonged elevation of proangiogenic factors. Strikingly, some early-recovery mRNAs, including

Snail, were elevated first during apoptosis, implying that dying cells poise to recover, even while under apoptotic stress. Snail was also required for recovery. This study reveals similarities in the anastasis genes, pathways, and cell behaviors to those activated in wound healing and identifies a repertoire of potential targets for therapeutic manipulation.

Introduction

Apoptosis is a cell suicide program that is conserved in multicellular organisms and functions to remove excess or damaged cells during development, regulation of the immune system, and stress (Elmore, 2007; Fuchs and Steller, 2011). Excessive apoptosis contributes to degenerative diseases, whereas blocking apoptosis can cause (Favaloro et al., 2012) or treat (Chen and Han, 2015) cancer. Apoptotic cells exhibit distinctive morphological changes (Kerr et al., 1972) caused by activation of proteases called caspases (Martin and Green, 1995; Kumar, 2007). Activation of executioner caspases is a necessary step during apoptosis (Kumar, 2007) and until recently was considered a point of no return (Green and Kroemer, 1998).

However, executioner caspase activation is not always sufficient to kill cells under apoptotic stress. For example, caspase 3 activation in cells treated with sublethal doses of radiation or chemicals does not cause morphological changes or death but rather allows cells to survive with caspase-dependent DNA damage that can result in oncogenic transformation (Lovric and Hawkins, 2010; Ichim et al., 2015; Liu et al., 2015). In addition, transient treatment of cells with lethal doses of certain apoptosis inducers causes

caspase 3 activation sufficient to cause apoptotic morphological changes, yet cells can survive after removing the toxin in a process called anastasis (Tang et al., 2012). Although most cells fully recover, a small fraction bear mutations and an even smaller fraction undergo oncogenic transformation. Cell survival after executioner caspase activation has also been reported in cardiac myocytes responding to transient ischemia, in neurons overexpressing Tau, and during normal Drosophila melanogaster development (de Calignon et al., 2010; Kenis et al., 2010; Ding et al., 2016; Levayer et al., 2016). Collectively, these studies suggest that cells can recover from the brink of apoptotic cell death and that this can salvage cells, limiting the permanent tissue damage that might otherwise be caused by a transient injury. However, the same process of anastasis in cancer cells might underlie recurrence after chemotherapy. Thus, defining the molecular changes occurring in cells undergoing this remarkable recovery from the brink of death is a critical step toward manipulating this survival mechanism for therapeutic benefit.

Results

Whole-transcriptome RNA sequencing (RNAseq) reveals that anastasis comprises two stages

To initiate apoptosis, we exposed HeLa cells to a 3-h treatment with EtOH, which was sufficient to induce cell shrinkage and membrane blebbing (Fig. 1, A and B). Removal of the EtOH by washing allowed a striking recovery to take place over the course of several hours, during which time ∼70% of the cells reattached to the culture matrix and spread out again (Fig. 1, C–G; and Video 1; Tang et al., 2012). 3 h of EtOH treatment was sufficient to cause activation of a fluorescent reporter of caspase 3 activity in ∼75% of the

cells (Fig. 1, H–J; and Video 2); cleavage of PARP1, which is a target of caspase 3/7 (Fig. 1 K); cleavage of caspase 9 (Fig. 1 L); and release of cytochrome *c* from mitochondria to the cytosol (Fig. 1 M). Therefore, EtOH activates the intrinsic apoptotic pathway. Inhibition of caspase activity blocked EtOH-induced cell death (Fig. 1 N).

To define anastasis at a molecular level, we performed RNAseq of untreated cells; apoptotic cells; and cells allowed to recover for 1, 2, 3, 4, 8, or 12 h (Fig. 1 O). These time points include and extend beyond the time needed for the major morphological changes, which appeared to be complete after 4 h (Fig. 1, A–F). Compared with untreated cells, 900–1,500 genes increased in abundance >1.5-fold at each time point, whereas 250–750 genes decreased >1.5-fold (false discovery rate [FDR] < 0.05; Fig. 1 P and Table S1). Well-characterized genes such as Fos, Jun, Klf4, and Snail were induced, as well as genes about which little is known, such as the long noncoding RNA LOC284454, a gene predicted to encode a deubiquitinating enzyme (OTUD1), a pseudokinase (TRIB1), and a phosphate carrier protein (SLC34A3).

We validated the expression patterns of 27 top-ranked differentially expressed (22 up-regulated and 5 down-regulated) genes using quantitative reverse transcription PCR (qRT-PCR). The results of RNAseq and qRT-PCR correlated well, with an R^2 of 0.89 (Fig. 1, Q–S; and Fig. S1).

Principal component analysis (PCA) of the RNAseq data showed that cells undergoing anastasis clustered into two distinct groups: one group composed of cells allowed to recover for 1–4 h and a second containing cells that recovered for 8 or 12 h. Both groups were also clearly different from apoptotic cells and untreated cells (Fig. 1 T). We therefore defined the first 4 h of recovery as the early stage and 8–12 h as the late stage.

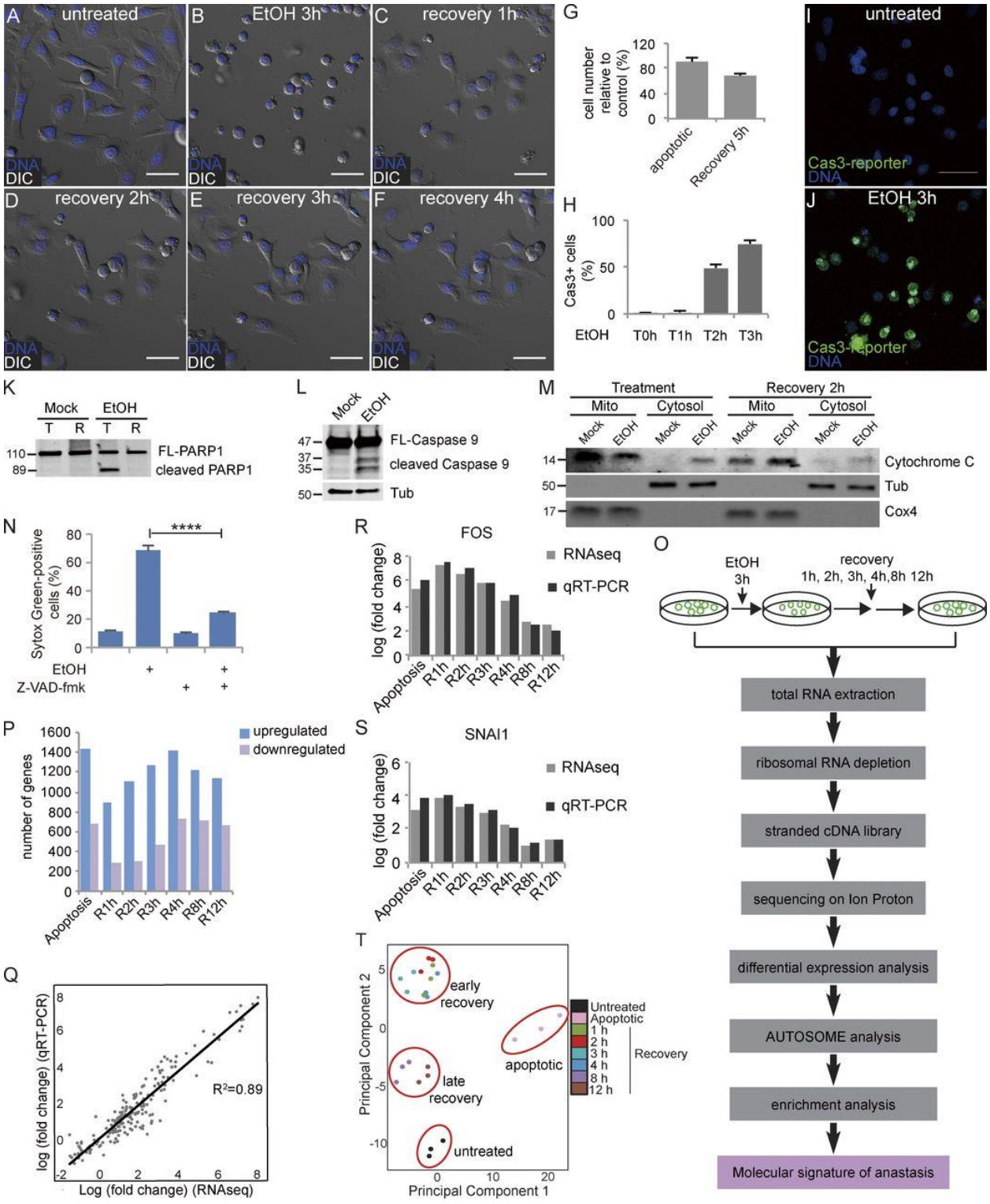
A untreated
B EtOH 3h
C recovery 1h
D recovery 2h
E recovery 3h
F recovery 4h
DNA
DIC
G
cell number relative to control (%)
120
80
40
0
apoptotic
Recovery 5h
H
Cas3+ cells (%)
100
50
0
EtOH
T0h
T1h
T2h
T3h
I untreated
Cas3-reporter
DNA
J EtOH 3h
Cas3-reporter
DNA
K
Mock
EtOH
T
R
T
R
110
89
FL-PARP1
cleaved PARP1
L
Mock
EtOH
47
37
35
50
FL-Caspase 9
cleaved Caspase 9
Tub
M
Treatment
Recovery 2h
Mito
Cytosol
Mito
Cytosol
Mock
EtOH
14
50
17
Cytochrome C
Tub
Cox4
N
Sytox Green-positive cells (%)
80
60
40
20
0
****
EtOH
Z-VAD-fmk
R
FOS
log (fold change)
8
6
4
2
0
RNAseq
qRT-PCR
Apoptosis
R1h
R2h
R3h
R4h
R8h
R12h
O
EtOH 3h
recovery 1h, 2h, 3h, 4h,8h 12h
total RNA extraction
ribosomal RNA depletion
stranded cDNA library
sequencing on Ion Proton
differential expression analysis
AUTOSOME analysis
enrichment analysis
Molecular signature of anastasis
P
number of genes
1600
1400
1200
1000
800
600
400
200
0
upregulated
downregulated
Apoptosis
R1h
R2h
R3h
R4h
R8h
R12h
S
SNAI1
log (fold change)
6
4
2
0
RNAseq
qRT-PCR
Apoptosis
R1h
R2h
R3h
R4h
R8h
R12h
Q
log (fold change) (qRT-PCR)
8
6
4
2
0
-2
0
2
4
6
8
R²=0.89
Log (fold change) (RNAseq)
T
Principal Component 2
5
0
-5
-10
early recovery
late recovery
apoptotic
untreated
0
10
20
Principal Component 1
Untreated
Apoptotic
1 h
2 h
3 h
4 h
8 h
12 h
Recovery

Figure 1. RNaseq defines anastasis as a two-stage, active process. (A–F) Time-lapse live imaging of HeLa cells before EtOH treatment (A), after 3 h of EtOH treatment (B), and after recovery for 1 h (C), 2 h (D), 3 h (E), and 4 h (F). (G) The ratio of the number of remaining cells immediately after washing away EtOH (apoptotic) or after 5 h of recovery to the number of cells after mock treatment (n = 3). (H) Quantification of the percentage of cells with active caspase 3 during EtOH treatment (n = 5). In G and H, error bars represent the standard error of the mean. (I and J) Caspase 3 activity (green fluorescence) in the same group of cells before (I) and after (J) 3 h of EtOH treatment. DAPI staining is shown in blue in A–F and I and J. Bars, 50 μm. (K) Western blots of full-length PARP1 (FL-PARP1) and cleaved PARP1 in cells after 3 h of mock or EtOH treatment (T) followed by 21 h of recovery (R). (L) Western blots of full-length caspase 9 (FL-Caspase 9) and cleaved caspase 9 in cells with or without EtOH treatment. (M) The level of cytochrome c in mitochondria (mito) and cytosol of cells with mock or EtOH treatment and of cells at 2 h of recovery after mock or EtOH treatment. Tubulin (Tub) was used as the control for the cytosol fraction, and Cox4 was used as the control for mitochondria. (N) The percentage of SYTOX Green–positive cells (dead cells) in cells with indicated treatment. Error bars represent the standard error of the mean. ****, $P < 0.0001$. (O) The workflow of RNAseq experiments. (P) Numbers of up-regulated and down-regulated genes in apoptotic cells and cells after 1, 2, 3, 4, 8, and 12 h of recovery compared with untreated cells (fold change > 1.5; FDR < 0.05). (Q) Correlation of RNAseq and qRT-PCR data for 27 genes. (R and S) Comparison of the changes in levels of FOS (R) and SNAI1 (S) mRNAs over time detected by RNAseq and qRT-PCR. In Q–S, fold change is compared with the expression level in untreated cells. (T) PCA of RNAseq data reveals four clusters: untreated cells, apoptotic cells, 1–4 h of recovery, and 8 and 12 h of recovery. Each color represents a different time point. Each time point was analyzed in triplicate.

Distinct features of early and late recovery

To compare the transcriptional profiles between early and late stages, we used the program AutoSOME (Newman and Cooper, 2010), which clusters genes according to similarities in their expression patterns over time (Table S2). This approach identified eight clusters containing a total of 1,172 genes up-regulated during early recovery and six clusters containing 759 genes up-regulated late (Table S3). We refer to these as early- and late-response genes, respectively (Fig. 2 A and Table S3). Gene ontology (GO) analysis revealed enrichment of expected categories such as “regulation of cell death” and “cellular response to stress” in the early response (Fig. 2 B). The GO term “transcription” was the most significantly enriched, indicating induction of transcription factors during initiation of anastasis (Fig. 2 B). The term “chromatin modification” was also enriched. Enrichment of early-response genes in “regulation of cell proliferation” and “regulation of cell cycle” terms suggested that removing apoptotic stress released cells from a growth-arrested state to reenter the cell cycle and proliferate (Fig. 2 B). Remarkably, the classes of early- and late-response genes were very different. The late response was enriched in posttranscriptional activities such as noncoding RNA processing and ribosome biogenesis (Fig. 2 B).

To identify pathways that are overrepresented in the early- and late-induced genes relative to untreated controls, we performed a pathway analysis based on the Kyoto Encyclopedia of Genes and Genomes (KEGG) database. Early-response genes were enriched in cell cycle and pro-survival pathways such as TGFβ, MAPK, and Wnt signaling (Fig. 2 C). The late response showed enrichment in general posttranscriptional pathways

such as ribosome biogenesis, RNA transport, protein processing, and endocytosis, as well as specific pathways such as focal adhesion and regulation of actin cytoskeleton (Fig. 2 C).

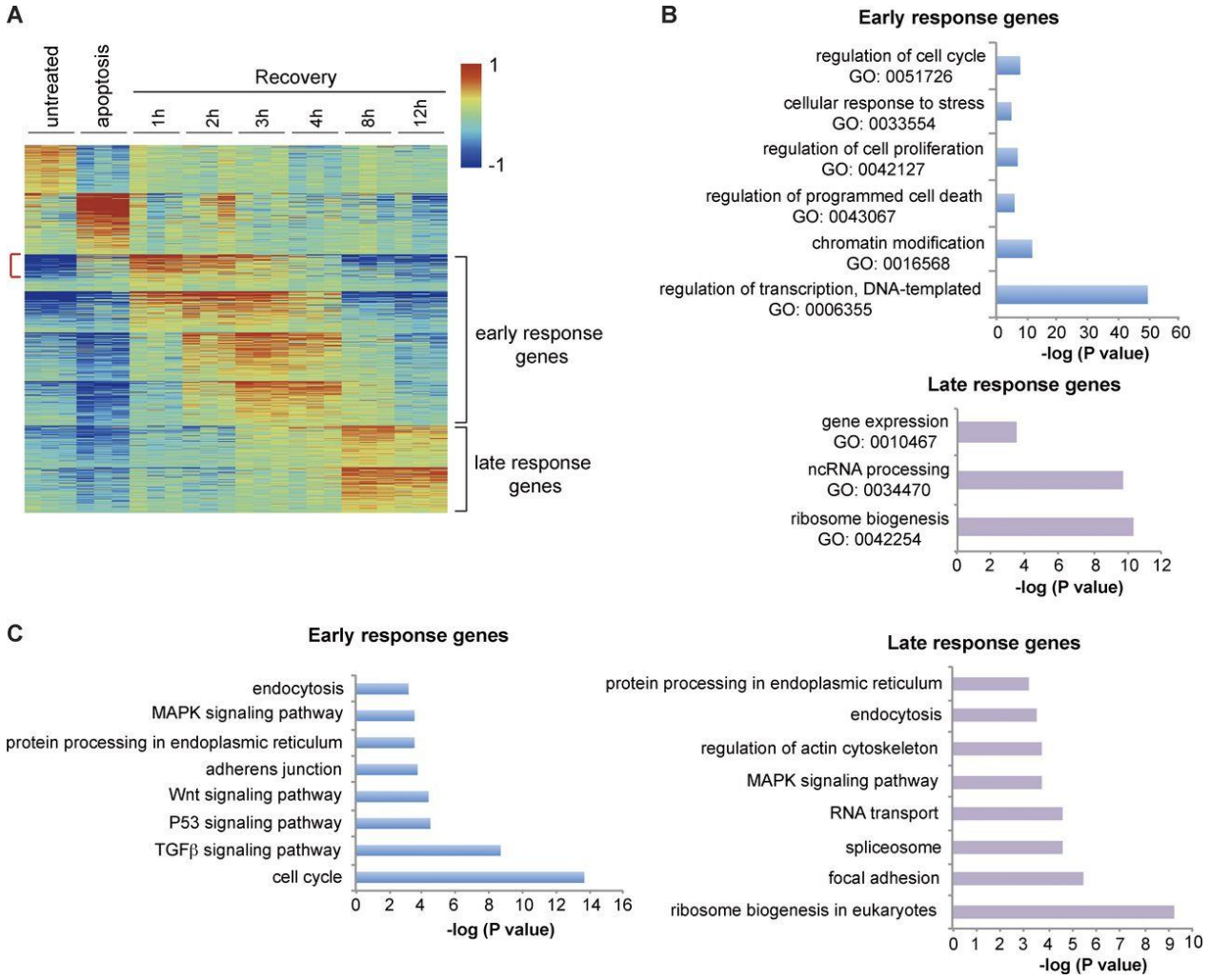

Figure 2. AutoSOME and enrichment analyses of early- and late-response genes. (A) AutoSOME analysis. Red indicates increases and blue indicates decreases in mRNA abundance. Genes most highly up-regulated during 1–4 h of recovery are defined as early-response genes, and those that peak at 8 or 12 h are defined as late-response genes. Red bracket points out the genes up-regulated in both apoptosis and early recovery. (B) GO enrichment analysis of early-response genes and late-response genes. (C) KEGG pathway enrichment analysis of early- and late-response genes. In B and C, the p-value is the Bonferroni p-value.

HeLa cells transition from proliferation to migration during anastasis

Consistent with enrichment of cell cycle and proliferation genes in the early response, cell numbers increased during the first 11 h of recovery (Fig. 3 A and Fig. S2), plateaued after 11 h, and began to increase again at ∼30 h. At even later time points (after replating), recovered cells exhibited a similar proliferation rate to control, mock-treated cells (Fig. 3 B).

Because of the enrichment of “focal adhesion” and “regulation of actin cytoskeleton” pathways in late-response gene clusters (Fig. 2 C), we hypothesized that cells might become migratory during the proliferation pause. To measure migration, we performed wound-healing assays. Scratch wounds made in monolayers of cells allowed to recover from EtOH treatment for 16 h closed faster than those in mock-treated monolayers (Fig. 3, C and D), even though they exhibited a lower cell number and a slightly slower proliferation rate (Fig. S3). In both mock-treated and EtOH-treated cells, those that migrated to fill the wound were more elongated than cells lagging behind (Fig. 3 E). A larger proportion of cells recovering from EtOH treatment showed this elongated morphology compared with mock-treated cells (Fig. 3, F and G), suggesting that this morphology might facilitate migration and wound closure.

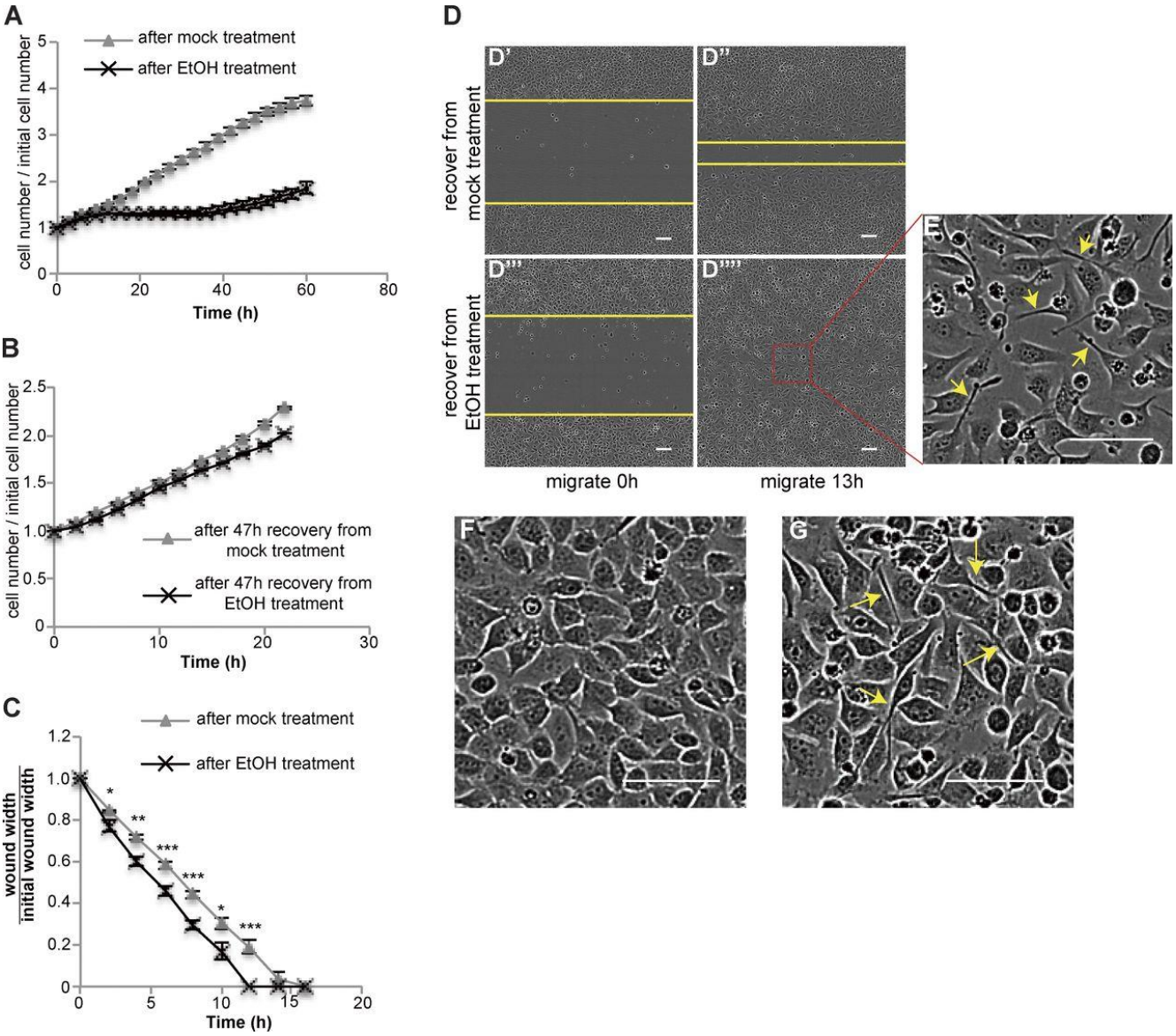

Figure 3. Cells transition from proliferation to migration during recovery. (A) Cell number during recovery after mock or EtOH treatment (n = 3). (B) Cells after 47 h of recovery from mock or EtOH treatment were trypsinized and replated at similar density. The curves show the change in the cell number over 22 h (n = 3). (C and D) Wound-healing assays. (C) Quantification of wound width over time (n = 8). The asterisks above each time point represent the statistical significance of the difference between cells after mock versus EtOH treatment. *, P < 0.05; **, P < 0.01; ***, P < 0.001; ****, P < 0.0001. (D) Images of wounds made in cells recovering from mock treatment (D' and D″) or EtOH treatment (D''' and D''''). The yellow lines mark the wound margins. (E) Magnified images of the outlined regions in D''''. (F and G) Images of confluent monolayers of cells recover from mock (F) or EtOH (G) treatment. In E and G, arrows point to elongated cells. In all plots, error bars represent the standard error of the mean. Bars, 100 µm.

Identification of the early-response genes common to multiple inducers and cell types

To identify which of the response genes induced during early recovery from EtOH treatment are common to recovery from other apoptotic inducers or in another cell line, we tested the expression of 69 top-ranked up-regulated early genes in H4 cells, a human glioma cell line, recovering from EtOH and in HeLa cells recovering from staurosporine (STS). Treatment of H4 cells with EtOH activated caspase 3, resulting in PARP1 cleavage (Fig. 4 A). Removal of EtOH after 4 h allowed 64% of the cells to recover (Fig. 4 B). 63 out of 69 genes were also up-regulated in H4 cells recovering from EtOH treatment (Fig. 4 C).

STS is a protein kinase inhibitor and a classic apoptosis inducer that activates the intrinsic pathway, as shown by cytochrome c release from mitochondria to cytosol, caspase 9 activation, and PARP1 cleavage (Fig. 4, D and E). As expected, inhibition of caspase blocked STS-induced cell death (Fig. 4 F). 76% of STS-treated cells recovered after removal of the drug (Fig. 4, G and H; and Video 3). 44 of 69 genes tested were up-regulated in cells recovering from STS (Fig. 4 C). GO analysis showed that the 44 genes up-regulated in both cells recovering from EtOH and cells recovering from STS were enriched in “regulation of transcription from RNA polymerase II promoter,” “regulation of cell cycle,” “response to stress,” and “blood vessel morphogenesis” (Fig. 4 I), similar to what we found using the full list of early-response genes in cells recovering from EtOH treatment (Fig. 2 B).

Both STS and EtOH induce apoptosis through the intrinsic pathway. To test if cells can survive apoptosis induced by extrinsic inducers, we treated HeLa cells stably expressing a caspase 3 reporter (HeLa-GC3AI) with TNFα and cycloheximide (CHX). Active caspase 3 induces a conformational change of the reporter, switching it from dark to green fluorescent (Zhang et al., 2013). As reported previously, cotreatment of TNFα and CHX induced caspase 8 activation and PARP1 cleavage and turned on the reporter (Fig. 4 J and Fig. S4). After washing away the TNFα and CHX, 5.6% of the caspase 3–positive cells recovered, possibly because of the poor reversibility of TNFα binding to its receptor. We tested the protein expression of Snail, one of the early-response genes, and found that GFP-positive cells that recovered contained a higher level of Snail (Fig. 4, K and L).

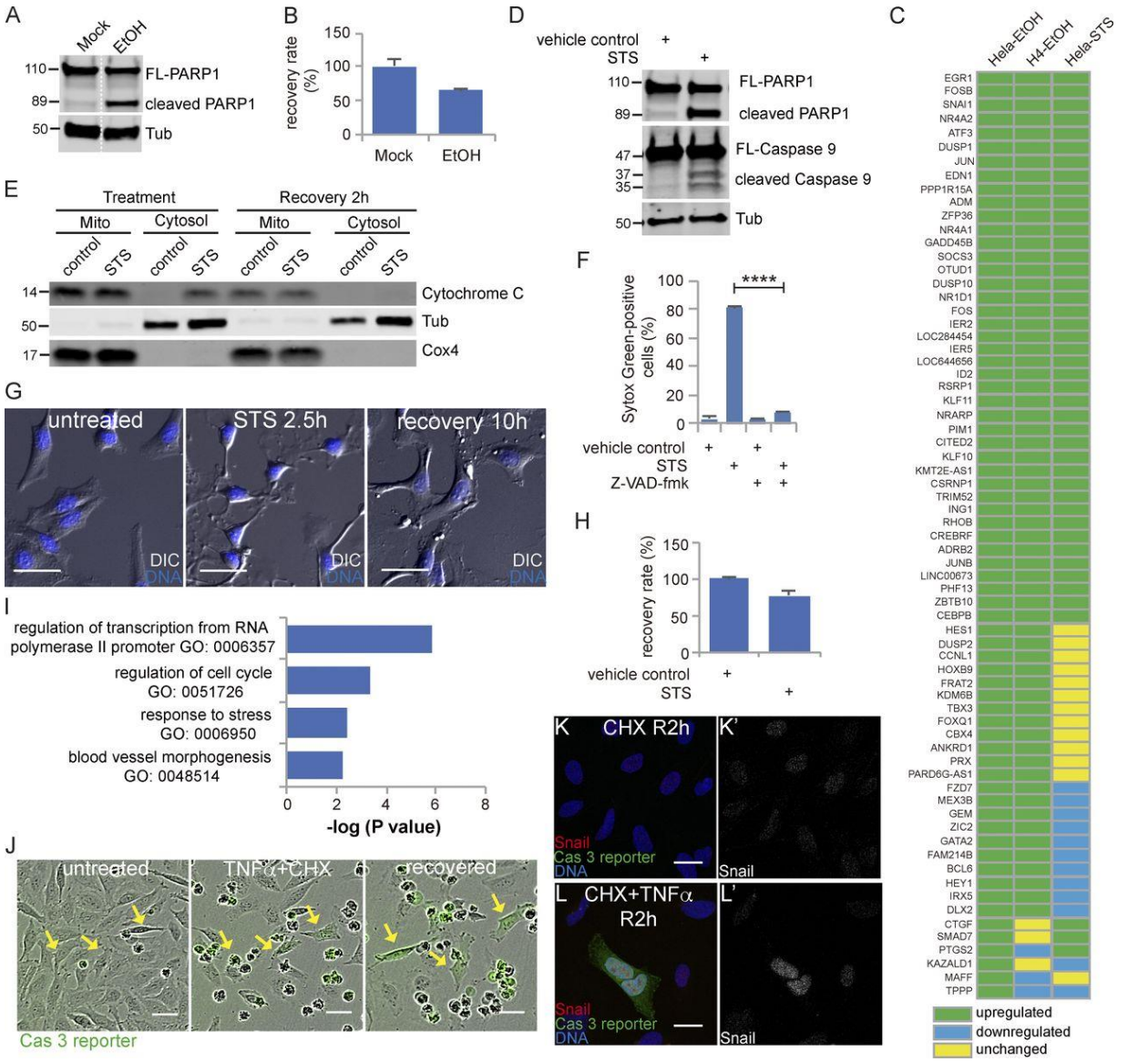

Figure 4. Identification of the early-response genes common to multiple inducers and cell types. (A) Western blots of full-length PARP1 (FL-PARP1) and cleaved PARP1 in H4 cells treated with or without 6.5% EtOH for 4 h. The white dotted line divides the lanes that were cropped from the same blot. (B) The percentage of recovering H4 cells after washing away EtOH. (C) The expression of the 69 top-ranking early-recovery genes in HeLa cells recovering from EtOH, H4 cells recovering from EtOH, and HeLa cells recovering from STS. Green: up-regulated compared with control; blue: down-regulated compared with control; yellow: unchanged compared with control. (D) Western blots of full-length PARP1 (FL-PARP1), cleaved PARP1, full-length caspase 9 (FL-Caspase 9), and cleaved caspase 9 in HeLa cells treated with 250 nM STS or 0.1% DMSO (vehicle control) for 2.5 h. (E) The level of cytochrome c in mitochondria (mito) and cytosol of cells with control or STS treatment and of cells at 2 h of recovery after control or STS treatment. Tubulin (Tub) was used as the control for the cytosol fraction, and Cox4 was used as the control for mitochondria. (F) The percentage of SYTOX Green–positive (dead) cells in cells with indicated treatment. ****, $P < 0.0001$. (G) Time-lapse live imaging of HeLa cells before STS treatment (untreated), after STS treatment (STS 2.5 h), and after recovery for 10 h (recovery 10 h). DNA is stained in blue. Bars, 50 μm. (H) The percentage of recovering HeLa cells after washing away STS. In B, F, and H, error bars represent the standard error of the mean. (I) GO enrichment analysis of common genes. (J) Time-lapse live imaging of HeLa-GC3AI cells before (untreated) and after treatment with TNFα together with CHX (TNFα + CHX) and cells after 12 h of recovery (recovered). Green indicates caspase 3 activity. Arrows point to cells recovered from caspase 3 activation induced by TNFα together with CHX. Bars, 50 μm. (K and L) Snail expression in cells after 2 h of recovery from CHX alone (K) and from TNFα together with CHX (L). Snail is shown in red, caspase 3 reporter is shown in green, and DNA is shown in blue. K' and L' show Snail signal only. Bars, 25 μm.

Recovery from apoptotic stress is distinct from recovery from autophagy

The observed enrichment of cell cycle components in the early response suggested that one facet of anastasis is reentry into the cell cycle after growth arrest during apoptosis. To distinguish which molecular features of anastasis were common to another type of growth arrest and recovery and to identify those more likely to be specific to anastasis, we evaluated the expression of the top-ranked, differentially expressed anastasis genes in cells undergoing recovery from nutrient deprivation. Nutrient deprivation induces growth arrest and autophagy, a process that can promote survival (Nikoletopoulou et al., 2013; Mariño et al., 2014). Autophagy results in degradation of cytoplasmic components in autophagosomes, which are double membrane–bound vesicles that sequester cytoplasm and fuse with lysosomes (Mariño et al., 2014). However, expression of autophagy genes was not induced during anastasis, suggesting that the two survival mechanisms differ. A time course showed that amino acid starvation for 2 h induced autophagy in HeLa cells, as shown by increased LC3 staining (Fig. 5, A–D), which is a marker for autophagosomes. LC3 staining is typically further augmented by blocking fusion between autophagsomes and lysosomes with bafilomycin A1 (Mizushima et al., 2010), and this was also true for nutrient-deprived HeLa cells (Fig. 5, A–D). 2 h of starvation did not induce caspase 3 activation (Fig. 5 E), although longer treatments did. Of the 24 genes up-regulated during anastasis that we tested, 10 were down-regulated or only slightly up-regulated during recovery from autophagy (Fig. 5, F–O). Thus, elevated transcription of these 10 genes distinguishes cells in early anastasis from those recovering from autophagy. Furthermore, cells recovering from autophagy showed no measurable difference in the rate of wound closure compared with that of mock-treated

cells (Fig. 5, P and Q). Thus, cells recovering from transient apoptotic stress exhibit both molecular and behavioral hallmarks that distinguish anastasis from recovery from other types of stress that induce growth arrest.

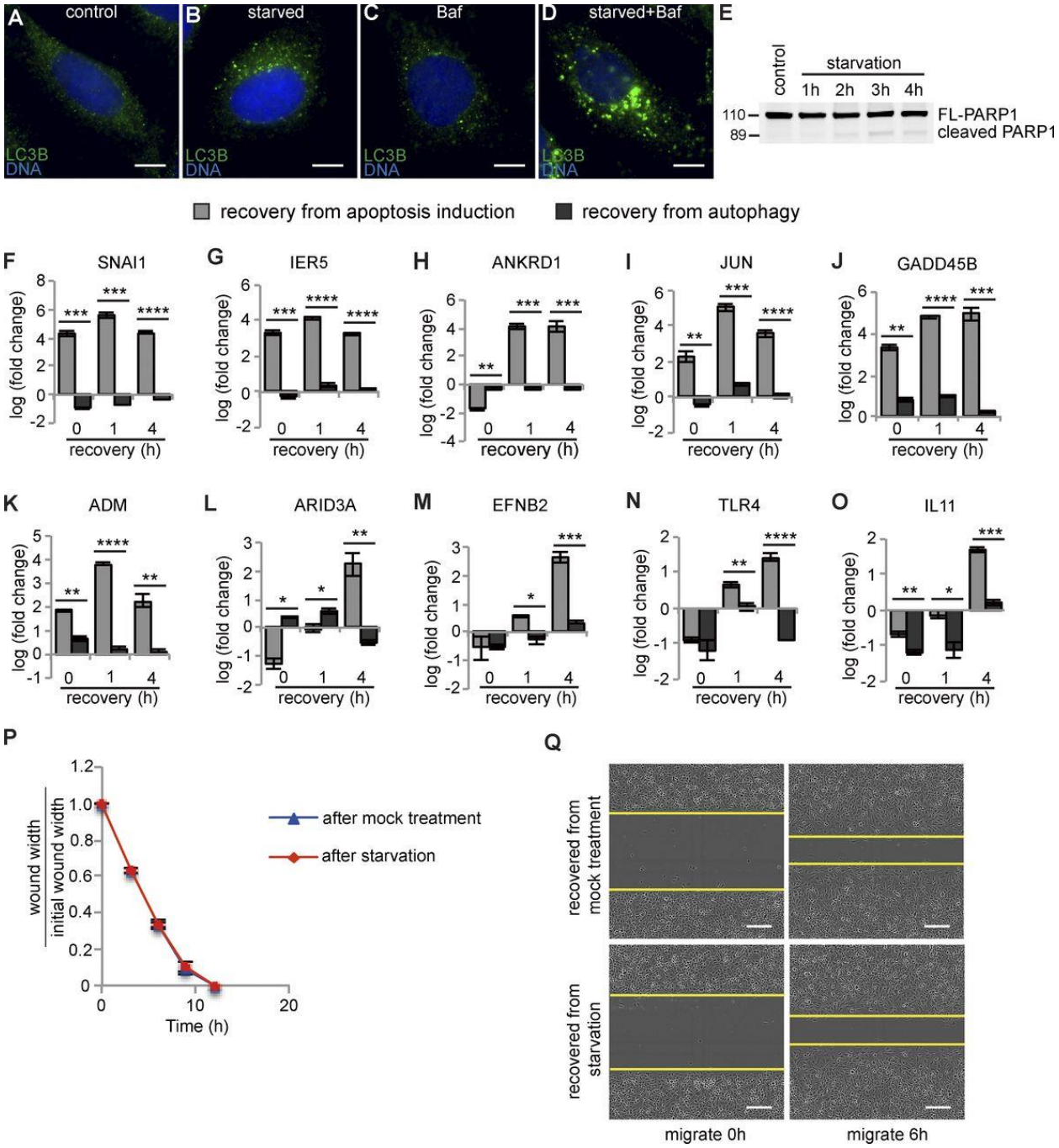

Figure 5. Comparison between anastasis and recovery from autophagy. (A–D) LC3B autophagosome marker staining (green) in cells incubated with growth medium containing 1% DMSO (control; A), HBSS containing 1% DMSO (B), growth medium containing 100 nM Bafilomycin A1 (C), or HBSS containing Bafilomycin A1 (D) for 2 h. Bars, 25 µm. (E) Western blot for PARP1 showing little cleavage during amino acid starvation. The 2-h time point was chosen for further studies. (F–O) Comparison between the mRNA levels of indicated genes after 0, 1, and 4 h of recovery from apoptosis induction (gray bars) or from autophagy (black bars). "Fold change" is compared with expression level of mock-treated cells. *, $P < 0.05$; **, $P < 0.01$; ***, $P < 0.001$; ****, $P < 0.0001$; $n = 3$. (P) Relative wound width over time in wound-healing assay ($n = 5$). (Q) Images of wounds made in cells recovering from mock treatment (upper two panels) or amino acid starvation (lower two panels). Yellow lines mark the margin of the wound. Bars, 200 µm. In all graphs, error bars represent the standard error of the mean.

Cells poise for recovery during apoptosis

The transcriptional profile of cells undergoing anastasis revealed an unknown feature of apoptotic cells that appears to contribute to the rapid transition to recovery. We noticed that transcripts corresponding to a subset of early-response genes that were induced during the first hour of anastasis were already elevated in abundance in apoptotic cells relative to untreated cells (Fig. 1, R and S; Fig. 2 A; and Fig. S1, A–G). One possible explanation is that these are genes that drive apoptosis and that apoptosis had not completely stopped 1 h after removal of the chemical stress. Alternatively, these could be genes encoding proteins that contribute to recovery, and cells prepare for the possibility of recovery even while caspase is activated. To distinguish between these opposing possibilities, we compared the levels of expression of 10 such early genes at 1 h of recovery after 3 h of EtOH treatment to the levels in cells left in EtOH for 4 h. The mRNA levels after 4 h of EtOH treatment were significantly lower than those at 1 h of recovery, indicating that accumulation of these mRNAs was associated with the survival response (Fig. 6, A–J). We analyzed the corresponding protein levels for five of the early-response targets for which antibodies were available. The protein levels remained unchanged or were slightly reduced during apoptosis (Fig. 6 K), suggesting that although the mRNAs accumulated, their translation was inhibited, consistent with prior observations of down-regulated protein synthesis in apoptotic cells (Liwak et al., 2012). This intriguing finding supports the idea that even during apoptosis, cells actually poise for recovery by synthesizing, or protecting from degradation, specific mRNAs encoding survival proteins, which are, however, not translated. If apoptotic stress persists, the mRNAs are degraded and the cells die. However, if the apoptotic stress disappears, cells are prepared to rapidly

synthesize survival proteins. This “poised for recovery” state may help to explain the rapid recovery after stress removal.

Snail knockdown impairs recovery

Snail is one of the mRNAs enriched in apoptotic cells and then highly induced in early recovery and has been reported to protect cells from apoptosis (Inukai et al., 1999; Metzstein and Horvitz, 1999; Franco et al., 2010; Wan et al., 2015). We found that Snail protein levels increased during recovery (Fig. 6 K). In addition, knocking down Snail expression by stably expressing shRNA reduced the endogenous Snail protein level (Fig. 7 A) and suppressed recovery from EtOH or STS treatment (Fig. 7, B and C). We also found increased PARP1 cleavage in Snail-depleted cells after EtOH or STS treatment (Fig. 7, A and D). Therefore, the poor recovery after Snail knockdown may result from enhanced caspase activation during treatment, impaired anastasis, or both.

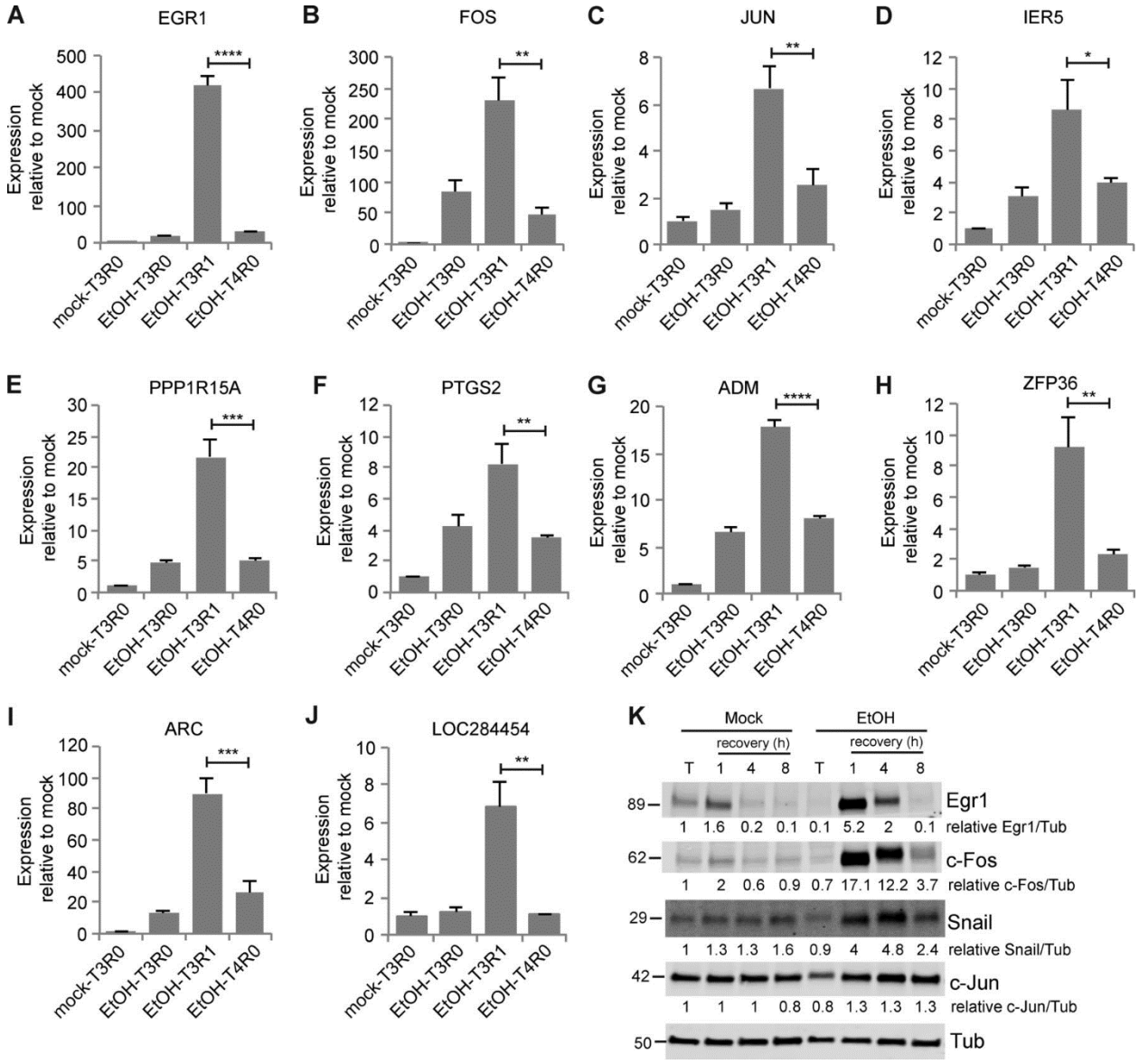

Figure 6. Apoptotic cells were poised for recovery. (A–J) mRNA levels of the indicated genes relative to mock-treated cells after 3 h of mock treatment (mock-T3R0), after 3 h of EtOH treatment (EtOH-T3R0), after 1 h of recovery from EtOH treatment (EtOH-T3R1), and after 4 h of EtOH treatment (EtOH-T4R0; n = 3). Error bars represent the standard error of the mean. Asterisks show statistical significance between EtOH-T3R1 and EtOH-T4R0. *, P < 0.05; **, P < 0.01; ***, P < 0.001; ****, P < 0.0001. (K) The protein levels of Egr1, c-Fos, c-Jun, and Snail of cells with mock or EtOH treatment (T) and of cells during recovery from mock treatment and EtOH treatment. The numbers below each blot are the normalized intensity of the bands.

Activation of TGFβ signaling contributes to Snail up-regulation and migration

One important upstream regulator of Snail is TGFβ signaling (Peinado et al., 2003), and this pathway was enriched in the early-recovery gene set. TGFβ signaling regulates transcription through phosphorylation and activation of the downstream transcription factors Smad2 and Smad3 (Massagué, 1998). Phosphorylation of Smad2/3 increased during apoptosis and in the first hour of recovery from EtOH treatment, then diminished after 4 h of recovery, indicating transient activation of TGFβ signaling (Fig. 7 E), which was also observed in HeLa cells recovering from STS treatment (Fig. 7 F).

To determine when and to what extent Snail induction depends on TGFβ signaling, we treated cells with the TGFβ receptor I–specific inhibitor LY364947. LY364947 did not affect basal cell survival or proliferation (Fig. S5 A). LY364947 also did not measurably affect Snail expression during EtOH treatment (Fig. 7 G). At 1 h of recovery, LY364947 treatment prevented induction of Snail mRNA and protein, reducing them to ∼40% of the control, and at 4 h, LY364947 eliminated Snail induction (Fig. 7, G and H). Whereas direct knockdown of Snail by shRNA decreased survival (Fig. 7, B and C), LY364947 treatment did not (Fig. S5, B and C), suggesting that the “poised” Snail is required at the earliest time points, before further induction by TGFβ. This is also consistent with the observation that dramatic transcriptional and morphological changes occur already within the first hour of recovery (Fig. 1, B–F and T).

We then tested whether the effect of TGFβ inhibition might occur later. TGFβ signaling activation can promote epithelial-to-mesenchymal transition (EMT) and cell migration (Xu

et al., 2009). To determine if the transient activation of TGFβ signaling was responsible for the increased migration later, we inhibited TGFβ signaling during apoptosis and the first 4 h of recovery and then tested cell migration using the wound-healing assay. LY364947 treatment reduced the mean migration speed of EtOH-treated cells from 45 to 37 μm/h while reducing the mean migration speed of mock-treated cells from 27 to 23 μm/h, suggesting that TGFβ signaling contributes to both basal motility and anastasis-induced migration in HeLa cells (Fig. 7 I). Interestingly, TGFβ signaling, Snail mRNA, and Snail protein were all down-regulated during autophagy and recovery (Fig. 5 F and Fig. 7 E). Recovery from autophagy did not stimulate cell migration (Fig. 5, P and Q). Thus, in HeLa cells, activation of TGFβ signaling, induction of Snail, and increased migration characterize the recovery from the brink of apoptotic cell death but not recovery from a nonapoptotic stress.

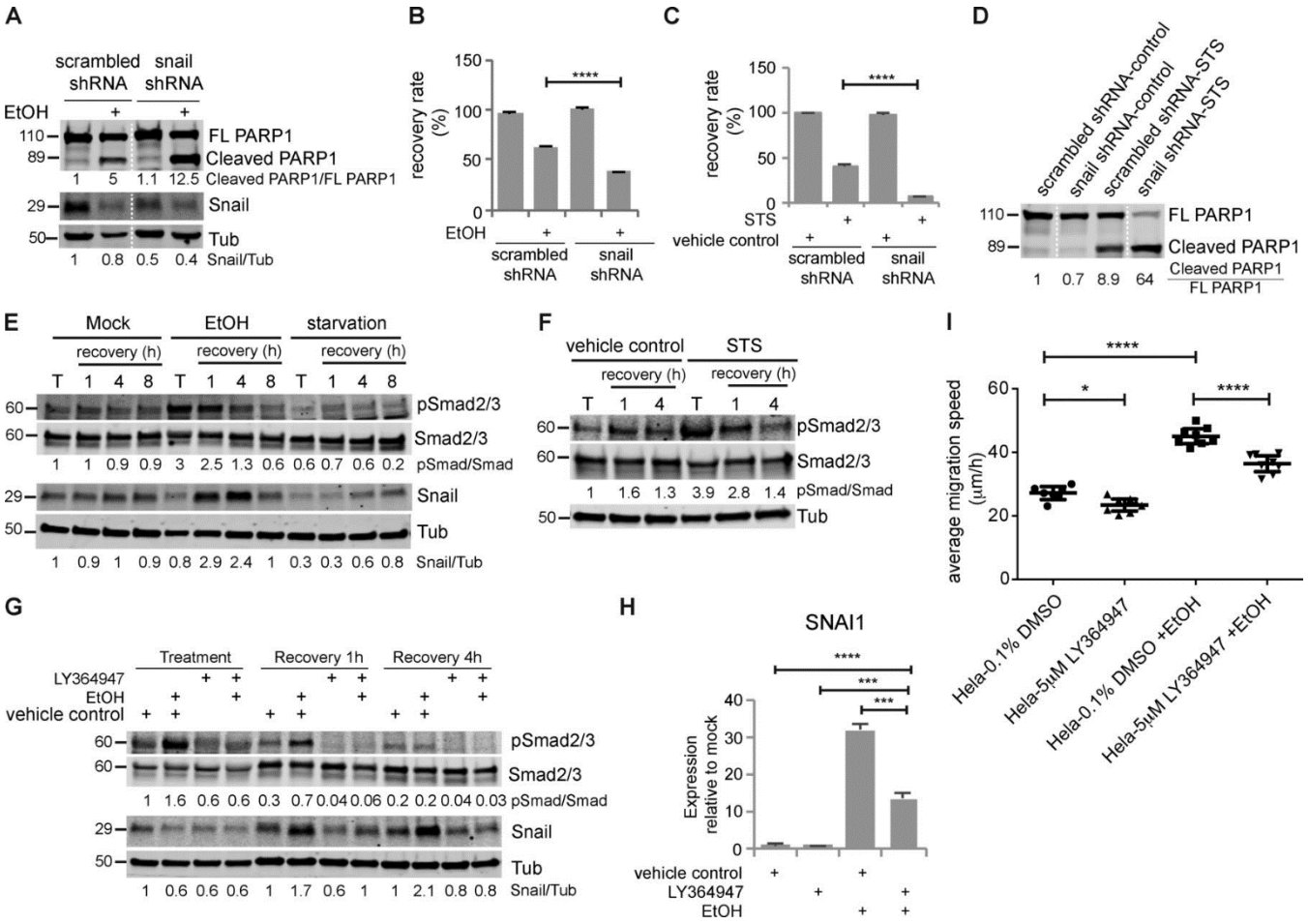

Figure 7. Transient activation of TGFβ signaling induced Snail up-regulation, which was required for anastasis, and caused increased migration in the late stage. (A) Cleavage of PARP1 and Snail protein in HeLa cells stably expressing scrambled shRNA or Snail shRNA treated with or without EtOH for 3 h. The white dotted line divides the lanes that were cropped from the same blot. (B) Recovery rate of HeLa-scrambled shRNA and HeLa-Snail shRNA cells after mock treatment or EtOH treatment (n = 3). (C) Recovery rate of HeLa-scrambled shRNA and HeLa-Snail shRNA cells after control treatment or STS treatment (n = 3). In all bar graphs, error bars represent the standard error of the mean. (D) Western blots of full-length PARP1 (FL PARP1) and cleaved PARP1 in HeLa-scrambled shRNA and HeLa-Snail shRNA cells treated with STS or control. The white dotted line divides the lanes that were cropped from the same blot. (E) Western blots of phosphor-Smad2/3 (pSmad2/3), total Smad2/3, Snail in cells after mock treatment, EtOH treatment, or starvation (T) and in cells recovering from these treatments (recovery). (F) The level of pSmad2/3 and Smad2/3 in HeLa cells treated with STS or vehicle control (T) and in cells recovering from STS or control treatment (recovery). (G) The level of pSmad2/3, Smad2/3, and Snail in apoptotic cells (treatment); cells after 1 h of recovery (recovery 1 h); and cells after 4 h of recovery (recovery 4 h). The addition of LY364497 and EtOH is indicated. The numbers under the blots are the intensity of the bands or the indicated ratio relative to the mock-treated sample. (H) The mRNA expression of Snail (SNAI1) after 1 h of recovery. The addition of LY364947 and EtOH is indicated. (I) Mean migration speed of the indicated group of cells during wound-healing assay (n = 8). Before wound-healing assay, cells were treated with or without EtOH together with 0.1% DMSO or 5 μM LY364947 for 3 h, followed by 4 h of recovery with 0.1% DMSO or 5 μM LY364947 and an additional 16 h of recovery without any inhibitor. Error bars represent 95% confidence interval. *, P < 0.05; **, P < 0.01; ***, P < 0.001; ****, P < 0.0001.

Induction of angiogenesis-related genes throughout recovery

Although TGFβ signaling and Snail expression were transiently elevated during early recovery, some angiogenesis-related genes were persistently elevated throughout the 12 h examined. Placenta growth factor (PGF) binds VEGF receptor (VEGFR) and stimulates endothelial cell proliferation and migration (De Falco, 2012). PGF was among the top 10 up-regulated genes at every time point during apoptosis and recovery (Table S1). PGF mRNA increased ~22-fold at 1 h of recovery, and even after 24 h of recovery, PGF mRNA was threefold higher in EtOH-treated cells compared with mock-treated cells (Fig. 8, A and B).

Ephrin and Ephrin receptor (EphR) signaling are also important in blood vessel development and angiogenesis (Salvucci and Tosato, 2012; Barquilla and Pasquale, 2015). Several EphRs (EPHA2, EPHB2, and EPHB4) and Ephrins (EFNB1, EFNB2) were up-regulated throughout recovery (Table S1). For example, expression of EFNB2 in the first hour of recovery was ~1.6-fold that of mock-treated cells and elevated approximately two- to threefold during 3–12 h of recovery (Fig. S1K). EPHA2 was significantly up-regulated after 24 h of recovery (Fig. 8 C). Sprouty 2 (SPRY2) is a common transcriptional target of VEGFR and EphR signaling (Cabrita and Christofori, 2008). SPRY2 expression was up-regulated from 4 to 24 h of recovery (Fig. 8, D–F), suggesting activation of VEGFR and EphR signaling during recovery.

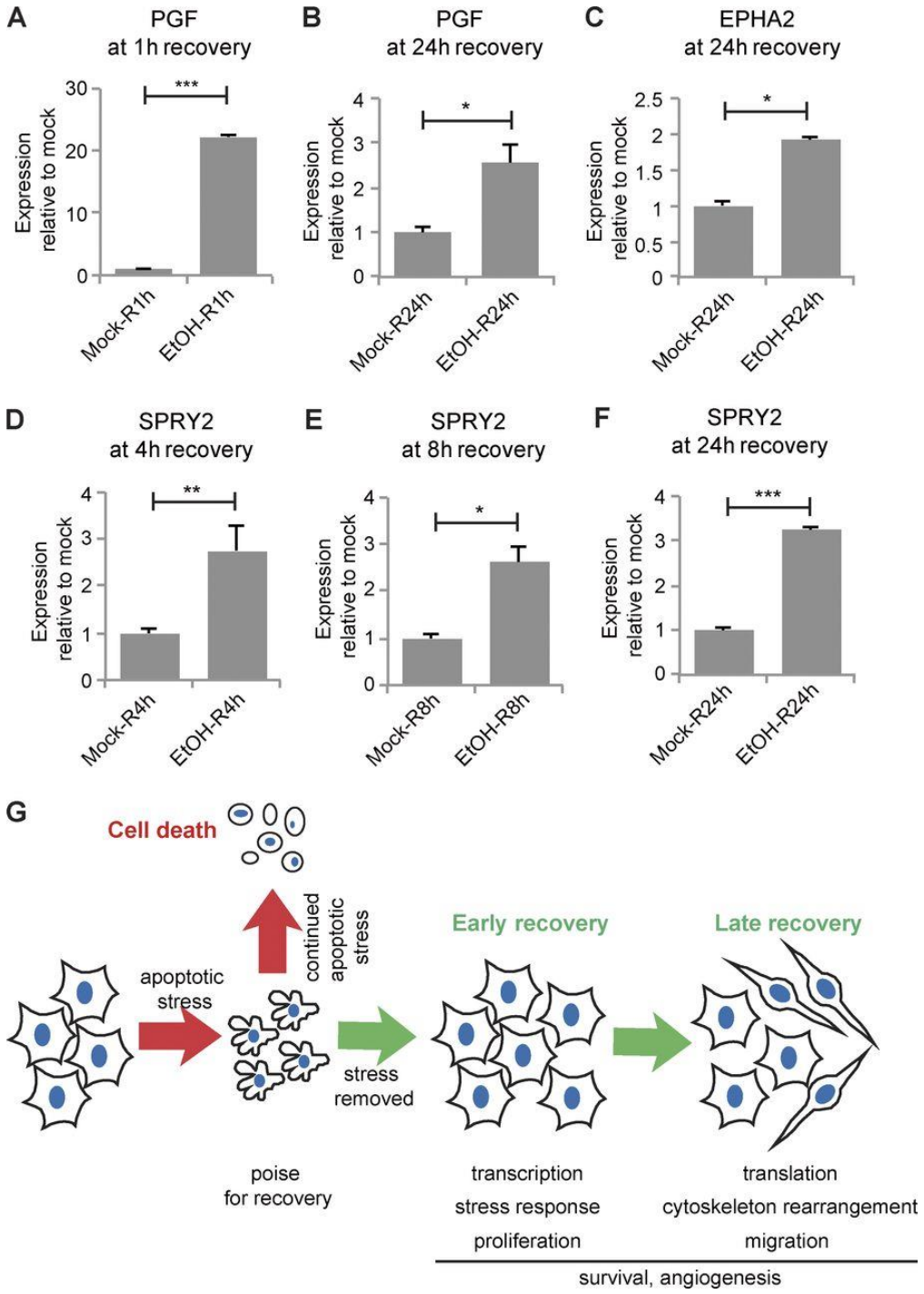

Figure 8. Angiogenesis-related genes were persistently up-regulated during recovery and schematic of events in anastasis. mRNA expression of PGF (A and B), EPHA2 (C), and SPRY2 (D–F) in cells recovering from mock or EtOH treatment for the indicated time (R). Error bars represent the standard error of the mean. *, $P < 0.05$; **, $P < 0.01$; ***, $P < 0.001$; ****, $P < 0.0001$. (G) Summary of events during anastasis. During apoptosis, cells poise for recovery. If the stress persists, cells die. If the stress is removed, cells undergo two stages of recovery.

Discussion

The ability of cells to survive caspase 3 activity has implications for normal development, cancer, and degenerative and ischemic diseases. Herein, we discuss the molecular characterization of cells recovering from the brink of apoptotic cell death. The data show that anastasis proceeds in two clearly defined stages that are characterized by distinct repertoires of genes. In the early stage, cells transcribe mRNAs encoding many transcription factors and reenter the cell cycle. In the late stage, cells pause in proliferation while increasing migration. Whereas the proliferation and migration responses were transient, others were longer lasting. For example, we found that cells that have undergone anastasis elevate expression of angiogenesis-related genes for 24 h. In vivo, these factors would be expected to exert a nonautonomous effect of stimulating blood vessel growth. Collectively, the results presented herein demonstrate that cells recovering from the brink of apoptotic cell death express factors that promote proliferation, survival, migration, and angiogenesis (Fig. 8 G). The cell biological processes involved in anastasis are thus reminiscent of wound-healing responses (Gurtner et al., 2008), consistent with the idea that cells evolved this capacity to limit permanent tissue damage after a transient injury.

Many of the same molecular pathways are up-regulated during wound healing and in cells undergoing anastasis, including TGFβ, receptor tyrosine kinase, MAPK signaling, and angiogenesis-promoting pathways (Gurtner et al., 2008). TGFβ signaling and Snail expression are thought to promote EMT and chemotherapy resistance during tumor progression (Kalluri and Weinberg, 2009; Kurrey et al., 2009; Brunen et al., 2013). HeLa

cells undergoing anastasis activate TGFβ signaling, activate Snail expression, and become migratory—all features of EMT. Two recent studies reported that EMT, although dispensable for tumor metastasis, is required for tumor recurrence after chemotherapy (Fischer et al., 2015; Zheng et al., 2015), suggesting that EMT is a survival strategy for tumor cells under stress in vivo. Our results suggest a possible relationship among tumor recurrence, EMT, and anastasis. If cancer cells exposed to radiation or chemotherapy during treatment escape death via anastasis, TGFβ signaling and Snail expression would be induced, and these critical regulators of EMT (Kalluri and Weinberg, 2009) would confer resistance to further chemotherapy and radiation (Kurrey et al., 2009). Therefore, anastasis could, in principle, drive EMT-dependent tumor recurrence.

In vivo, fast-growing tumors require formation of new blood vessels to supply nutrients and provide a route to metastasis (Nishida et al., 2006). Common cancer treatments, such as tumor resection, can induce extensive angiogenesis, which may promote tumor recurrence (Kong et al., 2010). In fact, elevated expression of angiogenic factors and/or increased blood vessel formation have been found in recurrent craniopharyngioma, bladder cancer, and squamous cell carcinoma after surgery or irradiation (Dinh et al., 1996; Sun et al., 2010; Agrawal et al., 2011). Our results imply that if tumor cells survive apoptosis triggered by chemotherapy, irradiation, or surgery, these survivors may up-regulate production of proangiogenic factors to promote angiogenesis and tumor recurrence.

In addition to providing insight into the molecular nature of anastasis, the work presented herein uncovers an unanticipated aspect of apoptosis. Even during apoptosis, cells poise for recovery by accumulating mRNAs encoding survival proteins. We propose that this facilitates rapid recovery upon removal of the apoptotic stimulus.

Apoptosis and caspase 3 have been linked to tumor recurrence. In cancer patients, the rate of recurrence is positively correlated with the amount of activated caspase 3 in tumor tissues (Huang et al., 2011; Flanagan et al., 2016). One explanation that has been offered for this somewhat paradoxical result is that after radiotherapy or chemotherapy, activated caspase 3 promotes production of progrowth signals that are released from dying cells to stimulate proliferation of living tumor cells, leading to tumor recurrence (Huang et al., 2011; Donato et al., 2014; Cheng et al., 2015). Dying cells can also secrete VEGF in a caspase-dependent way to promote angiogenesis after irradiation (Feng et al., 2015). These previous studies proposed that apoptotic cells induce nonautonomous compensatory proliferation in neighboring cells. The model is that cells that activate caspase 3 die and stimulate cells without activated caspase to proliferate and grow. However, our study suggests another possible mechanism underlying tumor recurrence: that tumor cells with activated caspase 3 themselves may eventually survive, proliferate, migrate, and trigger angiogenesis, contributing to tumor repopulation.

In addition to characterizing the process of anastasis using EtOH-treated HeLa cells, we found 41 genes up-regulated in early recovery in STS-treated HeLa and EtOH-treated H4 glioma cells. The GO analysis of these 41 genes indicates that the biological processes

involved in early recovery, like transcription regulation, cell cycle regulation, stress response, and angiogenesis, are common to anastasis in different cell lines and after treatment with different apoptotic inducers (Fig. 4 I). These 41 genes also serve as candidates for regulators of anastasis. Among them, we found that knocking down Snail impaired survival, whereas knocking down TGFβ impaired migration. Unfortunately, H4 cells were not amenable to the migration assay, so we were not able to test the effect of anastasis on motility in this additional cell type.

When facing tissue injury, anastasis could, in principle, facilitate repair and regeneration and limit the permanent damage that might otherwise occur in response to a powerful but temporary insult. However, anastasis would be detrimental if adopted by cancer cells in response to chemotherapy or radiation therapy, thus potentially promoting recurrence. Thus, the mechanisms described herein fit into the general idea that cancers mimic and co-opt wound-healing behaviors (Dvorak, 2015). Enhancing anastasis would be expected to be beneficial in the context of degenerative or ischemic disease, whereas inhibiting anastasis would be expected to be beneficial in cancer treatment. Further study will be required to determine which of the molecular markers and cell biological features described herein are general to many cells undergoing anastasis and in response to various inducers. Although some might be specific to particular cell types, both general and specific molecules and behaviors are of interest. General features may reveal a conserved molecular pathway. However, specific features may provide important therapeutic targets—if, for example, increased motility or a particular molecular pathway turns out to be characteristic of cancer cells but not normal cells or vice versa.

Materials and Methods

Cell culture

Human cervical cancer HeLa cells (cell line CCL-2; ATCC) were grown in MEM supplemented with GlutaMAX (Thermo Fisher Scientific), 10% FBS (Sigma), and 100 U/ml penicillin–streptomycin (Thermo Fisher Scientific). Human neuroglioma H4 cells (cell line HTB-148; ATCC) were grown in high-glucose DMEM supplemented with GlutaMAX (Thermo Fisher Scientific), 10% FBS, and 100 U/ml penicillin–streptomycin. All cells were maintained at 37°C with 5% CO2 and 90% humidity. Cells were tested for Mycoplasma contamination.

For RNAseq, 1.2 × 106 cells were seeded in each 100-mm dish and cultured overnight. The next day, cells were treated with either fresh growth medium or fresh growth medium with 4.3% EtOH (Thermo Fisher Scientific) for 3 h. Samples from untreated and apoptotic cells were collected at this moment. For recovery, medium was carefully removed and fresh growth medium was added. For each time point, three biological replicates were included.

For qRT-PCR, Western blotting, and immunofluorescent antibody staining, 2 × 105 cells were seeded in a 35-mm dish or six-well plate and cultured overnight. The next day, cells were treated with different chemicals. The concentration and time for different treatments were as follows: 4.3% EtOH on HeLa for 3 h, 250 nM STS (Santa Cruz Biotechnology) on HeLa for 2.5 h, 6.5% EtOH on H4 for 4 h, and HBSS (Thermo Fisher Scientific) on HeLa for 2 h. The precise concentrations and time points were chosen based on titration

studies to achieve the highest possible percentage of apoptotic cells that could recover. For recovery, medium was carefully removed and fresh growth medium was added for the indicated period of time.

For TGFβ signaling inhibition, 5 μM LY364947 (Sigma) was added to cells together with mock or EtOH treatment.

To test if cell death induced by STS or EtOH is caspase dependent, caspase inhibitor Z-VAD-fmk (10 μM) was applied to cells together with STS or EtOH. SYTOX Green was used to label permeabilized cells that entered secondary necrosis.

To activate the extrinsic apoptosis pathway, 100 μg/ml TNFα (Abcam) was cotreated with 10 μg/ml cycloheximide (Santa Cruz Biotechnology) for 6 h.

RNA extraction

For RNA sequencing, total RNA was extracted using a mirVana miRNA isolation kit (Thermo Fisher Scientific) and then treated with TURBO DNase (Thermo Fisher Scientific) to get rid of the genomic DNA. Ribosomal RNA (rRNA) was removed using RiboMinus Eukaryote System v2 (Thermo Fisher Scientific). The quality of RNA was examined using a fragment analyzer (Advanced Analytical).

For qRT-PCR, RNA was extracted using RNeasy Mini kit (QIAGEN) and treated with TURBO DNase to remove the genomic DNA.

RNA sequencing and data analysis

cDNA libraries used for sequencing were made from rRNA-depleted RNA using Ion Total RNA-seq kit v2 (Thermo Fisher Scientific) and sequenced on an Ion Torrent Proton sequencer (Thermo Fisher Scientific). Strand-specific, single-end reads were generated from sequencing with mean read lengths of 75 bp. Reads were mapped to University of California, Santa Cruz Human Reference Genome (hg19) using Tophat (v2.0.13; Trapnell et al., 2010). Reads covering gene coding regions were counted using htseq (v0.6.1; Anders et al., 2015), and the resulting count data were used for downstream analysis. Count data were first filtered by removing genes with low expression or genes with <50 reads in more than two replicates per sample. The remaining count data were normalized using the trimmed mean of the M-values method using edgeR (v3.14.0; Robinson et al., 2010). Normalized count distributions were fit to a generalized linear model to test for differential expression of genes ($P < 0.05$) among multiple samples. The differential expression test was corrected for multiple testing by applying the Benjamini–Hochberg method on p-values to control the FDR. AutoSOME (Newman and Cooper, 2010) was used for identification of gene clusters with similar expression patterns on counts per million (CPM) and log2-transformed count data.

GO enrichment analysis was performed using DAVID (https://david.ncifcrf.gov/) and PANTHER (http://pantherdb.org). Only common GO terms with Bonferroni p-values <0.001 and FDRs <0.001 were considered to be significantly enriched. KEGG pathway enrichment analysis was performed using WebGestalt (http://www.webgestalt.org) to identify the enriched pathways in the gene sets based on the KEGG database. The

pathways with adjusted p-values <0.001 and FDRs <0.01 were considered to be significantly enriched.

qRT-PCR

RNA samples were reverse transcribed into cDNA using the SuperScript III First-Strand Synthesis System (Thermo Fisher Scientific), and qPCR was performed on the QuantStudio 12K Flex Real-Time PCR System (Thermo Fisher Scientific) with the Power SYBR Green PCR Master Mix (Thermo Fisher Scientific) or on the CFX96 Touch Real-Time PCR Detection System (Bio-Rad Laboratories) with the SsoAdvanced Universal SYBR Green Supermix (Bio-Rad Laboratories). The primers used in qPCR are listed in Table S4.

Live imaging

2 × 105 cells were seeded in each glass-bottom, 35-mm dish (MatTek Corporation). Cells were incubated with Hoechst 33342 (Molecular Probes) for 20 min and imaged on a Zeiss LSM 780 or Leica DMi8 microscope with temperature and CO2 control. Images were taken every 10 or 5 min as indicated in the figure legends. Medium change for treatment and recovery was performed between scans. To live-monitor caspase 3 activation during EtOH treatment, NucView 488 (Biotium) was added. NucView 488 binds irreversibly to DNA and thus inhibits anastasis.

Mitochondria isolation

After treatment, 1.5 × 106 HeLa cells were scraped and pelleted. The cell pellets were resuspended in 300 µl of ice-cold fractionation buffer (250 mM sucrose, 20 mM Hepes, pH 7.4, 10 mM KCl, 1.5 mM MgCl2, 1 mM EDTA, 1 mM EGTA, and 1 mM DTT) supplemented with the protease inhibitor cocktail (Roche), 10 µM NaF, and 1 mM PMSF. The resuspended cells were placed on ice for 20 min and passed through a 26G needle 10–15 times to shear the cells. The needle-treated cell suspension was cleared from both nuclear fraction and nonsheared cells by centrifugation at 3,000 rpm for 5 min at 4°C. 200 µl of the supernatant (which represents the combined cytosolic and mitochondrial fractions) was transferred to new, prechilled tubes for further processing. To separate the mitochondrial fraction, the supernatant after nuclear fractionation was spun down for an additional 10 min at 10,000 rpm at 4°C. The supernatant was the cytosol fraction, and the pellet was the mitochondrial fraction. The pellet was resuspended in 50 µl of ice-cold fractionation buffer supplemented with inhibitors.

Western blotting

Cells were lysed in Laemmli sample buffer and run in 4–20% Mini-PROTEAN TGX precast protein gels (Bio-Rad Laboratories). The primary antibodies used were rabbit anti-Egr1 (no. 4154; Cell Signaling), rabbit anti–c-Fos (no. 2250; Cell Signaling), rabbit anti–c-Jun (no. 9165; Cell Signaling), mouse anti-Snail (no. 3895; Cell Signaling), rabbit anti-

PARP1 (no. 9532; Cell Signaling), rabbit anti-Smad2/3 (no. 8685; Cell Signaling), rabbit anti-pSmad2/3 (no. 8828; Cell Signaling), mouse anti–cytochrome c (no. sc-13560; Santa Cruz Biotechnology), mouse anti-Cox4 (no. 11967; Cell Signaling), rabbit anti–caspase 9 (no. 9502; Cell Signaling), mouse anti–caspase 8 (no. 9746; Cell Signaling), rabbit anti-Tubulin (no. 2128; Cell Signaling), and mouse anti–α-Tubulin (T6199; Sigma). The secondary antibodies used were IRDye 800CW donkey anti–rabbit IgG (H+L), IRDye 680LT donkey anti–mouse IgG (H+L), and IRDye 800CW donkey anti–mouse IgG (H+L; LI-COR Biosciences). The blots were scanned on an Odyssey imaging system (LI-COR Biosciences). Cell treatment, sample collection, and Western blotting were repeated at least three times, and the representative blots are shown in the figures.

Immunofluorescent staining

Cells were seeded in six-well plates with a coverslip. After treatment, cells were washed once with PBS and fixed with cold MeOH for 5 min. Cells were then rinsed with PBS twice and washed with PBS containing 0.2% Triton X-100 (Thermo Fisher Scientific). Thereafter, cells were blocked with PBS containing 0.2% Triton X-100 and 5% goat serum (Sigma). The primary and secondary antibodies used were rabbit anti-LC3B (no. 2775; Cell Signaling), rabbit anti-Snail (no. 3879; Cell Signaling), and Alexa Fluor 488–conjugated goat anti–rabbit IgG (H+L) secondary antibody (Thermo Fisher Scientific). The images were acquired on an DMi8 microscope (Leica). Cell treatment and staining were repeated three times, and the representative images are shown in the figures.

shRNA construct, transfection, and stable cell line

shRNA constructs were made in the pLVX vector. The sequences of Snail shRNA and scrambled shRNA were
5′-GGATCTCCAGGCTCGAAAGTCAAGAGCTTTCGAGCCTGGAGATCCTTTTTT-3′

(Lee et al.,2012) and
5′-CCTAAGGTTAAGTCGCCCTCGCTCGAGCGAGGGCGACTTAACCTTAGGTTTTT-3′
(no. 1864; Addgene). The constructs were transfected into HeLa cells using TurboFect transfection reagent (Thermo Fisher Scientific) and selected using 2 µg/ml puromycin (Thermo Fisher Scientific) to obtain stable cell lines.

The GC3AI caspase 3 reporter plasmid was obtained from B. Li (Tianjin Medical University, Tianjin, China). The plasmid was transfected into HeLa cells and selected using puromycin (Thermo Fisher Scientific) to obtain stable cell lines.

Proliferation assay

HeLa NucLight Red cells (Essen BioScience) were seeded in six-well plates and cultured overnight. After EtOH treatment, cells were cultured in growth medium and imaged using IncuCyte Zoom (Essen BioScience) every hour. Nine fields of view were taken per well, and the number of red fluorescent nuclei was counted using IncuCyte Zoom.
Wound-healing assay

HeLa NucLight Red cells were seeded in 100-mm dishes and cultured overnight. After treatment and 16 h of recovery, cells were trypsinized and seeded in Matrigel-coated 96-well ImageLock plates (Essen BioScience) at 4 × 104 cells per well. After 4 h, a wound was made in each well using WoundMaker (Essen BioScience). The wound closure process was imaged in IncuCyte Zoom every hour.

Recovery rate quantification

Before treatment, cells seeded in six-well plates were incubated with growth medium with DRAQ5 (Thermo Fisher Scientific) for 10 min at 37°C and imaged in IncuCyte Zoom to quantify the original cell number. After 4 h of recovery, cells were washed twice with PBS to remove floating dead cells and stained with DRAQ5 again. The cell number was quantified again as the number of survivors. The recovery rate was calculated as the ratio between the number of survivors and the original cell number.

Statistical analyses

The statistical analysis used in RNAseq data analysis is described in the RNA sequencing and data analysis section. For other experiments, statistical significance was determined using unpaired, two-tailed t tests with Welch's correction for comparison between two samples and one-way ANOVA to compare more than two samples, with $P < 0.05$ set as

the criteria for significance. The Tukey test was used to derive the adjusted p-values for pairwise comparison among multiple samples. Sample size was not predetermined.

Data availability

The RNAseq data have been deposited in the National Center for Biotechnology Information Gene Expression Omnibus under accession no. GSE86480.

Online supplemental material

Fig. S1 shows qRT-PCR validation of differentially expressed genes. Fig. S2 shows examples of cell division in early recovery stage. Fig. S3 shows change of cell number during wound-healing assay. Fig. S4 shows that treatment of TNFα together with CHX induces apoptosis through the extrinsic pathway. Fig. S5 shows inhibition of TGFβ signaling does not affect cell proliferation and recovery from EtOH or STS treatment. Video 1 shows live imaging of HeLa cells undergoing EtOH-induced apoptosis and recovery. Video 2 shows live imaging of caspase 3 activation in HeLa cells treated with EtOH. Video 3 shows live imaging of HeLa cells undergoing STS-induced apoptosis and recovery. Table S1 is a list of differentially expressed genes. Table S2 shows the results of AutoSOME gene clustering. Table S3 is a list of early- and late-response genes. Table S4 is a list of qPCR primers.

Acknowledgments

The authors thank Ugochukwu Ihenacho, Jing Xiong, and Rebecca Cheng for technical assistance. This work was supported by National Institutes of Health grants DP1OD019313-01 and 5DP1CA195760-02 to D.J. Montell. The authors declare no competing financial interests.

Author contributions: E. Guzman participated in preparing libraries for RNAseq and carried out bioinformatics analyses of the data. H.R. Zhou carried out the mapping of RNAseq reads. V. Balasanyan tested the cytochrome c level in cells with different treatments. C.M. Conner imaged HeLa cells recovering from STS treatment. K. Wong performed qPCR and Western blotting. K.S. Kosik provided advice on the design, execution, and interpretation of the RNAseq analysis. G. Sun carried out the majority of experiments presented, participated in preparing libraries for RNAseq, and carried out bioinformatics analyses. G. Sun also prepared the figures and wrote the first draft of the manuscript. D.J. Montell conceived and coordinated the study, advised G. Sun in all aspects of the work, contributed to the experimental design and interpretation of the results, and revised the manuscript.

References

Agrawal, U., A.K. Mishra, P. Salgia, S. Verma, N.K. Mohanty, and S. Saxena. 2011. Role of tumor suppressor and angiogenesis markers in prediction of recurrence of non muscle invasive bladder cancer. *Pathol. Oncol. Res.* 17:91–101. http://dx.doi.org/10.1007 /s12253-010 -9287-1

Anders, S., P.T. Pyl, and W. Huber. 2015. HT Seq-A Python framework to work with high-throughput sequencing data. *Bioinformatics.* 31:166–169. http://dx.doi.org/10.1093 /bioinformatics /btu638

Barquilla, A., and E.B. Pasquale. 2015. Eph receptors and ephrins: Therapeutic opportunities. *Annu. Rev. Pharmacol. Toxicol.* 55:465–487.
http ://dx.doi.org/10.1146/annurev-pharmtox-011112-140226

Brunen, D., S.M. Willems, U. Kellner, R. Midgley, I. Simon, and R. Bernards. 2013. TGF-β : An emerging player in drug resistance. *Cell Cycle.* 12:2960–2968.
http://dx.doi.org/10.4161/cc.26034

Cabrita, M.A., and G. Christofori. 2008. Sprouty proteins, masterminds of receptor tyrosine kinase signaling. *Angiogenesis.* 11:53–62. http://dx.doi.org/10.1007/s10456-008-9089-1

Chen, L., and X. Han. 2015. Anti-PD-1/PD-L1 therapy of human cancer: Past, present, and future. *J. Clin. Invest.* 125:3384–3391. http://dx.doi.org/10.1172 /JCI80011

Cheng, J., L. Tian, J. Ma, Y. Gong, Z. Zhang, Z. Chen, B. Xu, H. Xiong, C. Li, and Q. Huang. 2015. Dying tumor cells stimulate proliferation of living tumor cells via caspase-dependent protein kinase C δ activation in pancreatic ductal adenocarcinoma. *Mol. Oncol.* 9:105–114. http ://dx.doi.org/10 .1016/j.molonc.2014.07.024

de Calignon, A., L.M. Fox, R. Pitstick, G.A. Carlson, B.J. Bacskai, T.L. Spires-Jones, and B.T. Hyman. 2010. Caspase activation precedes and leads to tangles. *Nature.* 464:1201–1204. http://dx.doi.org/10.1038/nature08890

De Falco, S. 2012. The discovery of placenta growth factor and its biological activity. *Exp. Mol. Med.* 44:1–9. http://dx.doi.org/10.3858/emm.2012.44.1.025

Ding, A.X., G. Sun, Y.G. Argaw, J.O. Wong, S. Easwaran, and D.J. Montell. 2016. CasExpress reveals widespread and diverse patterns of cell survival of caspase-3 activation during development in vivo. eLife.5:e10936.
http://dx.doi.org/10.7554/eLife.10936

Dinh, T.V., E.V. Hannigan, E.R. Smith, M.J. Hove, V. Chopra, and T. To. 1996. Tumor angiogenesis as a predictor of recurrence in stage Ib squamous cell carcinoma of the cervix. *Obstet. Gynecol.* 87:751–754. http://dx.doi.org/10.1016 /0029-7844(96)00039-7

Donato, A.L., Q. Huang, X. Liu, F. Li, M.A. Zimmerman, and C.-Y. Li. 2014. Caspase 3 promotes surviving melanoma tumor cell growth after cytotoxic therapy. *J. Invest. Dermatol.* 134:1686–1692. http://dx.doi.org/10.1038/jid.2014.18

Dvorak, H.F. 2015. Tumors: Wounds that do not heal—Redux. *Cancer Immunol. Res.* 3:1–11. http://dx.doi.org/10.1158/2326-6066.CIR-14-0209

Elmore, S. 2007. Apoptosis: A review of programmed cell death. *Toxicol. Pathol.* 35:495–516. http://dx.doi.org/10.1080/01926230701320337

Favaloro, B., N. Allocati, V. Graziano, C. Di Ilio, and V. De Laurenzi. 2012. Role of apoptosis in disease. *Aging (Albany NY).* 4:330–349. http://dx.doi.org/10.18632/aging.100459

Feng, X., L. Tian, Z. Zhang, Y. Yu, J. Cheng, Y. Gong, C.-Y. Li, and Q. Huang. 2015. Caspase 3 in dying tumor cells mediates post-irradiation angiogenesis. *Oncotarget.* 6:32353–32367. http://dx.doi.org/10.18632/oncotarget.5898

Fischer, K.R., A. Durrans, S. Lee, J. Sheng, F. Li, S.T.C. Wong, H. Choi, T. El Rayes, S. Ryu, J. Troeger, et al. 2015. Epithelial-to-mesenchymal transition is not required for lung metastasis but contributes to chemoresistance. *Nature.* 527:472–476. http://dx.doi.org/10.1038 /nature15748

Flanagan, L., M. Meyer, J. Fay, S. Curry, O. Bacon, H. Duessmann, K. John, K.C. Boland, D.A. McNamara, E.W. Kay, et al. 2016. Low levels of Caspase-3 predict favourable response to 5FU-based chemotherapy in advanced colorectal cancer: Caspase-3 inhibition as a therapeutic approach. *Cell Death Dis.* 7:e2087. http://dx.doi.org/10.1038/cddis.2016.7

Franco, D.L., J. Mainez, S. Vega, P. Sancho, M.M. Murillo, C.A. de Frutos, G. Del Castillo, C. López-Blau, I. Fabregat, and M.A. Nieto. 2010. Snail1 suppresses TGF-β-induced apoptosis and is sufficient to trigger EMT in hepatocytes. *J. Cell Sci.* 123:3467–3477. http://dx.doi.org/10.1242/jcs.068692

Fuchs, Y., and H. Steller. 2011. Programmed cell death in animal development and disease. *Cell.* 147:742–758. http://dx.doi.org/10.1016/j.cell.2011.10.033

Green, D., and G. Kroemer. 1998. The central executioners of apoptosis: Caspases or mitochondria? *Trends Cell Biol.* 8:267–271. http://dx.doi.org/10.1016/S0962-8924(98)01273 -2

Gurtner, G.C., S. Werner, Y. Barrandon, and M.T. Longaker. 2008. Wound repair and regeneration. *Nature.* 453:314–321. http://dx.doi.org/10.1038/nature07039

Huang, Q., F. Li, X. Liu, W. Li, W. Shi, F.-F. Liu, B. O'Sullivan, Z. He, Y. Peng, A.-C. Tan, et al. 2011. Caspase 3-mediated stimulation of tumor cell repopulation during cancer radiotherapy. *Nat. Med.* 17:860–866. http://dx.doi.org/10.1038/nm.2385

Ichim, G., J. Lopez, S.U. Ahmed, N. Muthalagu, E. Giampazolias, M.E. Delgado, M. Haller, J.S. Riley, S.M. Mason, D. Athineos, et al. 2015. Limited mitochondrial permeabilization causes DNA damage and genomic instability in the absence of cell death. *Mol. Cell.* 57:860–872. (published erratum appears in *Mol. Cell* 2015. 58:900) http://dx.doi.org/10.1016/j.molcel.2015.01.018

Inukai, T., A. Inoue, H. Kurosawa, K. Goi, T. Shinjyo, K. Ozawa, M. Mao, T. Inaba, and A.T. Look. 1999. SLUG, a ces-1-related zinc finger transcription factor gene with antiapoptotic activity, is a downstream target of the E2A-HLF oncoprotein. *Mol. Cell.* 4:343–352. http://dx.doi.org/10.1016/S1097-2765(00)80336-6

Kalluri, R., and R.A. Weinberg. 2009. The basics of epithelial-mesenchymal transition. *J. Clin. Invest.* 119:1420–1428. http://dx.doi.org/10.1172/JCI39104

Kenis, H., H.R. Zandbergen, L. Hofstra, A.D. Petrov, E.A. Dumont, F.D. Blankenberg, N. Haider, N. Bitsch, M. Gijbels, J.W.H. Verjans, et al. 2010. Annexin A5 uptake in ischemic myocardium: Demonstration of reversible phosphatidylserine externalization and feasibility of radionuclide imaging. *J. Nucl. Med.* 51:259–267. http://dx.doi.org/10.2967/jnumed .109 .068429

Kerr, J.F., A.H. Wyllie, and A.R. Currie. 1972. Apoptosis: A basic biological phenomenon with wide-ranging implications in tissue kinetics. *Br. J. Cancer.* 26:239–257. http://dx.doi.org/10.1038/bjc.1972.33

Kong, B., C.W. Michalski, H. Friess, and J. Kleeff. 2010. Surgical procedure as an inducer of tumor angiogenesis. *Exp. Oncol.* 32:186–189.

Kumar, S. 2007. Caspase function in programmed cell death. *Cell Death Differ.* 14:32–43. http://dx.doi.org/10.1038/sj cdd.4402060

Kurrey, N.K., S.P. Jalgaonkar, A.V. Joglekar, A.D. Ghanate, P.D. Chaskar, R.Y. Doiphode, and S.A. Bapat. 2009. Snail and slug mediate radioresistance and chemoresistance by antagonizing p53-mediated apoptosis and acquiring a stem-like phenotype in ovarian cancer cells. *Stem Cells.* 27:2059–2068. http://dx.doi.org/10.1002 /stem .154

Lee, S.Y., H.M. Jeon, M.K. Ju, C.H. Kim, G. Yoon, S.I. Han, H.G. Park, and H.S. Kang. 2012. Wnt/Snail signaling regulates cytochrome *c* oxidase and glucose metabolism. *Cancer Res.* 72:3607–3617. http://dx.doi.org/10.1158/0008-5472.CAN-12-0006

Levayer, R., C. Dupont, and E. Moreno. 2016. Tissue crowding induces caspase dependent competition for space. *Curr. Biol.* 26:670–677.

http://dx.doi.org/10.1016/j.cub.2015 .12 .072

Liu, X., Y. He, F. Li, Q. Huang, T.A. Kato, R.P. Hall, and C.-Y. Li. 2015. Caspase-3 promotes genetic instability and carcinogenesis. *Mol. Cell.*58:284–296. http://dx.doi.org/10.1016/j.molcel.2015.03.003

Liwak, U., M.D. Faye, and M. Holcik. 2012. Translation control in apoptosis. *Exp. Oncol.* 34:218–230.

Lovric, M.M., and C.J. Hawkins. 2010. TRAIL treatment provokes mutations in surviving cells. *Oncogene.* 29:5048–5060. http://dx.doi.org/10.1038/onc.2010.242

Mariño, G., M. Niso-Santano, E.H. Baehrecke, and G. Kroemer. 2014. Selfconsumption: The interplay of autophagy and apoptosis. *Nat. Rev. Mol. Cell Biol.* 15:81–94. http://dx.doi.org/10.1038/nrm3735

Martin, S.J., and D.R. Green. 1995. Protease activation during apoptosis: Death by a thousand cuts? *Cell.* 82:349–352. http://dx.doi.org/10.1016/0092-8674(95)90422-0

Massagué, J. 1998. TGF-β signal transduction. *Annu. Rev. Biochem.* 67:753–791. http://dx.doi.org/10.1146/annurev.biochem.67.1.753

Metzstein, M.M., and H.R. Horvitz. 1999. The *C. elegans* cell death specification gene *ces-1* encodes a Snail family zinc finger protein. *Mol. Cell.* 4:309–319. http://dx.doi.org/10.1016/S1097-2765(00)80333-0

Mizushima, N., T. Yoshimori, and B. Levine. 2010. Methods in mammalian autophagy research. *Cell.* 140:313–326. http://dx.doi.org/10.1016/j.cell.2010.01.028

Newman, A.M., and J.B. Cooper. 2010. AutoSOME: A clustering method for identifying gene expression modules without prior knowledge of cluster number. *BMC Bioinformatics.* 11:117. http://dx.doi.org/10.1186/1471-2105-1-117

Nikoletopoulou, V., M. Markaki, K. Palikaras, and N. Tavernarakis. 2013. Crosstalk between apoptosis, necrosis and autophagy. *Biochim. Biophys. Acta.* 1833:3448–3459. http://dx.doi.org/10.1016/j.bbamcr.2013.06.00
Nishida, N., H. Yano, T. Nishida, T. Kamura, and M. Kojiro. 2006. Angiogenesis in cancer. *Vasc. Health Risk Manag.* 2:213–219. http://dx.doi.org /10.2147/vhrm.2006.2.3.213

Peinado, H., M. Quintanilla, and A. Cano. 2003. Transforming growth factor β -1 induces Snail transcription factor in epithelial cell lines: Mechanisms for epithelial mesenchymal transitions. *J. Biol. Chem.* 278:21113–21123. http://dx.doi.org/10.1074/jbc.M211304200

Robinson, M.D., D.J. McCarthy, and G.K. Smyth. 2010. edgeR: A Bioconductor package for differential expression analysis of digital gene expression data. *Bioinformatics.* 26:139–140. http://dx.doi.org/10.1093/bioinformatics/btp616

Salvucci, O., and G. Tosato. 2012. Essential roles of EphB receptors and Ephrin B ligands in endothelial cell function and angiogenesis. *Adv. Cancer Res.* 114:21–57. http://dx.doi.org/10.1016/B978-0-12-386503-8.00002-8

Sun, H.I., E. Akgun, A. Bicer, A. Ozkan, S.U. Bozkurt, O. Kurtkaya, D.Y. Koc, M.N. Pamir, and T. Kilic. 2010. Expression of angiogenic factors in craniopharyngiomas: Implications for tumor recurrence. *Neurosurgery.* 66:744–750. http://dx.doi.org/10.1227/01.NEU.0000367553.65099.14

Tang, H.L., H.M. Tang, K.H. Mak, S. Hu, S.S. Wang, K.M. Wong, C.S.T. Wong, H.Y. Wu, H.T. Law, K. Liu, et al. 2012. Cell survival, DNA damage, and oncogenic transformation after a transient and reversible apoptotic response. *Mol. Biol. Cell.* 23:2240–2252. http://dx.doi.org/10.1091/mbc.E11-11-0926

Trapnell, C., B.A. Williams, G. Pertea, A. Mortazavi, G. Kwan, M.J. van Baren, S.L. Salzberg, B.J. Wold, and L. Pachter. 2010. Transcript assembly and quantification by RNA-Seq reveals unannotated transcripts and isoform switching during cell differentiation. *Nat. Biotechnol.* 28:511–515. http://dx.doi.org/10.1038/nbt.1621

Wan, Z., H. Pan, S. Liu, J. Zhu, W. Qi, K. Fu, T. Zhao, and J. Liang. 2015. Downregulation of SNAIL sensitizes hepatocellular carcinoma cells to TRAIL-induced apoptosis by regulating the NF-κB pathway. *Oncol. Rep.* 33:1560–1566.

Xu, J., S. Lamouille, and R. Derynck. 2009. TGF-β-induced epithelial to mesenchymal transition. *Cell Res.* 19:156–172. http://dx.doi.org/10.1038/cr.2009.5

Zhang, J., X. Wang, W. Cui, W. Wang, H. Zhang, L. Liu, Z. Zhang, Z. Li, G. Ying, N. Zhang, and B. Li. 2013. Visualization of caspase-3-like activity in cells using a genetically encoded fluorescent biosensor activated by protein cleavage. *Nat. Commun.* 4:2157. http://dx.doi.org/10.1038/ncomms3157

Zheng, X., J.L. Carstens, J. Kim, M. Scheible, J. Kaye, H. Sugimoto, C.-C. Wu, V.S. LeBleu, and R. Kalluri. 2015. Epithelial-to-mesenchymal transition is dispensable for metastasis but induces chemoresistance in pancreatic cancer. *Nature.* 527:525–530. http://dx.doi.org/10.1038/nature16064

III. Cell Biological Consequences of Transient Apoptotic Stress in HeLa Cells

Abstract

During intrinsic apoptosis, mitochondrial outer membrane permeabilization (MOMP) results in the release of cell-death promoting factors into the cytosol. Mitochondrial release of cytochrome c activates the caspase proteases that ultimately dismantle the cell. Mitochondrial dysfunction is sufficient to kill cells even when caspase activity is blocked. However, a growing body of data demonstrates cell survival following mitochondrial damage and caspase activation. Here, we report major phenotypic changes following transient exposure to the apoptosis inducer staurosporine (STS). HeLa cells recover from STS induced mitochondrial damage and collapse. Limiting caspase activity during STS treatment enhances survival and enriches for cells with low mitochondrial membrane potential ($\Delta\Psi m$). Strikingly, low $\Delta\Psi m$ cells are viable and show healthy nuclear morphology. Our data reveal a previously unknown relationship between apoptosis survival and mitochondrial respiration.

Introduction

Mitochondrial outer membrane permeabilization (MOMP) is thought to represent a point-of-no-return during apoptosis (Tait and Green, 2008). Cell death is often inevitable as MOMP usually occurs throughout the entire mitochondrial network within minutes and is sufficient to kill cells even if caspase activity is blocked (Goldstein et al., 2000; Latrigue et al., 2009). However, recent reports show cell survival following MOMP provided the entire network is not compromised (Tait et al., 2010; Ichim et al., 2015; Xu et al., 2020). In possibly related processes, cell survival following transient apoptotic stress has been reported during fractional killing, failed apoptosis, abortive apoptosis, and pseudo-apoptosis (Raina et al., 2001; Mackenzie et al., 2005; Roux et al., 2015; Berthenet et al., 2020; Pandya et al., 2020). Sublethal caspase activity has also been reported during radiation and over-expression of the oncogene MYC (Liu et al., 2015; Cartwright et al., 2017). In addition, our lab and others have observed cell survival following transient executioner caspase activation in a process termed anastasis (Tang et al., 2012; Tang et al., 2015; Ding et al., 2016; Sun et al., 2017; Seervi et al., 2019; Sun et al., 2020). Hereafter, we refer to cells surviving transient apoptotic stress as anastatic. Elucidating the molecular mechanisms, cell biological consequences, and physiological function of these processes remains an area of active study.

Due to the central role of mitochondria in both apoptosis and energy production, we sought to characterize the mitochondrial network in anastatic cells. To facilitate our study of mitochondrial events, we developed a protocol to enhance the frequency of anastasis for HeLa cells exposed to the classic apoptosis inducer staurosporine (STS). We observed that anastatic cells survive MOMP and mitochondrial collapse. Strikingly, under

some experimental conditions a population of cells lacking mitochondrial membrane potential (ΔΨm), yet retaining mitochondria and normal nuclear morphology, persists for three days. Low-ΔΨm suggests that limited mitochondrial respiration is compatible with cell viability and may represent a survival strategy. Our data reveal a previously unrecognized relationship between anastasis and mitochondrial respiration.

Simultaneous Treatment with Staurosporine and QVD Engages Sublethal Caspase Activity Promoting Anastasis

We previously reported anastasis following transient exposure of HeLa cells to staurosporine (STS), (Sun et al., 2017), which is a broad-spectrum kinase inhibitor commonly used to induce apoptosis via the intrinsic pathway. However, in the absence of a biosensor for active caspase, it was not possible to monitor precisely the fates of individual cells with activated caspase-3. Therefore, we generated cervical cancer HeLa cells stably expressing a caspase biosensor (HeLa-GC3Ai) (Zhang et al., 2013). After a 5 h treatment with STS, cells shrank and activated caspases (Figure 3.1A). To quantify anastasis, we washed away the STS, allowed the cells to recover for 20 h, removed dead cells by additional washes, and measured the percentage of cells that remain GC3Ai positive. After recovery from STS, ~50% of cells were GC3Ai positive (Figure 3.1, B and C). Including 1μM of the pan-caspase inhibitor quinolyl-valyl-O-methylaspartyl-[2,6-difluorophenoxy]-methyl ketone (QVD) during STS exposure increased the fraction of caspase-positive surviving cells to ~80% (Figure 3.1, B and C). 1μM QVD prevented STS-induced cell death in propidium iodide (PI) uptake assay (Figure 3.1D). We next characterized this condition using live-cell imaging. We observed individual cells

activating GC3Ai and recovering (Figure 3.1E). Within 5 h of STS-QVD treatment, ~80% of cells shrank and showed nuclear condensation (Figure 3.1F). Upon washout with fresh cell culture media, ~50% of cells recover morphology (Figure 3.1F and Supplemental Figure S3.1A). 1μM dose of QVD was not sufficient to prevent cell death without washout (Supplemental Figure S3.1B). These data suggest that STS initiates caspase activity, and 1μM QVD prevents plasma membrane rupture thus enhancing the anastasis frequency. From these data, we conclude that low level of caspase inhibition promotes anastasis suggesting that heterogeneous caspase expression or activity levels might determine survival versus death in a population.

Our observation that 1μM QVD promotes anastasis without blocking caspase activity raises the question as to the mechanism of enhanced survival. Previously, we performed an RNA-seq of anastatic HeLa cells recovering from EtOH and identified 69 top-ranked up-regulated “early response” genes during the first hours of anastasis (Sun et al., 2017). 44 of those were also upregulated during STS recovery (Sun et al., 2017). Therefore, we reasoned to measure the expression levels of 10 “early response” genes at 2 h recovery after 4 h of STS-QVD treatment. All 10 genes were upregulated when compared to vehicle controls (Figure 3.2A-J). We conclude that these genes represent a common transcriptional signature for anastatic cells. We next sought to characterize anastasis at the cell biological level.

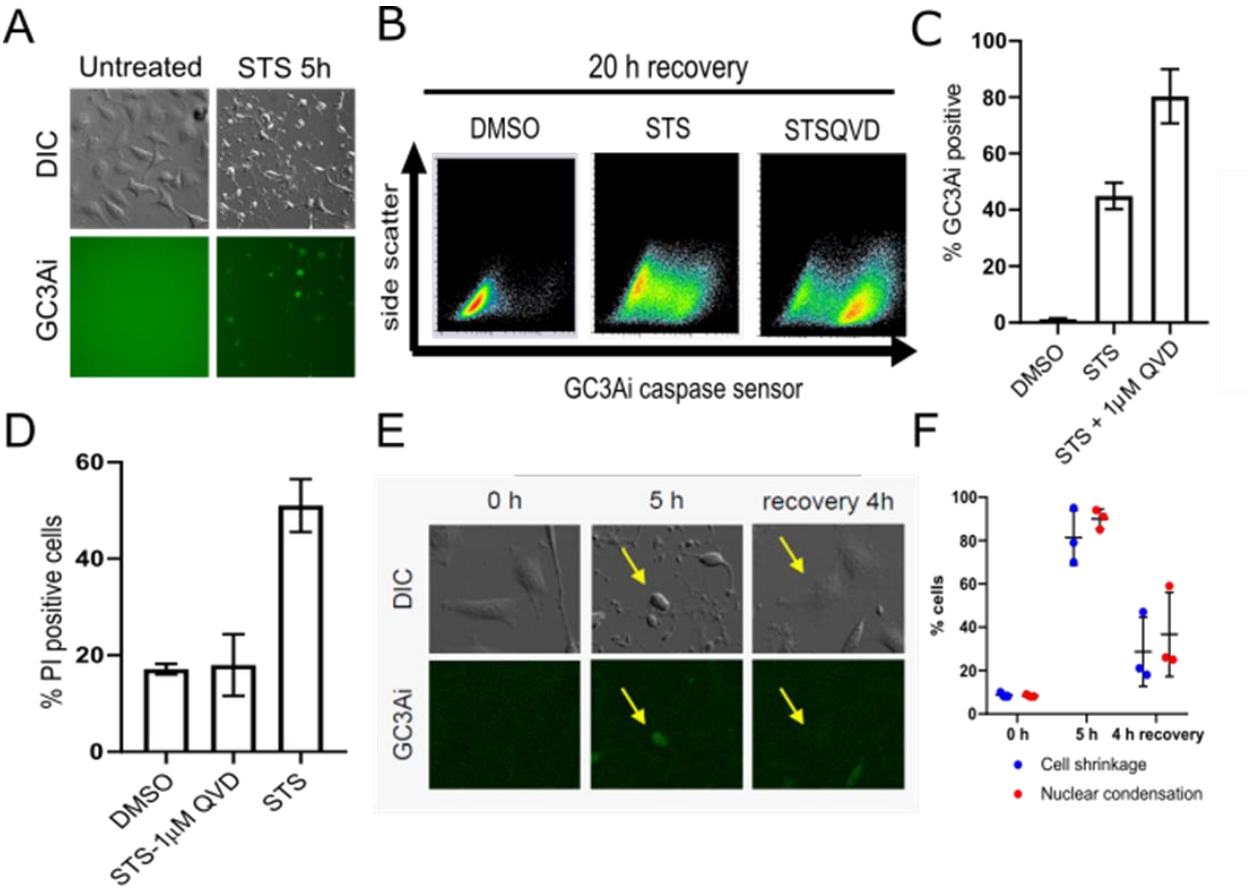

FIGURE 3.1: Simultaneous treatment with staurosporine and QVD engages sublethal caspase activity enhancing the frequency of anastasis. (A) Imaging of HeLa-GC3Ai cells untreated or treated with STS for 5 h. DIC and GC3Ai (green) were visualized by fluorescence microscopy. (B) Flow cytometry plots showing side scatter (y axis) and GC3Ai caspase sensor fluorescence (x axis) for DMSO, STS, and STS-QVD treated samples. Each sample was treated for 5 h followed by 20 h recovery before analysis. Colors represent increasing number of events in same position, white being lowest, red being the highest. (C) Quantification of flow cytometry plots in B. (D) Propidium iodide uptake assay at 24 h of cells treated with either DMSO, STS-QVD, or STS alone. (E) Time-lapse live-cell imaging of HeLa-GC3Ai cells before treatment (0 h), STS-QVD treatment (5 h), and after recovery (recovery 4 h). Yellow arrow marks an anastatic cell. (F) Quantification of morphological response to 5 h STS-QVD exposure. Error bars denote SD. Dots represent independent experiments in F. At least three independent experiments were performed.

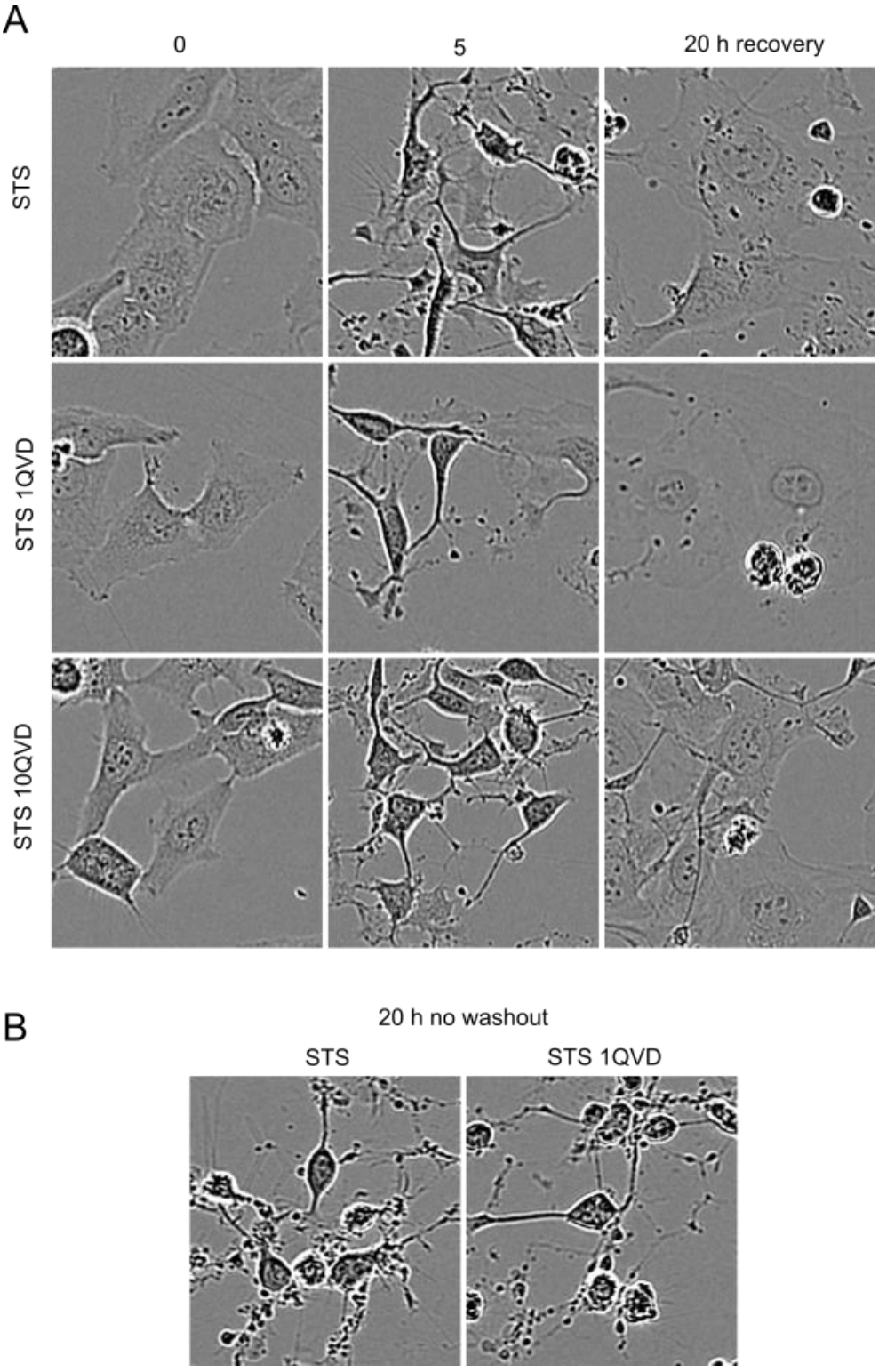

SUPPLEMENTAL FIGURE 3.1: Morphological response to STS conditions. (A) IncuCyte live-cell imaging of HeLa cells before (0), at 5 h treatment (5), and 20 h recovery. (B) IncuCyte live-cell imaging of HeLa cells at 20 h timepoint without washout occurring at 5 h treatment.

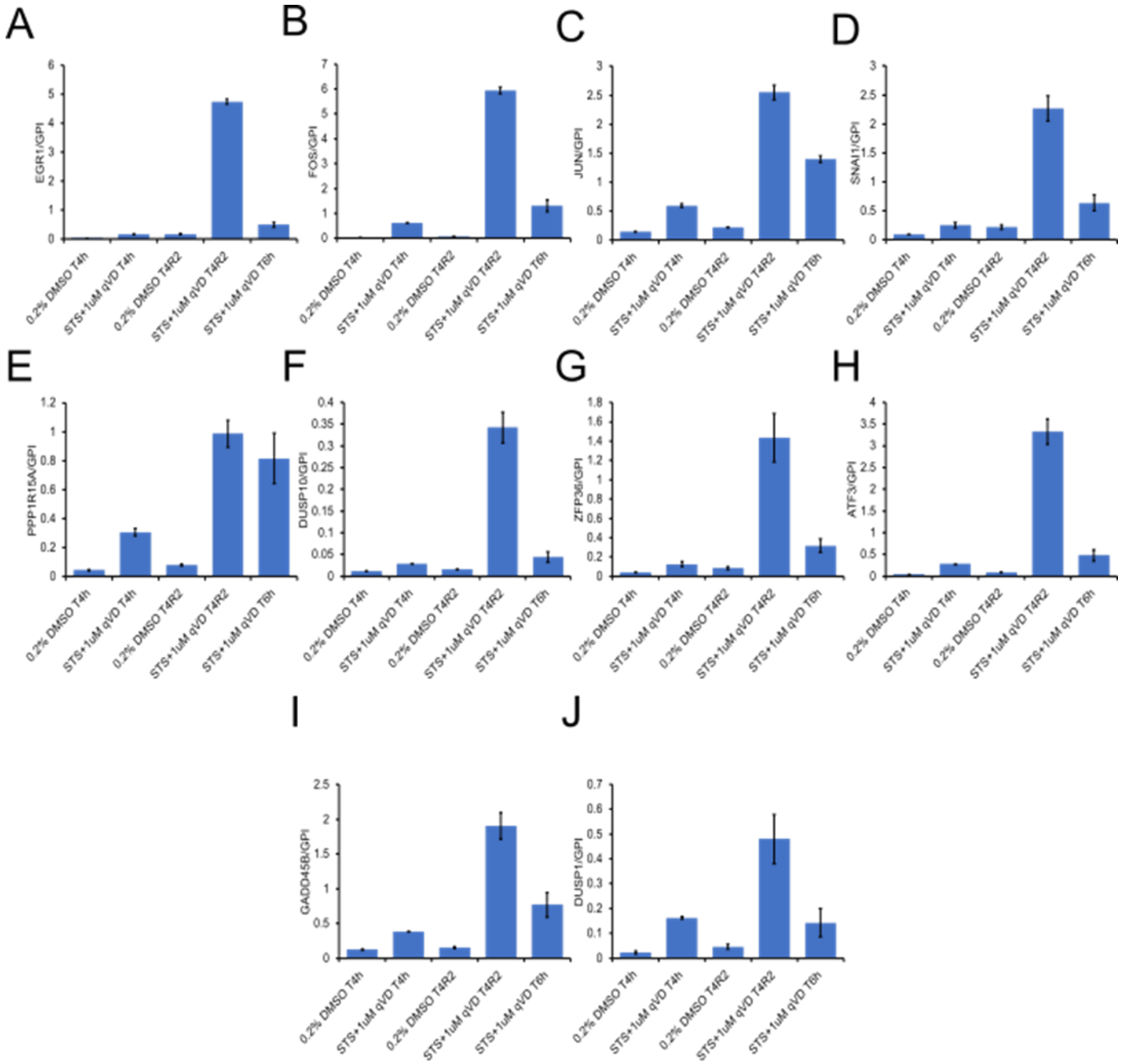

FIGURE 3.2: Early-response genes are upregulated in STS-QVD anastasis. (A-J) The expression of 10 early-response genes in HeLa cells recovering from STS-QVD. Error bars denote SEM. Data was kindly provided by Gongping Sun.

Surviving Cells Enlarge

We hypothesized that sublethal caspase activity may have long-term consequences to cells. To address this, we kept surviving cells in culture for days after transient stress. To better visualize changes in cell size we labeled the cytosol of cells by generating HeLa cells stably expressing HA-mCherry. 2 d after STS exposure we observed enlarged cell morphology (Figure 3.3A). Surviving cells enlarged 2X to 4X their original area (Figure 3.3B). Limiting caspase activity by addition of 1μM QVD increased the proportion of cells maintaining normal cell area (Figure 3.3B). Interestingly, at 10μM QVD, a dose that sufficiently blocks caspase activity, even more cells maintain original cell area (Figure 3.3A and B). This suggests that the enlarged cell phenotype is downstream of caspase activity during STS exposure.

Large and flat morphology is characteristic of senescent cells and we did not observe cell division events in our experiment. Therefore, the data suggests that transient STS exposure induces a senescent-like state whereas limiting caspase activity by QVD increases the proportion of cells capable of division. We conclude that heterogeneous caspase activity may determine senescence versus growth. However, our experiment does not differentiate cell-autonomous effects of caspase activity versus non-autonomous ones.

Anastatic Cells Survive Mitochondrial Damage

MOMP is considered a point-of-no-return in cells experiencing apoptotic induction. Therefore, we wanted to investigate the extent of mitochondrial damage and repair in single cells undergoing apoptosis and anastasis.

To do this, we visualized cytochrome c and the mitochondria membrane protein Tom20 by immunofluorescent antibody staining. At 5 h of STS or STS-QVD treatment, most cells exhibited cytosolic cytochrome c, a marker of MOMP (Figure 3.4, A and B). Approximately 80% of cells exhibited evidence of MOMP and about half of these cells recovered (Figure 3.4C), and inclusion of 1μM QVD during STS exposure enhanced the survival frequency (Figure 3.4C). These data show that cells can survive mitochondrial damage and that downstream caspase activity determines survival versus death. We conclude that in response to STS, MOMP induced caspase activity kills most cells, whereas addition of QVD limits caspase activity following MOMP thus promoting anastasis.

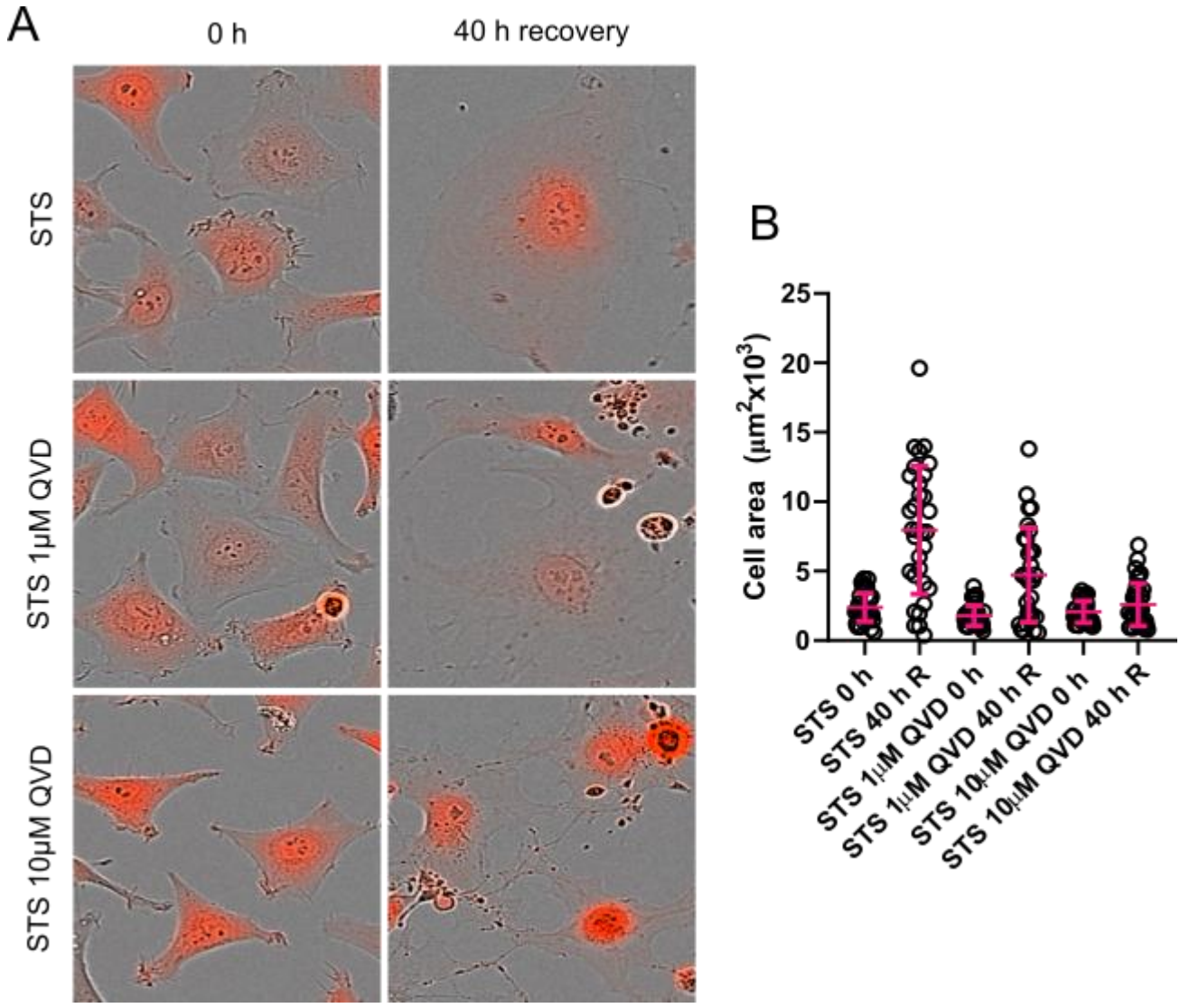

FIGURE 3.3: Surviving cells enlarge. (A) Live-cell imaging of HeLa-HA mCherry cells at time 0 h and time 40 h recovery following 5 h of indicated treatment. (B) Quantification of cell area. Each dot represents an individual cell. Data is from 1 imaging experiment and excludes dead cells. Error bars denote SD.

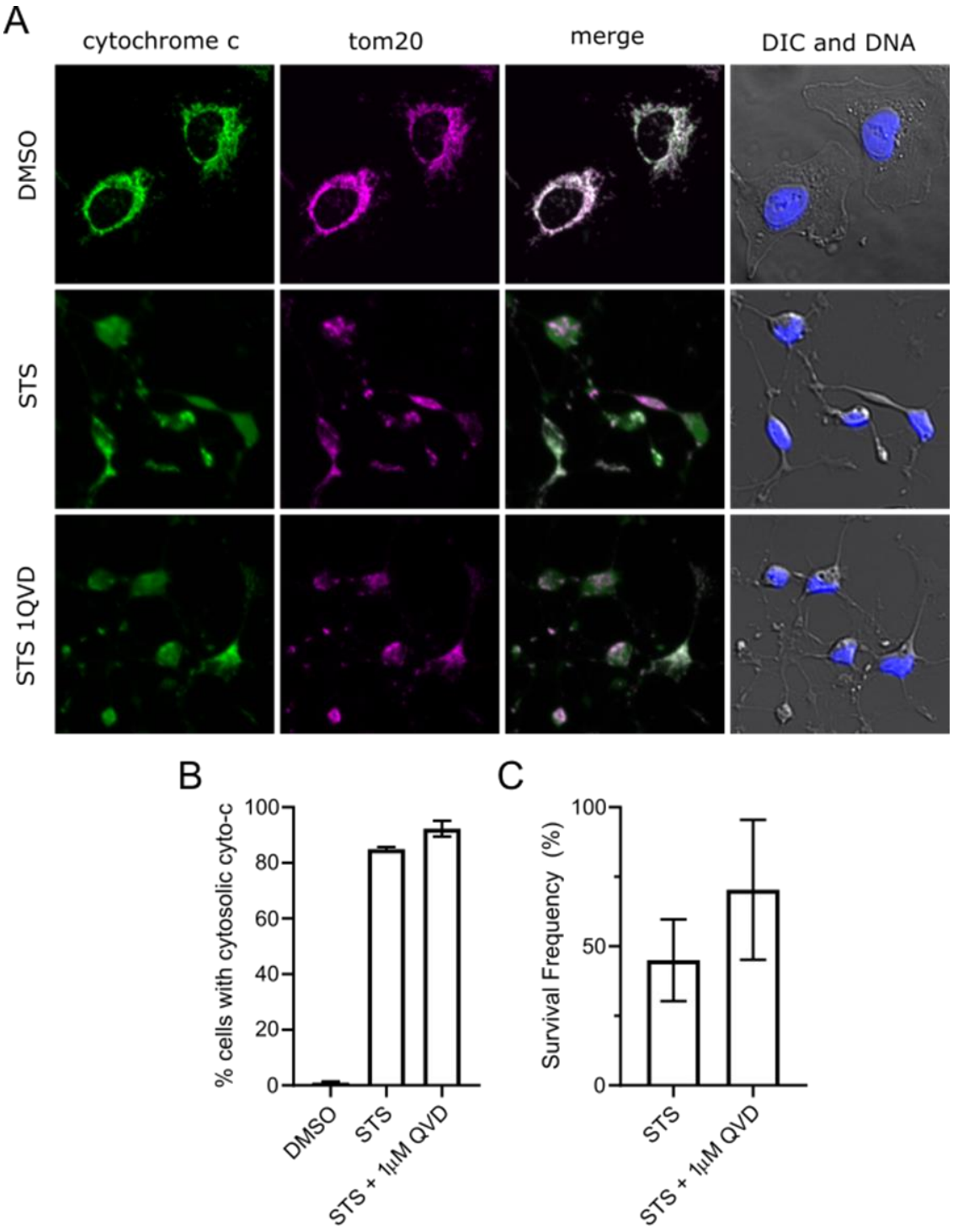

FIGURE 3.4: Anastatic cells survive mitochondrial damage. (A) Immunofluorescent antibody staining for cytochrome c (green) and Tom20 (magenta). Merge shows merged images of cytochrome c and Tom20. DIC and DNA merge is shown at right. (B) Quantification of percentage cells showing cytosolic cytochrome c from imaging data in A. (C) IncuCyte survival frequency quantification. Error bars denote SD. Images are representative of at least three independent experiments and at least 5 randomly selected imaging fields.

Mitochondrial Organization in Anastatic Cells

The mitochondrial network constantly undergoes cycles of fusion and fission (Youle and van der Bliek 2012). Fusion can promote mitochondrial activity by complementation of faulty mitochondrion with healthy ones and fission can support removal of damaged mitochondria (Otera and Mihara 2012). Mitochondrial fission occurs during apoptosis (Youle and Karbowski 2005) and anastasis has been observed following mitochondrial fragmentation in response to ethanol (EtOH), DMSO, and cucurbitacin I exposure (Tang et al., 2012). However, it is unclear what occurs during STS anastasis and the fate of mitochondria following extensive MOMP is unclear.

To gain insight into mitochondrial organization throughout anastasis, we visualized Tom20 in anastatic cells at treatment and recovery time points. During STS treatment, the mitochondrial network collapses (Figure 3.5A). This is observed even in the presence of 1μM and 10μM QVD suggesting that cellular and mitochondrial collapse occurs independent of caspase activation (Figure 3.5A). Upon washout, the mitochondrial network recovers (Figure 3.5A). This data shows anastatic cells recover from mitochondrial collapse.

Qualitatively, a variety of mitochondrial morphologies are observed in recovered cells when caspase activity is blocked with 10μM QVD (Figure 3.6). Cells surviving STS exposure alone mostly show healthy interconnected mitochondria (Figure 3.6A). Recovery following STS-10μM QVD resulted in at least three classes of mitochondrial phenotypes – fragmentated (Figure 3.6B), fused (Figure 3.6C), and perinuclear (Figure

3.6D). This suggests that limiting caspase activity, during STS exposure, allows for cellular viability downstream of MOMP yielding a variety of mitochondrial states.

As mentioned previously, both mitochondrial fusion and fission can have pro-survival effects. We propose that in response to STS, robust caspase activation succeeds MOMP usually resulting in cell death. Limiting caspase activity allows for survival with mitochondrial damage. The data suggests a heterogenous response to MOMP. We hypothesize that cells fragment individually damaged mitochondrion for recycling and fuse mitochondria together to preserve energy output. We conclude that mitochondrial reorganization enhances survival during anastasis.

One limitation of our interpretation is that we cannot formally rule out the possibility that fragmentation, fusion, or perinuclear accumulation of mitochondria represent transient states at different stages of recovery. To follow up on our hypothesis that mitochondrial fusion may function to preserve energy output, we next tested if anastatic cells maintain mitochondrial activity.

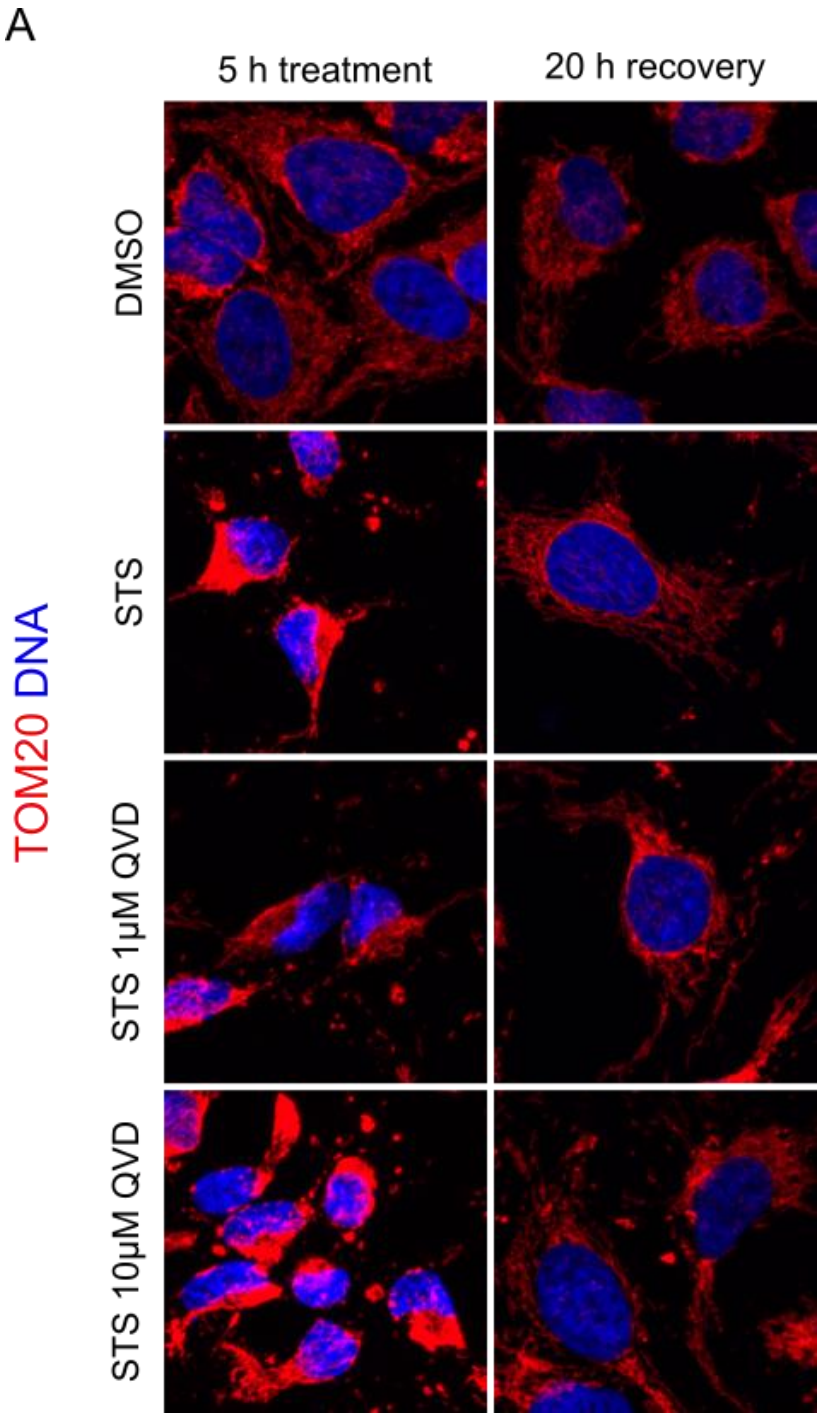

FIGURE 3.5: Mitochondrial organization in anastatic cells. (A) Immunofluorescent antibody staining for Tom20 (red) with Dapi stain (blue). HeLa cells were treated for 5 h with indicated treatment or recovered for 20 h after 5 h of indicated treatment. Maximum intensity projections are shown. Staining and imaging was performed by Maddalena Nano.

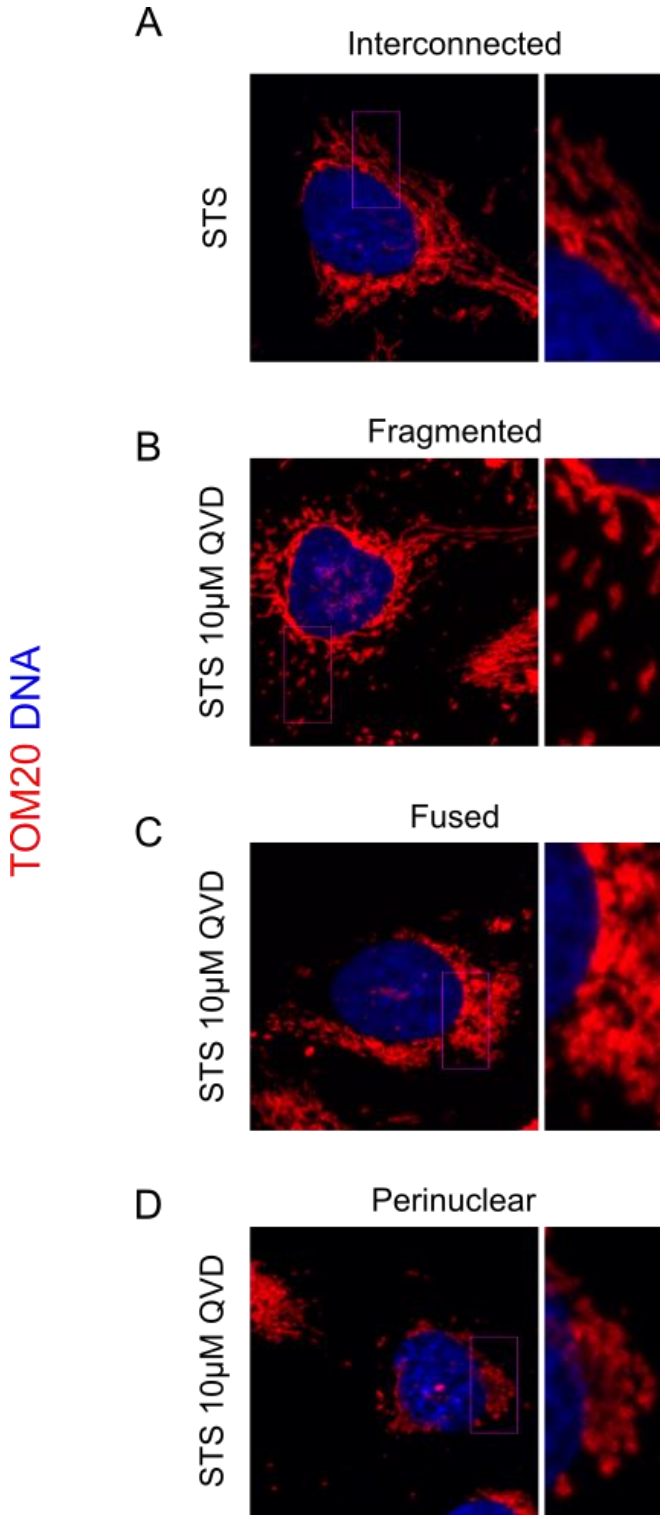

FIGURE 3.6 Mitochondria morphologies following STS 10μM QVD exposure. Immunofluorescent antibody staining for Tom20 (red) with Dapi stain (blue). All cells were treated for 5 h with indicated treatment and recovered for 20 h followed by staining. (A) HeLa cells surviving STS alone show interconnected healthy mitochondria. HeLa cells surviving STS 10μM QVD exposure show fragmented (B), fused (C), and perinuclear (D) mitochondrial morphologies. Pink box denotes the higher magnification crop shown at right.

Anastatic Cells are Characterized by Loss of ΔΨm

Mitochondrial damage and the dramatic changes in mitochondrial morphology raised the question as to whether anastatic cells maintain mitochondrial function. Mitochondria produce energy by generating an electrochemical protein motive force across their membrane. So, we used the cationic dye tetramethylrhodamine methyl ester (TMRM), which accumulates in proportion to the magnitude of the mitochondrial membrane potential (ΔΨm) (Ehrenberg et al., 1988).

Cells recovering from STS readily take up TMRM, suggesting mitochondria are functional (Figure 3.7A). Addition of 1μM QVD resulted in a population of TMRM-negative cells (Figure 3.7, A and B). Increasing to 10μM QVD reduces the proportion of cells generating ΔΨm even further (Figure 3.7B). These preliminary data suggests that caspase inhibition enriches for low-ΔΨm cells. Together with our MOMP data, we conclude that QVD limits caspase activity downstream of MOMP permitting cells to survive with mitochondrial dysfunction. We next asked if low-ΔΨm cells remain viable days following initial stress.

Low-ΔΨm Cells Persist and Show Healthy Nuclear Morphology

To test if low-ΔΨm cells remain viable, we visualized ΔΨm at 3 d recovery following apoptotic stress. Surviving cells show a strong TMRM signal (Figure 3.8A). Addition of QVD again resulted in recovered cells maintaining low-ΔΨm even after 3 d recovery (Figure 3.8A) and 10μM QVD again increased the percentage of cells lacking strong ΔΨm (Figure 3.8A and B). Strikingly, cells with low-ΔΨm maintained healthy nuclear morphology when compared to cells with high-ΔΨm and the percentage of cells with

nuclear defects decreased with increasing QVD concentration (Figure 3.8A and C). Of importance, loss of ΔΨm is not due to mitochondrial loss (Figure 3.9). This suggests that low-ΔΨm cells are viable long-term and maintain healthy nuclei.

Taken together, the morphological data and ΔΨm results show that anastatic cells survive MOMP, show low mitochondrial activity, and maintain healthy nuclear structure. From this data, we conclude that decreased mitochondrial respiration occurs during anastasis and benefits the long-term health of the cell.

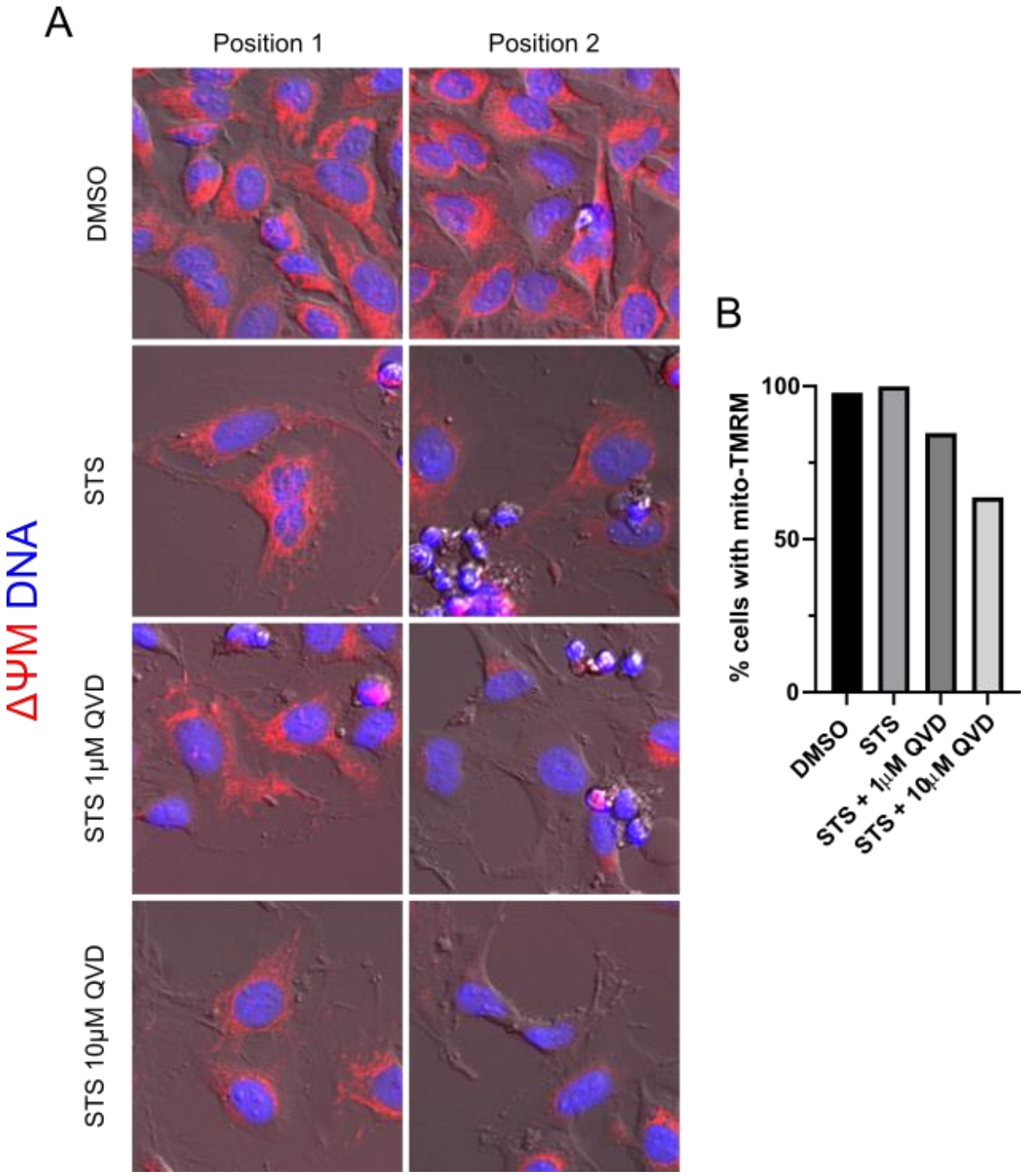

FIGURE 3.7: Caspase inhibition selects for cell state characterized by loss of ΔΨm. (A) Live-cell imaging of HeLa cells at 20 h recovery following 5 h of indicated treatments. DNA shown in blue and TMRM shown in red. Position 1 shows cells of robust TMRM staining. Position 2 shows examples of cells showing low TMRM staining. (B) Preliminary quantification of cells showing TMRM staining at 20 h recovery.

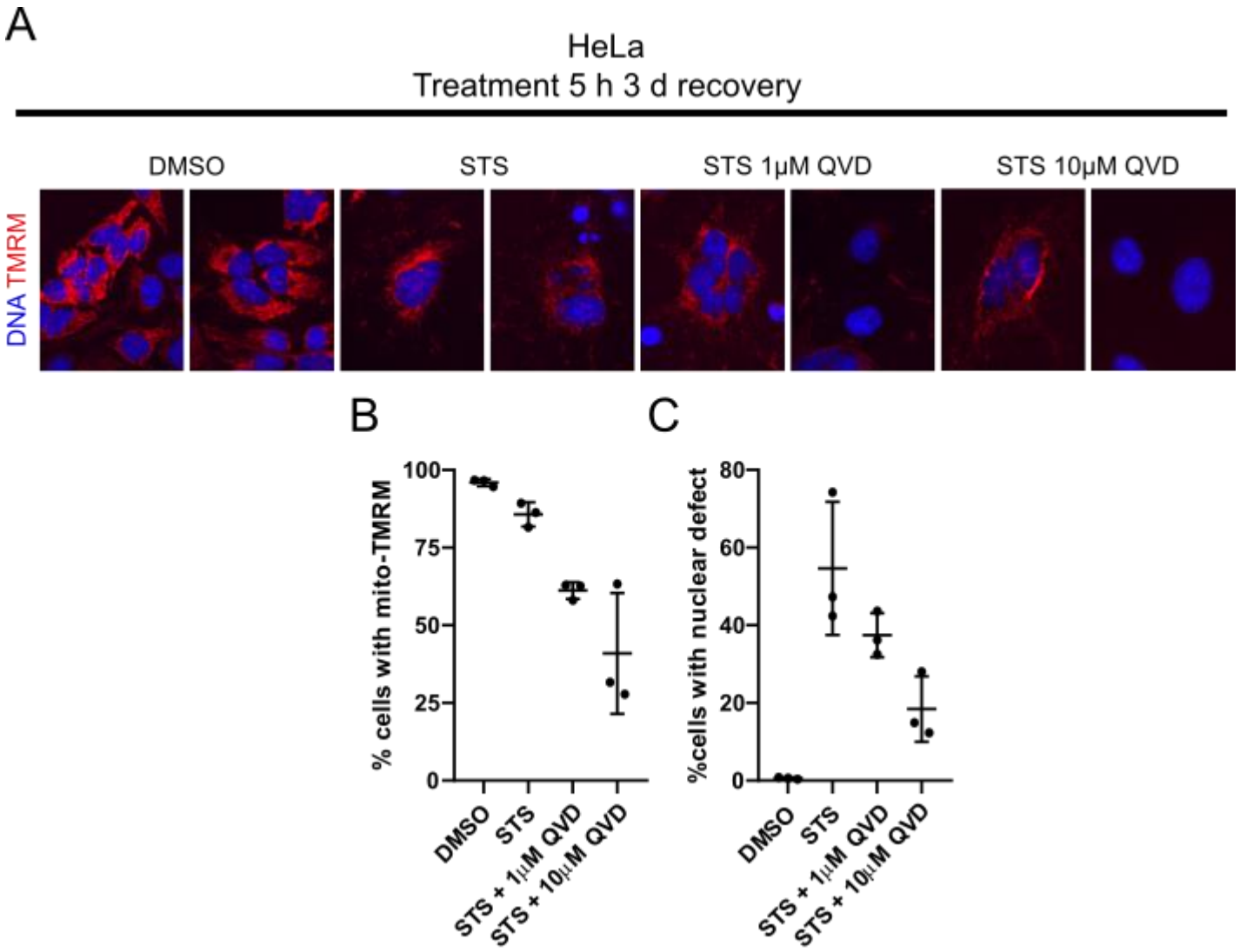

FIGURE 3.8: Low-ΔΨm cells persist for 3 d and show healthy nuclear morphology. (A) Live-cell imaging of HeLa cells at 3 d recovery following 5 h of indicated treatments. DNA shown in blue and TMRM shown in red. Two separately cropped locations are shown for each condition. (B) Quantification of cells showing TMRM staining. (C) Quantification of cells showing nuclear defects. Quantifications exclude dead cells, and each dot represents an independent experiment. Error bars denote SD.

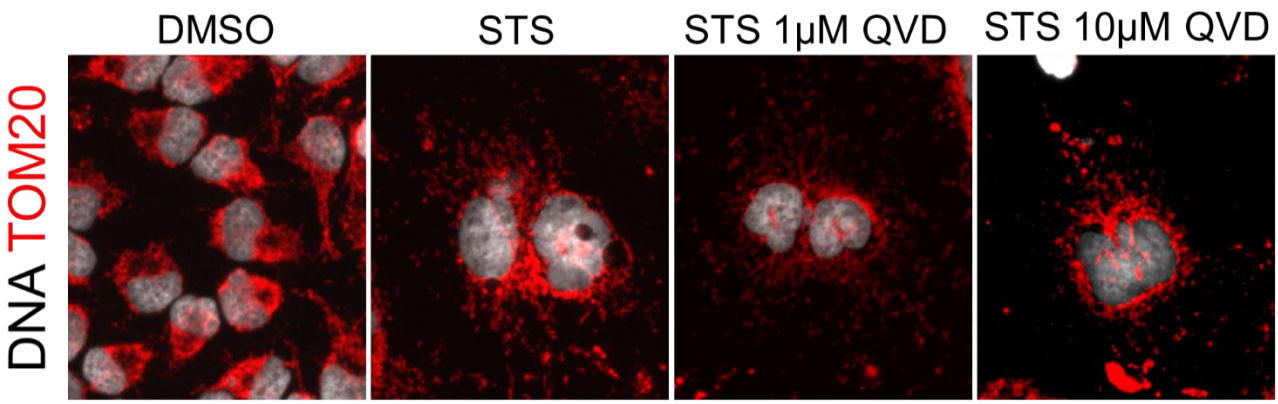

FIGURE 3.9: Loss of overall mitochondrial membrane potential is not due to loss of mitochondria. Fixed-cell imaging of HeLa cells at 3 d recovery following 5 h treatment of indicated treatments. DNA is shown in grey and Tom20 is shown in red.

Discussion

Here we report major mitochondrial events throughout anastasis. We found that limiting caspase activity by QVD promotes anastasis (Figure 3.1). Previously identified “early response” genes are also upregulated during STS-QVD anastasis (Figure 3.2). Without QVD, surviving cells induce a senescent-like state and enlarge 2X to 4X in area (Figure 3.3). Further, anastatic cells survive mitochondrial damage and recover from mitochondrial collapse (Figure 3.4 and 3.5). Strikingly, provided caspases are limited, surviving cells are characterize by loss in ΔΨm (Figure 3.7). These cells remain viable for 3 d following stress and low ΔΨm correlated with nuclear healthy (Figure 3.8). Collectively, our data reveal that cells surviving sublethal caspase activity are characterized by a loss in mitochondrial activity.

Previous work has reported that mitochondria remain functional after MOMP and use cytosolic cytochrome c to transiently recover ΔΨm, however, eventually the authors observe a loss in ATP production and cell death (Waterhouse et al., 2001). Sympathetic neurons can survive cytochrome c release, but recovery is not observed after ΔΨm loss and MOMP is reported to kill cells from loss of mitochondrial respiration (Deshmukh et al., 2000; Lartigue at al., 2009). Our data reveal an unexpected aspect of apoptosis recovery. Cancer cells recovering from transient caspase activity survive with mitochondrial dysfunction and maintain healthy nuclear morphology. This data suggests that cancer cells not only survive with mitochondrial dysfunction but that this benefits nuclear health.

Cellular recovery despite mitochondrial dysfunction is surprising, however, metabolic reprogramming is a hallmark of cancer (Hanahan and Weinberg 2011). Otto Warburg first observed that despite the presence of oxygen, tumor cells preferentially perform glycolysis and hypothesized that this occurs due to mitochondrial dysfunction (Warburg et al., 1927; Warburg 1956). The function of aerobic glycolysis or the “Warburg Effect” in tumorigenesis remains controversial as many cancer cells typically maintain healthy mitochondrial networks and can perform mitochondrial respiration (Liberti and Locasale 2016).

Glucose metabolism has been linked to suppression of apoptosis. In HeLa cells, glucose metabolism through the pentose phosphate pathway results in the reduced form of cytochrome c which is less efficient at inducing apoptosis and glucose deprivation increases sensitivity to cytochrome c induced apoptosis (Vaughn and Deshmukh 2008). Additional studies show that increased glucose uptake stabilizes the anti-apoptotic Bcl-2 protein Mcl-1 and suppresses pro-apoptotic Bcl-2 family protein Puma upregulation during growth factor withdrawal (Zhao et al., 2007; Zhao et al., 2008). In line with this work, we show that cancer cells experiencing MOMP lose ΔΨm yet persist. We hypothesize that anastatic cells upregulate glycolysis even further as a result of mitochondrial damage to maintain energy demands and suppress apoptosis. Our data suggest that cell survival is dictated by caspase activity, however, we cannot formally rule out the role of the redox state of cytochrome c. Altogether, our study reveals a previously unrecognized relationship between anastasis and mitochondrial respiration.

Future work is necessary to determine if anastatic cells are in fact more glycolytic, if mitochondrial dysfunction is pro-survival, to determine the physiological relevance of this cell state, and to study if loss of ΔΨm represents a general anastatic phenotype or is specific to HeLa cells in response to STS.

Materials and Methods

Further information and resource requests should be directed and will be fulfilled by the corresponding author Denise J. Montell (dmontell@ucsb.edu).

Expression constructs, transfection, and stable cell lines

For transient transfection, cells were transfected using Xtreme Gene transfection reagent (Sigma). The GC3Ai caspase reporter plasmid was obtained from B. Li (Tianjin Medical University, Tianjin, China). The plasmid was delivered by lentivirus and selected using puromycin (Thermo Fisher Scientific) to obtain stable cell lines. Monoclonal cell lines were generated by serial dilution.

Mammalian cell culture

Human cervical carcinoma HeLa cells (cell line CCL-2; ATCC) were purchased from the American Type Culture Collection (Manssas, VA). The cells were maintained in high glucose (4.5g/L) DMEM (Gibco) supplemented with GlutaMAX (Thermo Fisher Scientific) and 10% FBS (Sigma) at 37°C with 5% CO2 and 90% humidity. All cells were passaged by trypsinization (Trypsin-EDTA; Gibco). Cells were seeded onto tissue culture plates for at least 1 d allowing growth to 70% confluency before experimentation. Culture medium was exchanged every 24-36 h. Apoptosis was induced using 250nM STS ± 1μM QVD. For washout, media was carefully removed by aspiration and cells were washed twice with warm culture medium. Control cells were treated with 0.1% - 0.2% DMSO at the same time as experiment groups.

Flow cytometry and fluorescence activated cell sorting

Cells were grown in T75 flasks. After treatment, cellular debris was removed by a PBS wash, cells were harvested by trypsinization, spun down, and resuspended in either culture medium or PBS. Cells were incubated with 1µg/mL propidium iodide (PI) for 10 min before samples were analyzed. For each sample, at least 10,000 cells were evaluated. For cell sorting, gates were created to select for singlets and at least 100,000 cells were sorted. Data was collected on either the Accuri BD Cytometer or Sony FACS.

Immunofluorescence antibody staining and fluorescence microscopy

200K cells per well were seeded onto coverslips in 6 well culture plates. At 70% confluency, cells were treated as indicated followed by fixation with 4% paraformaldehyde for 15 min at room temperature (RT). After fixation, samples were blocked at RT for 30 min (5% normal goat serum in PBS). After blocking, samples were incubated in primary antibodies overnight followed by incubation in secondary antibodies for 30 min at RT. Samples were mounted in media containing DAPI. Images were acquired on an DMi8 microscope (Leica). Treatment and staining were repeated at least three independent times and representative images are shown in figures. At least 5 randomly selected fields were imaged per sample.

Live-cell microscopy

150K-200K cells were seeded onto 35-mm glass bottom dishes (MatTek Corporation) and allowed to grow overnight. At 70% confluency, cells were placed onto Leica DMi8 incubator chambers with temperature and CO2 control and allowed to equilibrate for 10

min before experimentation. At least 5 random fields per sample were selected for live imaging.

Image analysis and statistics

Two-tailed Student's t test with Welch's correction was performed for comparison between two groups. Differences were considered statistically significant if p value was <0.05. Statistical analysis and data visualization was performed in GraphPad Prism software.

References

Berthenet, K, Castillo Ferrer, C, Fanfone, D, Popgeorgiev, N, Neves, D, Bertolino, P, Gibert, B, Hernandez-Vargas, H, and Ichim, G (2020). Failed Apoptosis Enhances Melanoma Cancer Cell Aggressiveness. Cell Reports 31, 107731.

Cartwright, IM, Liu, X, Zhou, M, Li, F, and Li, C-Y (2017). Essential roles of Caspase-3 in facilitating Myc-induced genetic instability and carcinogenesis. ELife 6, e26371.

Deshmukh, M, Kuida, K, and Johnson, EM (2000). Caspase Inhibition Extends the Commitment to Neuronal Death Beyond Cytochrome c Release to the Point of Mitochondrial Depolarization. Journal of Cell Biology 150, 131–144.

Ding, AX, Sun, G, Argaw, YG, Wong, JO, Easwaran, S, and Montell, DJ (2016). CasExpress reveals widespread and diverse patterns of cell survival of caspase-3 activation during development in vivo. ELife 5, e10936.

Ehrenberg, B, Montana, V, Wei, MD, Wuskell, JP, and Loew, LM (1988). Membrane potential can be determined in individual cells from the nernstian distribution of cationic dyes. Biophysical Journal 53, 785–794.

Goldstein, JC, Waterhouse, NJ, Juin, P, Evan, GI, and Green, DR (2000). The coordinate release of cytochrome c during apoptosis is rapid, complete and kinetically invariant. Nat Cell Biol 2, 156–162.

Hanahan, D, and Weinberg, RA (2011). Hallmarks of Cancer: The Next Generation. Cell 144, 646–674.

Ichim, G et al. (2015). Limited Mitochondrial Permeabilization Causes DNA Damage and Genomic Instability in the Absence of Cell Death. Molecular Cell 57, 860–872.

Lartigue, L, Kushnareva, Y, Seong, Y, Lin, H, Faustin, B, and Newmeyer, DD (2009). Caspase-independent Mitochondrial Cell Death Results from Loss of Respiration, Not Cytotoxic Protein Release. MBoC 20, 4871–4884.

Liberti, MV, and Locasale, JW (2016). The Warburg Effect: How Does it Benefit Cancer Cells? Trends in Biochemical Sciences 41, 211–218.

Liu, X, He, Y, Li, F, Huang, Q, Kato, TA, Hall, RP, and Li, C-Y (2015). Caspase-3 Promotes Genetic Instability and Carcinogenesis. Molecular Cell 58, 284–296.

Mackenzie, AB, Young, MT, Adinolfi, E, and Surprenant, A (2005). Pseudoapoptosis Induced by Brief Activation of ATP-gated P2X $_7$ Receptors. J Biol Chem 280, 33968–33976.

Otera, H, and Mihara, K (2012). Mitochondrial Dynamics: Functional Link with Apoptosis. International Journal of Cell Biology 2012, 1–10.

Pandya, V, Githaka, JM, Patel, N, Veldhoen, R, Hugh, J, Damaraju, S, McMullen, T, Mackey, J, and Goping, IS (2020). BIK drives an aggressive breast cancer phenotype through sublethal apoptosis and predicts poor prognosis of ER-positive breast cancer. Cell Death Dis 11, 448.

Raina, AK, Hochman, A, Zhu, X, Rottkamp, CA, Nunomura, A, Siedlak, SL, Boux, H, Castellani, RJ, Perry, G, and Smith, MA (2001). Abortive apoptosis in Alzheimer's disease. Acta Neuropathol 101, 305–310.

Roux, J, Hafner, M, Bandara, S, Sims, JJ, Hudson, H, Chai, D, and Sorger, PK (2015). Fractional killing arises from cell-to-cell variability in overcoming a caspase activity threshold. Mol Syst Biol 11, 803.

Seervi, M, Sumi, S, Chandrasekharan, A, Sharma, AK, and Santhosh Kumar, TR (2019). Molecular profiling of anastatic cancer cells: potential role of the nuclear export pathway. Cell Oncol 42, 645–661.

Sun, G, Ding, XA, Argaw, Y, Guo, X, and Montell, DJ (2020). Akt1 and dCIZ1 promote cell survival from apoptotic caspase activation during regeneration and oncogenic overgrowth. Nat Commun 11, 5726.

Sun, G, Guzman, E, Balasanyan, V, Conner, CM, Wong, K, Zhou, HR, Kosik, KS, and Montell, DJ (2017). A molecular signature for anastasis, recovery from the brink of apoptotic cell death. Journal of Cell Biology 216, 3355–3368.

Tait, SWG, and Green, DR (2008). Caspase-independent cell death: leaving the set without the final cut. Oncogene 27, 6452–6461.

Tait, SWG, Parsons, MJ, Llambi, F, Bouchier-Hayes, L, Connell, S, Muñoz-Pinedo, C, and Green, DR (2010). Resistance to Caspase-Independent Cell Death Requires Persistence of Intact Mitochondria. Developmental Cell 18, 802–813.

Tang, HL et al. (2012). Cell survival, DNA damage, and oncogenic transformation after a transient and reversible apoptotic response. MBoC 23, 2240–2252.

Tang, HL, Tang, HM, Fung, MC, and Hardwick, JM (2015). In vivo CaspaseTracker biosensor system for detecting anastasis and non-apoptotic caspase activity. Sci Rep 5, 9015.

Vaughn, AE, and Deshmukh, M (2008). Glucose metabolism inhibits apoptosis in neurons and cancer cells by redox inactivation of cytochrome c. Nat Cell Biol 10, 1477–1483.

Warburg, O (1956). On the Origin of Cancer Cells. Science 123, 309–314.

Warburg, O, Wind, F, and Negelein, E (1927). THE METABOLISM OF TUMORS IN THE BODY. Journal of General Physiology 8, 519–530.

Waterhouse, NJ, Goldstein, JC, von Ahsen, O, Schuler, M, Newmeyer, DD, and Green, DR (2001). Cytochrome C Maintains Mitochondrial Transmembrane Potential and Atp Generation after Outer Mitochondrial Membrane Permeabilization during the Apoptotic Process. Journal of Cell Biology 153, 319–328.

Xu, Y et al. (2020). Bile acid-induced “Minority MOMP” promotes esophageal carcinogenesis while maintaining apoptotic resistance via Mcl-1. Oncogene 39, 877–890.

Youle, RJ, and van der Bliek, AM (2012). Mitochondrial Fission, Fusion, and Stress. Science 337, 1062–1065.

Youle, RJ, and Karbowski, M (2005). Mitochondrial fission in apoptosis. Nat Rev Mol Cell Biol 6, 657–663.

Zhang, J et al. (2013). Visualization of caspase-3-like activity in cells using a genetically encoded fluorescent biosensor activated by protein cleavage. Nat Commun 4, 2157.

Zhao, Y et al. (2007). Glycogen Synthase Kinase 3α and 3β Mediate a Glucose-Sensitive Antiapoptotic Signaling Pathway To Stabilize Mcl-1. MCB 27, 4328–4339.

Zhao, Y, Coloff, JL, Ferguson, EC, Jacobs, SR, Cui, K, and Rathmell, JC (2008). Glucose Metabolism Attenuates p53 and Puma-dependent Cell Death upon Growth Factor Deprivation. Journal of Biological Chemistry 283, 36344–36353.

IV. Open Questions and Additional Observations

Introduction

This chapter includes a more detailed discussion of metabolic reprogramming in cancer, open questions from chapter 3, and presents experiments to help address them. I also discuss preliminary observations I made during my study. This includes preliminary work on the Golgi complex in anastatic cells, tracking cell cannibalism, and imaging of ESCRT proteins during STS treatment.

The Warburg Effect and Open Questions

Otto Warburg observed that tumors preferentially perform glycolysis even in the presence of oxygen, coining the term aerobic glycolysis, and attributed this to permanent mitochondrial dysfunction (Warburg 1956). Even though aerobic glycolysis is observed in most cancers, drives malignant progression and is associated with poor prognosis, cancer cell mitochondria are typically intact and functional (Gaude and Frezza 2016; Vaupel et al., 2019). Consistently, upon inhibition of glycolysis, some cancer cells can adapt and upregulate oxidative phosphorylation (McGuirk et al., 2020) and our data show that control HeLa cells readily uptake TMRM (Figure 3.7). This raises interesting questions about the functional advantage of aerobic glycolysis and its origin.

Cancer is thought of as a genetic disease with mutations in oncogenes and tumor suppressors principally driving tumorigenesis (National Cancer Institute; Alexandrov et al., 2013). Many of the most commonly mutated genes in cancer can impact metabolism directly or indirectly. For example, KRAS mutations are associated with enhanced glycolysis, MYC directly upregulates expression of hexokinase II and glucose transport I, and wild type p53 represses expression of the glucose transport genes GLUT1 and GLUT4 (Luo et al., 2020). Recent data show that in some cancers, mutations in metabolic genes themselves can drive tumorigenesis (Schmidt et al., 2020). The consensus is that mutations in genes regulating metabolism result in mitochondrial dysfunction and a shift to aerobic glycolysis.

Our data suggests an interesting possibility – transient apoptotic stress results in mitochondrial permeabilization forcing a metabolic shift toward glycolysis. This may be important in the context of chemotherapy. Most chemotherapeutic agents kill cancer cells by inducing apoptosis; however, relapse remains a major problem. As mentioned in chapter 2, anastatic cells upregulate aggressive properties such as motility and expression of angiogenesis genes and the rate of cancer recurrence is positively correlated with amount of active caspase 3. Cancer cells surviving chemotherapy may survive with mitochondrial damage, upregulate glycolysis even further in response, and acquire aggressive characteristics. Future research is necessary to tease apart the relationship between anastasis and metabolic reprogramming in cancer.

Next, we discuss some open questions and present experiments to help address them.

Are anastatic cancer cells more glycolytic?

We hypothesize that loss of mitochondrial membrane potential (ΔΨm) corresponds with decreased mitochondrial respiration and increased glycolysis. To test this directly, a metabolic assessment using a Seahorse XFe96 Analyzer (Agilent) instrument may be performed. If our hypothesis is correct, we expect to see increased extracellular acidification rate (ECAR) and a decreased oxygen consumption rate (OCR). If this is observed, it would be of great interest to test if anastatic cells rely on increased glycolysis for recovery. To test this, addition of glycolysis inhibitors, such as 2-Deoxy-D-Glucose (2-DG), may be added. It is critical to troubleshoot concentrations of inhibitors that do not impact HeLa cell viability prior to STS exposure.

Is loss of ΔΨm a consequence of MOMP?

We have shown that QVD selects for sublethal caspase activity promoting anastasis (Figure 3.1) and that these cells survive mitochondrial damage (Figure 3.4). During STS exposure, MOMP, caspase activation, kinase inhibition, and a stress response are all occurring. It is not clear which event, or combination of events, dictates loss of ΔΨm.

A first hypothesis is that mitochondrial damage results in dysfunction causing loss of ΔΨm. However, mitochondrial damage is observed in both STS and STS-QVD conditions, yet loss of ΔΨm is only observed in STS-QVD recovered cells. Our data does suggest that QVD permits recovery with mitochondrial damage whereas cells likely die from STS induced MOMP. To directly test if ΔΨm loss is consequence of MOMP,

overexpression of Bcl-2 or Bcl-xL or knockdown of Bax and Bak may prevent MOMP in response to STS. ΔΨm then may be measured in cells surviving STS stress independent of MOMP. If our hypothesis is correct, ΔΨm loss will no longer be observed without MOMP.

Another approach may be to artificially induce caspase activity itself. Chemical dimerization techniques can activate caspases directly (Straathof et al., 2005). Using this system, we can ask if ΔΨm loss occurs after transient caspase activity itself. In theory, direct activation of caspases would not induce MOMP and kinase inhibition which is seen during STS treatment.

Are anastatic cancer cells with low-ΔΨm more aggressive?

Another open question concerns the significance of low ΔΨm for cancer cells. It is unknown how low ΔΨm cancer cells compare to high ΔΨm cells phenotypically. To address this, cell sorting may be performed based on TMRM or other mitochondrial membrane potential dyes such as JC-1. After sorting has separated low from high-ΔΨm cells, cells can be assessed for proliferation, motility, expression of angiogenesis genes, and resistance to a second exposure of STS. If we hypothesize that low ΔΨm cancer cells are more aggressive, we expect to see higher rates of proliferation, increases motility, upregulation of angiogenesis factors, and/or acquisition of resistance to STS.

The physiological relevance of anastatic cells has not been studied. HeLa cells upregulate motility during EtOH anastasis, however, if this enhances metastasis *in vivo* is unknown.

Xenograft experiments and tracking of anastasis in tumorigenesis models should be performed.

Are mitochondrial-nuclear interactions required for nuclear defect phenotype?

Mitochondrial retrograde response (MRR) refers to communication between the mitochondria and nucleus (Butow and Avadhani 2004). Consistent with our data (Figure 3.6), a study shows that STS treatment results in mitochondria accumulation around the nucleus and this induces the nuclear accumulation of NF-kB and expression of pro-survival genes (Desai et al., 2020). The translocator protein (TSPO) is required for this interaction (Desai et al., 2020). Experimentally, mitochondria-nuclear communication can be blocked by knockdown of TSPO. If MMR is required for our observed nuclear defects, we would expect to see a reduction of nuclear deformities in anastatic cells with TSPO knockdown.

Is loss of ΔΨm a general property of anastatic cells? Does it occur in response to chemotherapy?

It is unknown if loss of ΔΨm represents a general characteristic of anastatic cells or is specific to STS treatment or even possibly specific to HeLa cells. Mitochondrial activity and metabolic changes should be measured in anastatic cells of different cancer cell types in response to different apoptotic stresses.

Next, we discuss preliminary observations that may serve as jumping off point for future work.

The Golgi Apparatus in Anastatic Cells

The Golgi is an essential organelle for protein and lipid trafficking and modification (Day et al., 2013). Local recruitment of apoptotic machinery can occur at organelles distinct from mitochondria including the Golgi (Ferri and Kreomer 2001). Additionally, fragmentation of the Golgi has been observed during STS induced apoptosis (Mukherjee et al., 2007). However, the Golgi complex has not been studied during anastasis.

To gain insight into Golgi structure during anastasis, we visualized trans-golgi network protein 2 (TGN46). We observed increased Golgi mass in surviving cells (Figure 4.1). This occurred with and without QVD, suggesting that increased Golgi mass occurs generally in response to STS and does not require caspase activity (Figure 4.1).

Increased Golgi mass occurs in HeLa cells during interphase and Golgi dispersal is observed in senescent HeLa cells following BrdU treatment (Cho et al., 2011; Sin and Harrison 2016). Taken together with our cell size data in chapter 3, we hypothesize that some cells become senescent following transient STS exposure. Future work should be aimed at deciphering the relationship between anastasis and senescence and test the requirement of Golgi expansion for anastasis.

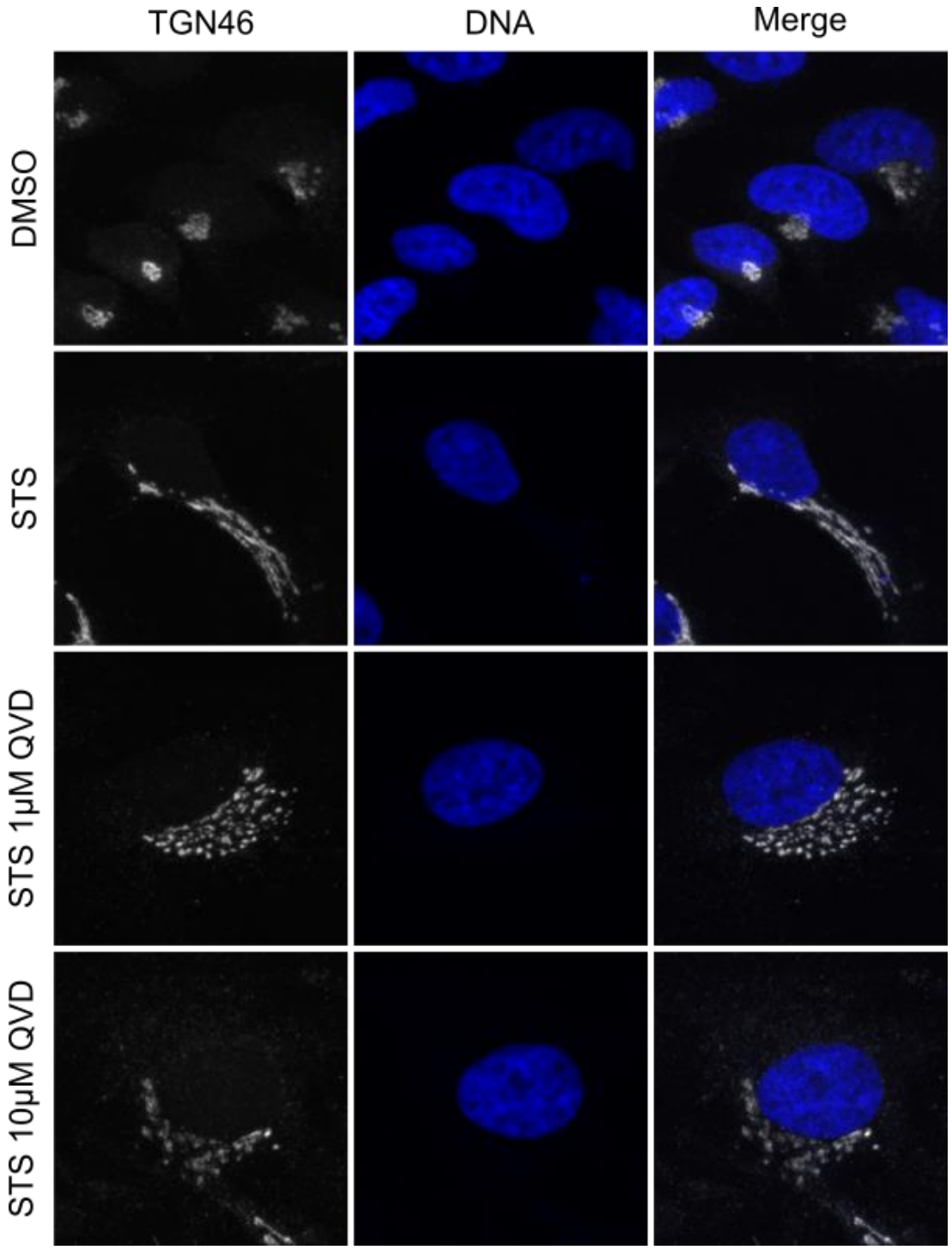

FIGURE 4.1 The Golgi apparatus in anastatic cells. Following 5 h of indicated treatments, HeLa cells were recovered for 20 h followed by fixation and staining for TGN46 (grey) and Dapi (blue).

Stress Induced Cancer Cell Cannibalism

Cells have been observed to engulf each other during processes termed entosis and phagoptosis (Overholtzer et al., 2007; Brown and Neher 2012). Another report shows that chemotherapy-induced senescent cancer cells engulf each other (Tonnessen-Murray et al., 2019). We hypothesized that anastatic cells may also turn on their neighbors and engulf.

To test this, we generated HeLa and breast cancer MCF-7 cells stably expressing an mCherry-conjugated marker. We then created co-cultures of recovered mCherry cells together with untreated, unlabeled cells. We did not observe HeLa cell on cell engulfment following STS exposure. Strikingly, we did observe nuclei inside gaps of mCherry cytosol of MCF-7 cells recovered after transient exposure to paclitaxel (Figure 4.2A).

We observed examples of cells engulfing multiple untreated cells and degradation of engulfed cell nuclei (Figure 4.2A, 4.2B, and 4.2C). We observed that longer co-culture incubation time resulted in higher engulfment frequencies (Figure 4.2B, bar graph). Engulfment was also documented in colon cancer HCT-116 cells (Figure 4.C). These preliminary data, together with previous reports, suggest that engulfment represents a stress induced phenotype and may function as a survival mechanism. Future work should be aimed at deciphering the relationship between caspases, anastasis, and cell cannibalism.

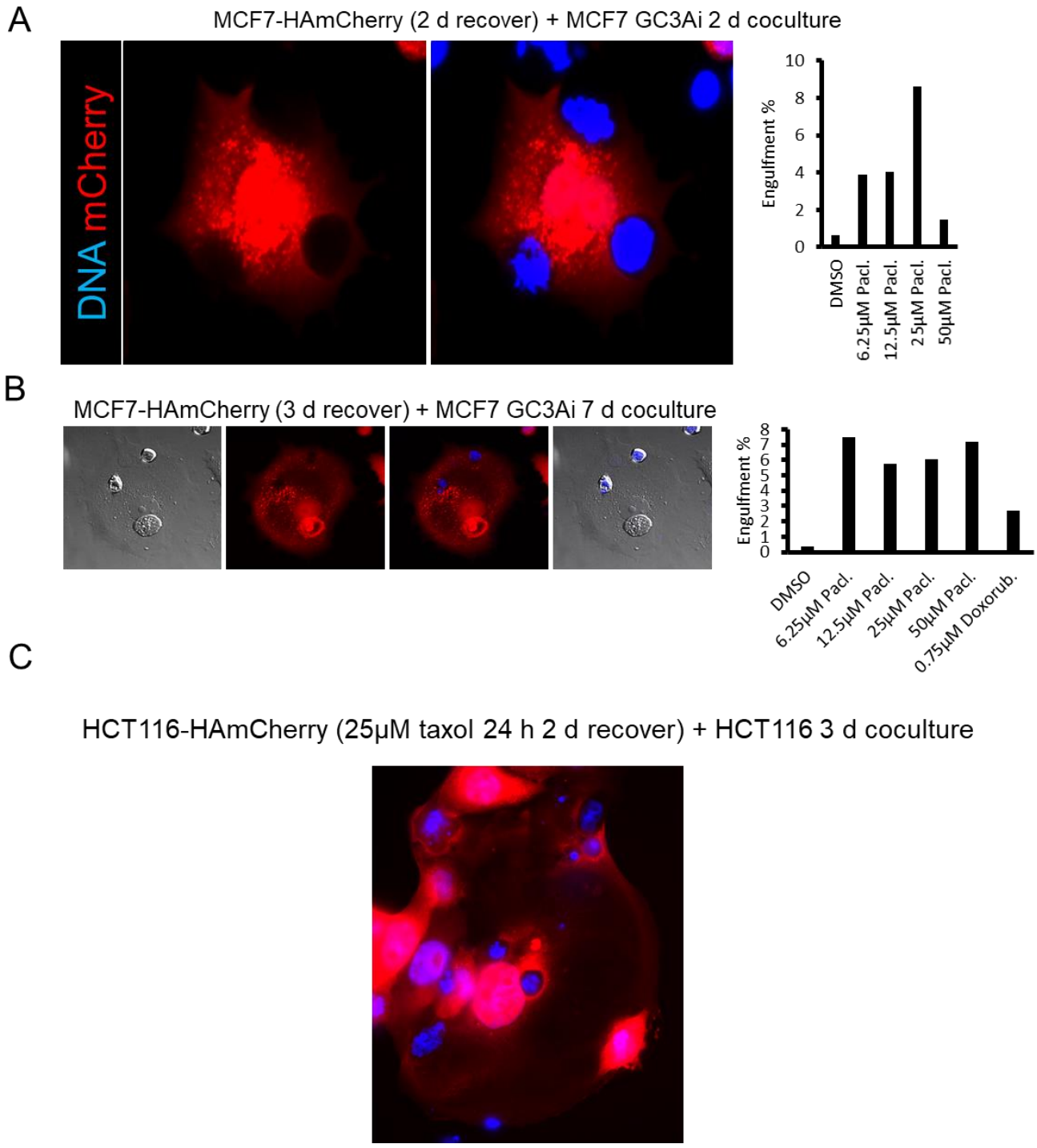

FIGURE 4.2 Stress induced cancer cell cannibalism. (A) Fixed imaging of mCherry MCF-7 cells treated with paclitaxel for 24 h followed by 2 d recovery and 2 d co culture with untreated unlabeled MCF-7 cells. Quantification shows engulfment percentage of MCF-7 cells treated and recovered from indicated paclitaxel concentrations. (B) Engulfment percentage is increased with longer recovery time and co-culture time. (C) Example of HCT-116 cell engulfing multiple untreated unlabeled HCT-116 cells.

Imaging of ESCRT Proteins During STS Treatment

The endosomal sorting complex required for transport (ESCRT) machinery functions in a variety of cellular processes including biogenesis of endosomes and cytokinetic abscission (Christ et al., 2017). The ESCRT machinery repairs plasma membrane wounds following laser damage (Jimenez et al., 2014). Recent work has shown ESCRT mediated membrane repair during necroptotic and pyroptotic induction (Gong et al., 2017a; 2017b; and Ruhl et al., 2018). In this work, ESCRT proteins counteract necroptotic and pyroptotic machinery to maintain cellular integrity. Classically, apoptosis does not result in damage to the plasma membrane, however, mitochondria permeabilization occurs. This leaves an interesting hypothesis – do cancer cells use the endosomal machinery to repair mitochondrial wounds?

Rab endosomal machinery can regulate mitophagy and Rab5 is recruited to mitochondria during apoptotic stress (Hammerling et al., 2017; Hsu et al., 2018; and Yamano et al., 2018). Additionally, overexpression of Rab5 slowed hydrogen peroxide induced cytochrome c release (Hsu et al., 2018). Rab5 machinery may involve the recruitment of ESCRT machinery to repair mitochondria wounds. To test this, I imaged a series of GFP-tagged ESCRT proteins in response to STS. The ESCRT components CHMP4B, VPS4A, or CHMP4C did not form puncta and no increase in mitochondrial localization was observed in response to STS (Figure 4.3A and B). Puncta formation of CHMP1B was observed prior to loss of mitochondrial membrane potential (Figure 4.3C). This preliminary data suggests CHMP1B may function to repair STS induced damage. Future work should be aimed to test the requirement of CHMP1B for anastasis.

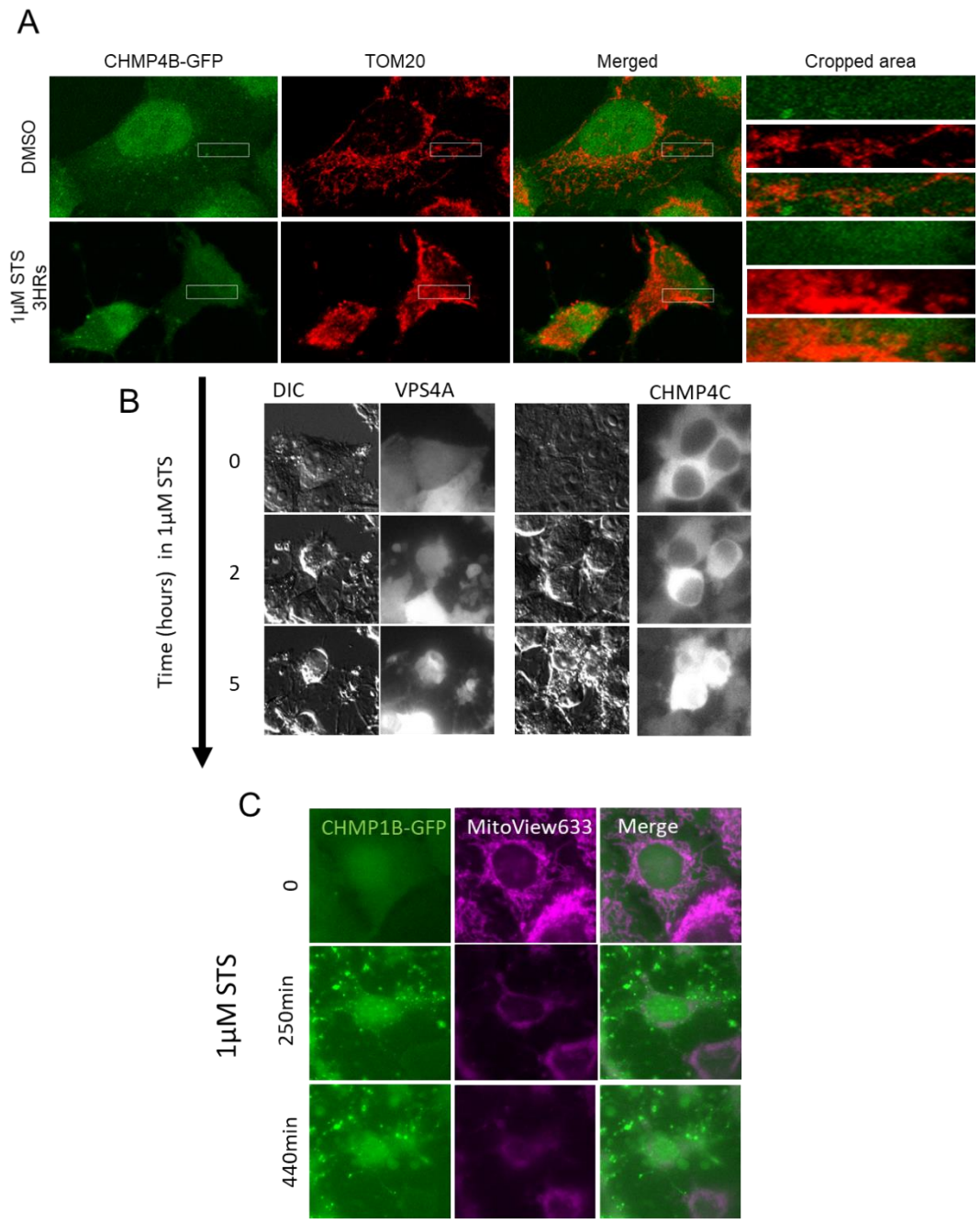

FIGURE 4.3 Imaging of ESCRT proteins during STS treatment. (A) HeLa-CHMP4B GFP cells were treated with either DMSO or STS for 3 h followed by fixed imaging. CHMP4B (green) and Tom20 (red) are shown. Box denote cropped area shown at right. (B) Live-cell imaging of HeLa-VPS4A or HeLa-CHMP4C response to STS. (C) Live-cell imaging of HeLa-CHMP1B GFP cells incubated with MitoView633 (magenta) in response to STS.

References

Alexandrov, LB et al. (2013). Signatures of mutational processes in human cancer. Nature 500, 415–421.

Brown, GC, and Neher, JJ (2012). Eaten alive! Cell death by primary phagocytosis: 'phagoptosis.' Trends in Biochemical Sciences 37, 325–332.

Butow, RA, and Avadhani, NG (2004). Mitochondrial Signaling. Molecular Cell 14, 1–15.

Cho, J-H, Saini, DK, Karunarathne, WKA, Kalyanaraman, V, and Gautam, N (2011). Alteration of Golgi structure in senescent cells and its regulation by a G protein γ subunit. Cellular Signalling 23, 785–793.

Christ, L, Raiborg, C, Wenzel, EM, Campsteijn, C, and Stenmark, H (2017). Cellular Functions and Molecular Mechanisms of the ESCRT Membrane-Scission Machinery. Trends in Biochemical Sciences 42, 42–56.

Day, KJ, Staehelin, LA, and Glick, BS (2013). A three-stage model of Golgi structure and function. Histochem Cell Biol 140, 239–249.

Desai, R et al. (2020). Mitochondria form contact sites with the nucleus to couple prosurvival retrograde response. Sci Adv 6, eabc9955.

Ferri, KF, and Kroemer, G (2001). Organelle-specific initiation of cell death pathways. Nat Cell Biol 3, E255–E263.

Gaude, E, and Frezza, C (2016). Tissue-specific and convergent metabolic transformation of cancer correlates with metastatic potential and patient survival. Nat Commun 7, 13041.

Gong, Y-N, Guy, C, Crawford, JC, and Green, DR (2017a). Biological events and molecular signaling following MLKL activation during necroptosis. Cell Cycle 16, 1748–1760.

Gong, Y-N, Guy, C, Olauson, H, Becker, JU, Yang, M, Fitzgerald, P, Linkermann, A, and Green, DR (2017b). ESCRT-III Acts Downstream of MLKL to Regulate Necroptotic Cell Death and Its Consequences. Cell 169, 286-300.e16.

Hammerling, BC et al. (2017). A Rab5 endosomal pathway mediates Parkin-dependent mitochondrial clearance. Nat Commun 8, 14050.

Hsu, F, Spannl, S, Ferguson, C, Hyman, AA, Parton, RG, and Zerial, M (2018). Rab5 and Alsin regulate stress-activated cytoprotective signaling on mitochondria. ELife 7, e32282.

Jimenez, AJ, Maiuri, P, Lafaurie-Janvore, J, Divoux, S, Piel, M, and Perez, F (2014). ESCRT Machinery Is Required for Plasma Membrane Repair. Science 343, 1247136–

1247136.

Luo, Y, Ma, J, and Lu, W (2020). The Significance of Mitochondrial Dysfunction in Cancer. IJMS 21, 5598.

McGuirk, S, Audet-Delage, Y, and St-Pierre, J (2020). Metabolic Fitness and Plasticity in Cancer Progression. Trends in Cancer 6, 49–61.

Mukherjee, S, Chiu, R, Leung, S-M, and Shields, D (2007). Fragmentation of the Golgi Apparatus: An Early Apoptotic Event Independent of the Cytoskeleton. Traffic 8, 369–378.

Overholtzer, M, Mailleux, AA, Mouneimne, G, Normand, G, Schnitt, SJ, King, RW, Cibas, ES, and Brugge, JS (2007). A Nonapoptotic Cell Death Process, Entosis, that Occurs by Cell-in-Cell Invasion. Cell 131, 966–979.

Rühl, S, Shkarina, K, Demarco, B, Heilig, R, Santos, JC, and Broz, P (2018). ESCRT-dependent membrane repair negatively regulates pyroptosis downstream of GSDMD activation. Science 362, 956–960.

Schmidt, C, Sciacovelli, M, and Frezza, C (2020). Fumarate hydratase in cancer: A multifaceted tumour suppressor. Seminars in Cell & Developmental Biology 98, 15–25.

Sin, AT-W, and Harrison, RE (2016). Growth of the Mammalian Golgi Apparatus during Interphase. Mol Cell Biol 36, 2344–2359.

Straathof, KC, Pulè, MA, Yotnda, P, Dotti, G, Vanin, EF, Brenner, MK, Heslop, HE, Spencer, DM, and Rooney, CM (2005). An inducible caspase 9 safety switch for T-cell therapy. Blood 105, 4247–4254.

Tonnessen-Murray, CA et al. (2019). Chemotherapy-induced senescent cancer cells engulf other cells to enhance their survival. Journal of Cell Biology 218, 3827–3844.

Vaupel, P, Schmidberger, H, and Mayer, A (2019). The Warburg effect: essential part of metabolic reprogramming and central contributor to cancer progression. International Journal of Radiation Biology 95, 912–919.

Warburg, O (1956). On respiratory impairment in cancer cells. Science 124, 269–270.

Yamano, K et al. (2018). Endosomal Rab cycles regulate Parkin-mediated mitophagy. ELife 7, e31326.

Conclusion

Eukaryotic cell death is critical throughout animal development, tissue homeostasis, and disease. Millions of cells die every second in an adult human and apoptosis remains the most well characterized form of cell death. Induction of apoptosis results in mitochondrial permeabilization and caspase activity. Either event is sufficient to kill cells. However, an ever-growing body of research suggest that cells, including cancer cells, can survive transient damage to the mitochondria and subsequent caspase activity using a process termed anastasis. Evasion of cell death is a hallmark of cancer so studying the fundamental biology of anastasis is necessary to develop better cancer therapies. The basic cell biology of anastatic cancer cells remains largely understudied. In this dissertation I have used human cancer cell lines to study the biological consequences of transient apoptotic stress and characterize key mitochondrial events during anastasis.

The mitochondrial network is essential for cell death regulation and energy production. However, mitochondrial organization and function during anastasis was relatively understudied prior to this work. I developed a protocol which limits caspase activity to promote anastasis and enhances our study of mitochondrial hallmarks. I found that cancer cells recover following extensive mitochondrial permeabilization and collapse. I observed that anastatic cells maintain low mitochondrial activity. Anastatic cells of low mitochondrial membrane potential also show healthy nuclei suggesting an interplay between apoptosis survival, metabolic reprogramming, and nuclear viability.

Evasion of cell death and deregulated cellular energetics are two hallmarks of cancer that are controlled at the mitochondrial network. Altogether, this dissertation catalogs key mitochondrial events throughout anastasis and reveals a previously unknown connection between anastasis and mitochondrial respiration. My observations lay the foundation for future work aimed to understand the advantages of mitochondrial dysfunction following transient apoptotic stress. This is important as many chemotherapeutic agents induce apoptosis and tumor relapse remains a major clinical problem. This discovery represents a critical first step toward the development of novel therapies targeting dysregulation of apoptosis and metabolism in cancer.